Title

Multi-scale spatial ecology of an endangered alpine migrant, Sierra Nevada bighorn sheep

Permalink

https://escholarship.org/uc/item/079274sk

Author

John, Christian

Publication Date

2022

Peer reviewed|Thesis/dissertation

Multi-scale spatial ecology of an endangered alpine migrant, Sierra Nevada bighorn sheep

By

CHRISTIAN L. JOHN
DISSERTATION

Submitted in partial satisfaction of the requirements for the degree of

DOCTOR OF PHILOSOPHY

in

Ecology

in the

OFFICE OF GRADUATE STUDIES

of the

UNIVERSITY OF CALIFORNIA

DAVIS

Approved:

_____

Eric S. Post, Chair

_____

Justine A. Smith

_____

Thomas R. Stephenson

Committee in Charge

2022

Table of Contents

Acknowledgements

No five-year project comes to fruition without the support, guidance, and advice from a whole community, and this dissertation is no exception. I will be forever grateful to Eva Beyen, whose encouragement, wisdom, and patience improved many days spent in the field and "office" alike. A garage may make for small quarantine quarters, but I could not have asked for a better companion with whom to endure a pandemic.

My dissertation committee – Eric Post, Justine Smith, and Tom Stephenson – provided immensely helpful guidance and feedback throughout the course of graduate school. It has been a long time since I first met Eric, and it was through his work and counsel that I realized how my path might involve a career in ecology. He provided me an academic home where I had the freedom to pursue my own interests, develop my own ideas, and learn at my own pace. He also introduced me to Tom, who instilled in me a sense of awe and respect for the Sierra starting our first day hiking up McGee Creek in a lightning storm. Justine joined our department during my second year at UC Davis, and from the start has been an inspiration for both her breadth of experience and depth of expertise. The work described in this dissertation would have looked very different indeed without all of their input during the design, execution, and summarization of the Sierra phenology project.

Several faculty outside my dissertation committee contributed substantially to my development as a scholar at UC Davis. I am especially indebted to Hugh Dingle, Ben Houlton, Andrew Latimer, Sharon Lawler, and Rahel Sollmann for their service on my qualifying exam committee; discussions with each of them leading up to and during the exam helped shape the foundations of what would eventually become my dissertation. Don Strong provided me an

iv

Finally, I owe a great deal of thanks to my parents, who taught me to stick with commitments, encouraged me to seize opportunities, and helped me to overcome innumerable roadblocks. My father, Greg, maintains a childlike wonder about the natural world in spite of nearing 70, and my mother, Sally, is always dreaming up a new craft or form of entertainment. I hope that I will take their creativity and reverence with me in whatever lies ahead.

Through my blue fingers, pink grains are falling, haphazard, random, a disorganized stream of silicone that seems pregnant with the possibility of every conceivable shape . . . but this is illusion. Things have their shape in time, not space alone. Some marble blocks have statues within them, embedded in their future.

-Alan Moore, *Watchmen*

Abstract

Ecological dynamics have been altered by recent climate change in regions with pronounced warming trends. Landscape- and regional-scale ecological processes face change in both seasonal patterns and long-term trends as temperature and precipitation regimes shift. Interspecific interactions are especially sensitive to environmental change if one species responds flexibly to abiotic processes but the other does not. Herbivore movements, migrations, and distributions – each of which relate to biotic and abiotic environmental variation – are thus likely to change as effects of climate change cascade through ecosystems. Yet, multilevel relationships connecting climate with spatial dynamics of herbivores are poorly understood, in part due to the difficulties in generating consistent measurements of fine-scale ecological processes across broad geographic extents. Here, I use the Sierra Nevada mountains of California and Sierra Nevada bighorn sheep (*Ovis canadensis sierrae*, hereafter "Sierra bighorn") as a model to address three questions about space and time in ungulate ecology: First, how does landscape phenology vary along a desert-alpine gradient? Second, what drives nomadic migration in Sierra bighorn? And third, how can long-term climate forecasts inform conservation of large ungulates at the continental scale? I begin by outlining a niche-centric view of altitudinal migration and its marine counterpart, bathymetric migration. I then quantify relationships among topography, geography, and weather, and their collective effects on spatial patterns in resource phenology. Next, I address movement strategy, organization, and migration timing of an alpine specialist as they relate to the resource base. Finally, I contextualize ungulate conservation efforts in future climatic conditions, identifying which species are most susceptible to loss of protected climate space toward the end of the century.

Chapter 1: Seasonality, niche management, and vertical migration in landscapes of relief

Abstract

Landscapes of vertical relief, such as mountains and continental slopes, intensify ecological and climatological variation within narrow spatial windows. Seasonal vertical migrants exploit this variation during their residence in, and movements between, vertically stratified seasonal ranges. Animals in terrestrial, marine, and even human-ecological systems undergo similar patterns of seasonal vertical movements. The diversity of arenas in which vertical migration evolved lends insight to the factors promoting seasonal use of landscapes of relief. Because animals must contend with both endogenous circannual rhythms and exogenous environmental seasonality, vertical migrants may be sensitive to inconsistent change across stratified seasonal ranges under climate change. To better understand how ongoing and future climatic and environmental changes are likely to impact vertical migrants, we examine vertical migration in the context of niche tracking and niche switching. Whereas niche trackers minimize variation in realized environmental conditions throughout their seasonal movements, niche switchers undergo seasonal transitions in realized niche space. These strategies mediate the relationship between migrants and their changing environment, and can be used to forecast impacts of future change and effectively conserve systems of vertical migration. Niche tracking may be hindered by inconsistent or unpredictable environmental change along a single niche axis across strata, while niche switching may be sensitive to incongruous spatiotemporal change

across factors. We suggest that climate change will affect seasonal patterns in vertical

environments discontinuously across time, space, and strata, and that vertical migrants are

likely to face additional anthropogenic threats that interact with environmental seasonality.

Conservation of vertical migrants should prioritize the availability of, and facilitate movement

between, stratified seasonal ranges.

Keywords

altitudinal, bathymetric, migration, seasonality, climate change, niche breadth

biotopic space. Axes of positions in a physical environment, such as elevation or depth. **fundamental niche.** The range of biotic and abiotic conditions over which an organism can, theoretically, survive and produce viable offspring. **geographic migration.** Long-distance seasonal movements, such as latitudinal migration. **landscape**. Any environment with a substrate, including terrestrial and marine settings. **niche space**. Axes of positions in an n-dimensional hypervolume of conditions that define an organism's suitable environment. **realized niche.** The range of biotic and abiotic conditions over which an organism actually survives and produces viable offspring. This is a sub-set of the organism's fundamental niche constrained by realized environmental conditions at a specific location and time and by positive and negative interactions with other organisms. **season**. An intra-annual subset of any annual cycle, such as tropical precipitation patterns, Arctic sea ice formation and depletion, or endogenous rhythms in hormone release. **strata**. Two or more positions separated by vertical biotopic space, as in the case of movement along topographic or bathymetric slopes. **vertical migration**. Short-distance seasonal movements across strata such as altitudinal or bathymetric migrations.
Glossary

Introduction

Migration is a taxonomically and geographically widespread adaptation to temporal

variation in the environment. Migration is characterized by movements between spatially

isolated ranges, on a much greater scale than typical day-to-day movements (Dingle and Drake

2007). Seasonal ranges may be separated by hundreds or thousands of kilometers across geography, as is the case in long-distance migrations, or just a few hundred meters across topography or bathymetry, as is the case in vertical migrations. Whereas long-distance migrants face significant energetic demands and risks of mortality during their journeys, vertical migrants minimize costs of travel while still realizing considerable ecoclimatic variation. Amphibians, birds, and crustaceans are but a few of the taxa represented among Earth's vertical migrants (Aguzzi et al. 2013, Boyle 2017, Hsiung et al. 2018). These climbing creatures seasonally traverse mountain sides and marine canyons alike, in pursuit of resources, shelter, and mating opportunities.

Mountains cover a quarter of Earth's land surface, and shallow seas comprise over a tenth of the total global seabed area (Costello et al. 2010, Karagulle et al. 2017). While vast distances must be traveled to realize significant changes in ecology or climatology across latitudinal gradients, comparable variation can be experienced by traversing only a few hundred meters up or down a mountainside (Körner 2007, Klinges and Scheffers 2020). Similarly, physical properties of the water column generate abiotic and biotic gradients over small distances in depth, compared to the thousands of kilometers that would be required for the same apparent change across latitude (Sprintall and Cronin 2001). Together, elevation and depth constitute a continuous, 1-dimensional biotopic space which vertical migrants can navigate in order to realize or mitigate seasonal change in their environment (Figure 1.1).

The magnitude of seasonal rhythms with which migrants contend often varies across strata. For example, snowpack is deeper and the snow season is longer in temperate alpine regions than in the foothills below. Similarly, deep seafloors are more protected from seasonal

storms than shallow coastal waters. Two strategies are available to migrants for coping with spatially structured seasonal environmental variation: they can track spatiotemporal variation along niche axes ("niche tracking," Figure 1.1a,c) or undergo seasonal transitions in the niche space they occupy ("niche switching," Figure 1.1b) over the course of their migratory journey (Martínez-Meyer et al. 2004, Gómez et al. 2016). Whereas niche trackers maintain constancy or dampen seasonal oscillations in their realized niche (e.g. Somveille et al. 2019, Bay et al. 2021), niche switchers abandon niche space at the turn of the season and exacerbate variation along some niche axes (e.g. Ponti et al. 2020). If seasonal ranges undergo inconsistent environmental change, past strategies of niche tracking and niche switching may fail to accommodate novel conditions.

Prevailing patterns of seasonal change across stratified environments may be threatened by changes in the climate regime. Inconsistent change in the timing and magnitude of seasons across strata, as well as long-term trends in bioclimatic and species distributions, modify the pattern of emergence of seasons across landscapes of relief. If phenological shifts in exogenous seasonal factors are inconsistent across elevation or depth (e.g. Inouye et al. 2000), the ability of both niche trackers and niche switchers to cope with forecasted environmental change may be compromised. Inconsistent trends among axes of fundamental niche space may lead to the loss of suitable niche space within a range. Simultaneously, direct human impacts such as land use change and fencing infrastructure limit migrants' historical access to seasonal ranges. Effective conservation management plans for vertical migrants will account for the spatiotemporal complexities of landscapes of relief.

In this review, we ask the following questions: 1) *Why migrate vertically rather than geographically*? 2) *In what vertical migratory systems do niche tracking and switching emerge*? and 3) *How will anthropogenic change affect systems of vertical migration*? To answer these questions, we identify how landscapes of relief modify seasonal variation in limiting factors across vertical space, and examine the means by which vertical migrants cope with seasonal variation in the environment. We then explore how climate shapes the progression of seasons across strata, and discuss the mechanisms through which ongoing and future change are likely to affect vertical migrants. We conclude by outlining conservation priorities that will help protect vertical migrants in the face of forecasted change.

Environmental variation in landscapes of relief

Seasonal movements such as migration arise in response to temporal variation in endogenous or exogenous factors. Relative to the scale of seasonal migration, some environmental factors that vary spatially appear to be constant through time, with a similar spatial pattern of variation persisting across years. Migrants that experience significant seasonal endogenous variation (such as breeding or molting) may exploit temporally "static" variation by moving between disparate ranges as the need for - or challenges posed by - different conditions arises. Conversely, other environmental factors vary both spatially and seasonally due to Earth's axial tilt and position along its revolution around the Sun. Such dynamic exogenous variation may promote migratory movements regardless of the migrant's endogenous state if the relative favorability of seasonal ranges varies across seasons.

Static variation: space

Elevation and depth generate environmental variation over short distances through static influences on abiotic environmental factors. In general, solar radiation increases while air density and temperature decrease with increasing altitude (Körner 2007). Other factors such as precipitation and wind may vary across altitude but the pattern of their variation is locally or regionally idiosyncratic. For example, temperate latitudes tend to experience increasing annual precipitation at higher elevations, while in polar and equatorial latitudes the opposite trend is observed. Within regions, relationships among precipitation and elevation are nonlinear, and vary across seasons (Körner 2007). Water depth similarly imposes stratified abiotic variation: incoming light and solar radiation dramatically decrease through the photic zone, while buffering from atmospheric weather is increased. Conversely, temperature, oxygen concentration, and salinity vary with depth, but their profiles can be nonlinear and locally idiosyncratic (Paulmier and Ruiz-Pino 2009, Shadwick et al. 2015).

Stratified variation in abiotic factors drives vertical zonation in ecological communities, composed of species that are simultaneously adapted to a window of conditions and interspecific interactions. Physiological limits of animals and plants determine the vertical range of habitat available to them on both mountains (Janzen 1967) and in oceans (Carney 2005). The process through which relief generates community stratification is perhaps most famously illustrated by the upper limit of tree growth on mountainsides (Körner and Paulsen 2004). In the ocean, primary production is largely limited to the shallowest reaches, where sunlight is able to penetrate and the rate of photosynthesis is greater than that of respiration (Dennison 1987). Consequently, a steep decline in forage availability emerges for primary consumers with

6

increasing ocean depth. Similarly, a balance of pressure tolerance, temperature, and oxygen availability dictates the bathymetric range of many marine animals (e.g. Brown and Thatje 2011, Brown et al. 2017).

Dynamic variation: space-time

Seasonal variation in abiotic factors drives seasonal variation in ecological communities (Post 2019). Just as accumulated temperature and precipitation regulate plant growth in many terrestrial systems (Cleland et al. 2007), so too do these factors impact the timing, magnitude, and species composition of marine phytoplankton blooms (Thompson et al. 2015). Temperature, precipitation, and primary productivity cycles underlie the adaptive benefits of dormancy and emergence by many terrestrial animals. Seasonal pulsed reproduction by plants and animals alike are linked to cascading effects of abiotic seasons (e.g. madwort flowering: Gómez 1993, caribou and muskox parturition: Kerby and Post 2013, bivalve spawning: Philippart et al. 2014). When seasonal variation follows predictable cycles (e.g. Box 1.1), migrants can rely on temporal cues such as photoperiod to coordinate movements with anticipated change at the destination.

Because variation in abiotic and biotic factors is neither linear across strata nor uniform among factors, temporal environmental variation is spatially structured in landscapes of relief. Landscapes of relief modify the spatial structure of seasonal environmental variation in three forms of "seasonal transformation": phase shifts, phase differences and phase products (Figure 1.2). In phase shifts (Figure 1.2a), the timing of variation in a factor is shifted with respect to strata, but the magnitude, and baseline condition of variation in that factor, remain unchanged. For example, plant growth may be delayed with respect to elevation due to the recession of the

snowline and variation in accumulated temperature along an elevational gradient. In phase differences (Figure 1.2b), the baseline condition of a factor changes with respect to strata, but the timing and magnitude of variation in that factor remain unchanged. For example, the timing and magnitude of seasonal temperature variation may be consistent across a mountainside, while high elevations experience predictably colder temperatures than lower elevations. In phase products (Figure 1.2c), the magnitude of variation in a factor is adjusted with respect to strata, while the timing and baseline condition of the factor remain unchanged. For example, disturbance from seasonal atmospheric storms is greater in shallow waters than in protected waters deep below. Finally, landscapes of relief may introduce a combination of these phase modifications (Figure 1.2d), where two or more forms of spatiotemporal variation emerge. For example, the duration and magnitude of seasonal snow cover may be much greater in an alpine environment than the foothills below. Similarly, photosynthetic activity in the euphotic zone generates a primary productivity seasonality regime in shallow waters, while primary production in deeper waters may be negligible.

Geography and the relative role of relief

Migration may facilitate the pursuit of favorable conditions, or escape from unfavorable conditions (Winger et al. 2019). Across broad geographic distances, spatiotemporal variation in environmental conditions is generally reliable. For example, movement between a savanna and tropical rainforest ensures directional change in moisture and ecosystem structure (Whittaker 1970). This is also the case to a certain extent across topography or bathymetry (e.g. Whittaker and Niering 1968); however, regional variation in climate may predominate in spite of considerable local variation in some factors. For example, persistent snow is common at high

elevations in the Arctic, while seasonal snow cover characterizes variation across elevations (Hammond et al. 2018). Vertical migration would thus be insufficient as a means of complete escape from snow in the Arctic; geographical movements are the only available option if that region is to be utilized by migrants that cannot cope with snow. At more temperate and tropical latitudes, however, persistent snow is rare, and seasonal snow at high elevations is not matched at low elevations (Hammond et al. 2018). Altitudinal movements would facilitate a response to snow at these latitudes.

Conversely, vertical retreat from unfavorable winter conditions may be adaptive in marine settings at higher latitudes, where sea surface temperatures are most dramatically seasonal in shallow waters (Box 1.1). This combined phase difference and amplification at high latitudes introduces a strong seasonal signal in the depth gradient in water temperature, of particular importance for ectotherms. Tropical waters face comparatively little seasonal variation in temperature, but strong seasonality in sea surface salinity due to winds and fresh water inputs by precipitation and runoff (Delcroix and Hénin 1991). While vertical migration in these waters may satisfy seasonal endogenous requirements, so too may it allow migrants to cope with temporally dynamic exogenous factors.

Terrain structure further complicates general patterns of environmental variation along elevation or depth. Slope and aspect are particularly impactful factors in terrestrial temperate and Arctic settings, where increased direct solar irradiance on slopes facing the equator leads to increased temperature, reduced moisture, and advanced phenology (Jackson 1966, Griffiths et al. 2009, Geroy et al. 2011). In marine settings, topography underlies the mixing and movement of water masses (Huthnance 1995, Shapiro et al. 2003), impacting temperature,

deposition of organic matter, availability of oxygen and nutrients, and community diversity (Robertson et al. 2020). Coastal upwelling and its drivers add additional complexities to seasonal variation in environmental factors along depth, but simultaneously introduce cues that reliably predict imminent environmental change (Largier 2020). Upwelling in California (USA), for example, leads to a seasonal influx of nutrients from deeper waters, and consequently increases in production of phytoplankton and ultimately krill. Thus ensures seasonal arrival by geographically migratory blue whales (*Balaenoptera musculus*) when availability of their preferred food source is high there (Croll et al. 2005). Further from the coast, organic carbon deposition reliably follows upwelling events, leading to seasonal influxes of consumable detritus and visitation by mobile benthic species on the deep sea-floor (Smith et al. 2013). Thus, in spite of coarse regional patterns that underlie some unavoidable seasonal environmental, landscapes of relief introduce additional dimensions of local environmental variation along which migratory animals can track existing conditions, or seek out novel environments.

Niche management in multi-season space

The environmental variation introduced by landscapes of relief can be exploited without moving across vast distances, as would be required of long-distance migrants. This reduces the endogenous cost of migration, such as energy usage and storage limitations, as well as external pressures such as unfavorable conditions faced during long-distance migrations (Alerstam et al. 2003, Boyle 2017). Migrants must navigate a gamut of exogenous seasons while simultaneously facing seasonal variation in endogenous factors such as hormone release, body condition, and reproductive status. Animals may therefore use seasonal migration as a tactic to navigate

biotopic space while managing their use of niche space. For a given niche axis, migrants may

maintain access to consistent conditions ("niche tracking") or seek out completely different

conditions during a subset of year ("niche switching", Martínez-Meyer et al. 2004). Whereas

niche tracking involves the maintenance of niche space during migration, niche switching

involves a fundamental shift in the realized environmental factors during or as a result of

migration. Vertical migrants may employ either or both of these strategies to cope with the

numerous seasons of change they face.

Niche tracking

Niche tracking vertical migrants follow constant environmental conditions across strata

in landscapes of relief. Because the phenology of seasonal factors such as forage availability and

accumulated temperature may vary across strata (e.g. Hopkins 1920), niche trackers can

synchronize their vertical movements with spatially predictable change in their environment

(Riotte-Lambert and Matthiopoulos 2020). Migrants using this strategy can minimize

physiological or behavioral adjustments that would be required for major transitions in realized

environmental factors.

Many migrating ungulates follow the phase shift in spring plant growth upslope during

spring in a form of niche tracking called "surfing the green wave" (Albon and Langvatn 1992,

Mysterud et al. 2001, Merkle et al. 2016). Because newly emergent plant material is nutrient-

rich and easily digested, these migrants can extend the window of high-quality forage access

and increase fat reserves by tracking green-up through space (Middleton et al. 2018). Recent

evidence indicates that ungulates are able to more effectively track resource phenology when

vegetation growth is rapid and progresses sequentially across the landscape, as is the case in

many mountain settings (Aikens et al. 2020). Evidence of resource tracking in landscapes of

relief has also been reported in tortoises (Blake et al. 2013), hares (Rehnus and Bollmann 2020),

birds (Loiselle and Blake 1991), and human-ecological systems (Beck 1991).

Niche tracking vertical migrations are also useful for coping with seasonal variation in

temperature. For example, sea surface temperature off the coast of Maine (USA) is highly

seasonal, generating an attenuation in temperature variation toward deeper, more insulated

water. Seasonal bathymetric movements have been detected through mark-recapture of deep-

sea lobsters (*Homarus americanus*) in Maine, where they use shallower waters during the

summer before retreating to the continental slope for winter (Cooper and Uzmann 1971).

Migratory lobsters were able to maximize their growth rate, in part because they maintained a

warm narrow range of temperature across the year, while sympatric lobsters that remained

resident in shallow waters year-round experienced colder temperatures that were more

variable (Cooper and Uzmann 1971). In the Mediterranean Sea, similar seasonal variation in

bathymetric distributions of benthopelagic fish and crustaceans appears to coincide with

temperature and salinity variability introduced by seasonal subsurface water currents (Aguzzi et

al. 2013).

Niche switching

Niche switching vertical migrants face major shifts in realized niche space during or as a

result of their migration. Migrations associated with endogenous schedules, such as dormancy,

molting, and reproduction frequently include some element of niche switching. Because

seasonality in physiology and behavior may cyclically require different habitat parameters,

many niche switching vertical migrants exploit stratified environmental variation that is not

necessarily seasonal. By partitioning niche space over the course of the year, niche switchers

can adjust habitat use to accommodate seasonal life history requirements.

Seasonal dormancy allows organisms to cope with periodically harsh conditions, and is

frequently associated with vertical migratory movements. In Costa Rican dry forests, seasonal

variation in rainfall generates seasonality in vegetation growth. Skipper butterfly (*Aguna*

asander) caterpillars rely on leaves of *Bauhinia ungulata,* a shrub that produces leaves only

during the rainy season (Assunção et al. 2014). In the absence of *Bauhinia* leaves, the insects

migrate uphill to colder strata where they estivate in trees and among rocks. Once the seasonal

rains resume, *A. asander* return to the rejuvenated lowland forests to feed and reproduce

(Janzen 2004). Interestingly, a sympatric predatory paper wasp (*Polistes variabilis*) undergoes

similar vertical movements to reach dry season dormancy habitat (Hunt et al. 1999). Bears and

bats also undergo seasonal vertical movements to access hibernacula, which are separated

from habitat used during their waking life through amplified snowpack and stratified

geomorphology (Grachev 1976, Neubaum et al. 2006).

Niche switching may also facilitate reproductive tasks. A perhaps extreme example of

this occurs in a transit between terrestrial and marine environments. The ecotone between

land and sea is inherently stratified and delineates an impressive array of environmental

conditions. Soldier crabs (*Coenobita clypeatus*) of Mona Island (Puerto Rico, USA) undergo

seaward migrations during an annual summer spawning event called the *cobada* (Nieves-Rivera

and Williams 2003). Adult *C. clypeatus* spend most of their time in terrestrial habitat, but

migrate to the ocean where eggs are deposited, larvae develop, and juveniles claim shells.

Seaward migrations by land hermit crabs are timed to coincide with seasonal peaks in water

temperature, but also attuned to the lunar cycle for favorable tide and lighting conditions (Doi et al. 2016, Nio et al. 2019). Niche switching reproductive migrations are also observed among some birds, when seasonal courtship, foraging, and roosting habitat are vertically stratified (Mussehl 1960, Crawford and Pelren 2001, Zwickel and Bendell 2003), or when reproduction is seasonal and sensitive to stratified variation in predation (Boyle 2008).

Navigating the fundamental niche: the tracking-switching continuum

Across the entirety of a migrant's fundamental niche, both niche tracking and niche switching are no doubt employed over the course of a year. Any environmental condition that varies in space can be tracked or abandoned by a mobile organism, so long as relocation does not require exceeding some physiological constraint (i.e. departing from fundamental niche space). Because migrants face a crash of endogenous and exogenous seasons, they potentially realize inconsistent variation among niche axes while moving across strata. For example, ascending a marine canyon may increase access to forage, but simultaneously lead to changes in light, salinity, and hydrostatic pressure. By navigating physical space, migrants can realize considerable differentiation along one niche axis, but minimize variation along another. Incomplete migratory patterns, such as partial and facultative migrations, lend insight into how animals use vertical movements to track or switch among seasonal niche spaces.

Partial migration is common among vertically migratory species, wherein a subset of the population migrates while another does not (e.g. Cooper and Uzmann 1971, Boyle 2017). Whereas migration can facilitate tracking favorable environmental variation, remaining resident in a particular range may limit the extent to which niche tracking is possible (Laube et al. 2015, Gómez et al. 2016). For example, many Sierra Nevada bighorn sheep (*Ovis canadensis sierrae*)

in California (USA) move to low-elevation slopes during winter to avoid deep snow and seek

foraging opportunities, but they face increased predation pressure compared to those

remaining in the barren snowy alpine zone (Spitz et al. 2020). While individuals that remain

resident in the alpine zone may reduce interactions with predators, they must cope with

increased seasonal variation in temperature, wind speed, snow cover, and forage availability.

Other factors favoring partial migration include seasonal intraspecific competition and conflict,

intrapopulation niche differentiation, and thermal tolerance (Chapman et al. 2011). Coping

with, or evading, these factors, likely underlies how individuals manage niche space: evading

conditions that are sought after by conspecifics ensures a different realization of total annual

niche space occupied by the individual.

Facultative and sub-seasonal movements add flexibility to migrants' seasonal

distribution schedule. Niche tracking vertical migrants may be able to entrain their movements

with environmental conditions by making multiple vertical movements leading up to and during

the migratory season. The close geographic proximity of seasonal ranges afford vertical

migrants the opportunity to scout conditions and find refuge from unfavorable weather by

revisiting seasonal ranges (Horvath and Sullivan 1988, Hahn et al. 2004, Rice 2008, Boyle et al.

2010). Sub-seasonal vertical movements also arise among multiple-breeding animals, such as

some birds seeking to track high-quality conditions across reproductive attempts (Brambilla and

Rubolini 2009, Ceresa et al. 2020). Such fine-scale adjustments in vertical distribution may

enable some migrants to buffer climate change and maintain access to tracked niche space

throughout the season (Frey et al. 2016).

Tracking and switching lie on opposite ends of a continuum of strategies for managing

seasonal niche space. Migrants likely employ both approaches during vertical migration

because of the numerous factors that vary across strata in landscapes of relief. However, the

interaction between physiology, behavior, and environmental factors governs whether a

migrant generally tracks niche space across the year, or switches between seasonal subsets of

niche space. For example, ectotherms that face seasonal temperature variation without going

into dormancy track vertical zonation in temperature in order to maintain metabolic activity

(e.g. Cooper and Uzmann 1971, Crossin et al. 1998). Conversely, species that migrate to

hibernacula in order to escape unfavorable conditions undergo a massive shift in metabolism,

activity, and preferred habitat (e.g. Hunt et al. 1999, Haroldson et al. 2002, Neubaum et al.

2006). Niche switching is similarly dramatic for diadromous and semi-diadromous migrants as

they deposit larvae in ontogenic habitat (e.g. Elliott et al. 2007, Amorim et al. 2016). The niche

management strategy employed by vertical migrants, and the faculty to use alternative

approaches during migration, will likely determine their ability to persist under future climate

change.

Climate shapes configuration of seasonal niche space

Climate modifies stratified environmental variation in landscapes of relief by shaping

patterns within and relationships among niche axes across biotopic space (Colwell and Rangel

2009). Changes in temperature and precipitation, and the seasonality thereof, lead to ecological

response across strata and through time. Common ecological responses to warming include

advancing phenology due to more rapidly accumulated spring temperature, and range shifts to

accommodate physiological constraints (Parmesan 2006). However, the degree of phenological

change may vary across strata, as well as the propensity to shift ranges and the availability of novel, suitable habitat. Climate-induced changes in migratory propensity may influence reproductive exchange within partially migratory populations, ultimately impacting gene flow and genetic diversity, potentially driving, or limiting, evolutionary change. Vertical migrants' ability to "keep up" with climate change will depend on modifications to the spatiotemporal arrangement of environmental variation in their historic, current, and potentially future habitat, as well as change in the phenology and distribution of organisms with which migrants interact.

Seasonal niche space

Inconsistent alteration of stratified ranges by climate change will impact the relative timing of transitions between seasons, and consequently the ability of some migrants to track spatial variation along some niche axes (Figure 1.3, Niche 1). For example, in the European Alps, rapid phenological advance at high elevations has led to more uniform green-up across elevation (Vitasse et al. 2018). Earlier green-up and flowering by plants related to climatic warming were not matched by parturition of roe deer (*Capreolus capreolus*) in the Alps (Rehnus et al. 2020). Roe deer are income breeders and therefore depend on forage availability during the energetically expensive parturition and fawn rearing season. Thus, exacerbation of conditions that result in trophic mismatch can be consequential for offspring production and survival (Kerby and Post 2013). However, due to the elevational gradient in green-up timing, *C. capreolus* were able to buffer the expanding mismatch by adjusting their migratory schedule to account for shifting spatiotemporal dynamics of forage quality (Rehnus et al. 2020). The advantages of such a buffer may be stymied by more spatio-temporally uniform plant phenological dynamics. A similar pattern is expected for bark beetles (*Ips typographus*), as the

17

timing of diapause termination and swarming is expected to shift more rapidly at high

elevations and on south-facing slopes in the Alps (Jakoby et al. 2019). Adjustments to the

historic elevational trend in insect swarming phenology may impact insectivorous altitudinal

migrants that live there (e.g. grey wagtails, Klemp 2003). Inconsistent shifts across stratified

ranges can also be expected in marine settings, where effects of climate change are not

constant between surface waters and deep ocean (Capotondi et al. 2012).

Inconsistent climatic change across space also modifies the historic overlap and

adjacency of stratified niche spaces between seasons. Disruption of the historic relative timing

of seasonal niche availability may impact the seasonal migration schedule of some niche

switching vertical migrants (Figure 1.3, Niches 2 and 3). For example, grizzly bears (*Ursus arctos*

horribilis) in the greater Yellowstone ecosystem undergo a partial downhill migration after

emerging from high-elevation dens in spring (Haroldson et al. 2002). They then follow the

elevational progression of snowmelt into high-elevation habitat in the summer, coincident with

the summertime aggregations of Army cutworm moths (*Euxoa auxiliaris*) that migrate to the

alpine from the Great Plains (Pruess 1967, Servheen 1983, French et al. 1994, White et al.

1998). This influx of forage facilitates the hyperphagia required of bears leading up to

hibernation (Nelson et al. 1983, French et al. 1994). Throughout the Rocky Mountains, the

predictability of seasonal variation in snow cover has changed during recent years (Box 1.1).

Warming winters and reduced snow accumulation are expected in that area for the coming

decades (Lapp et al. 2005). If emergence and departure timing of *E. auxiliaris* in the Great Plains

becomes decoupled from snowmelt and den emergence by *U. a. horibilis* in the Rocky

Mountains, the efficacy of migratory bears' switch from hibernating to foraging may be compromised.

Fundamental niche space

Response to climate change through range shifts is additionally limited for vertical migrants. Abiotic stressors covary with both altitude and depth, imposing novel pressures on animals that undergo distributional shifts in response to increasing temperatures (Spence and Tingley 2020). In mountains, a finite upper biotopic limit (mountain peaks and ridgelines) prohibits indefinite upslope response. The available surface area of mountains is furthermore not constant across strata (Körner 2004, Elsen and Tingley 2015) and presents an added constraint on altitudinal migrants, particularly if density dependent factors like intraspecific competition for resources underlies the elevational distribution of seasonal ranges. In marine systems, range shifts toward deeper water are a common response to warming surface waters (Pinsky et al. 2013). However, physical and chemical factors prevent an indefinite retreat to deeper waters. The twilight zone introduces an absolute maximum depth for visual animals, while the sea surface delimits a minimum depth available to marine obligates. Reduced oxygen and increased hydrostatic pressure in deep water impose limits on metabolism, introducing a barrier that can only be overcome through physiological adaption (Brown and Thatje 2015). Because hypoxia tolerance is strongly linked to temperature in some depth migrants (Bigford 1979, Deutsch et al. 2015), change in ocean temperature and oxygenation, and shifts in the depth of the oxygen minimum zone, may be especially limiting for depth shifts by seasonal vertical migrants in the ocean.

Conserving systems of vertical migration

While the emergence of suitable niche space across vertical biotopic space is prone to adjustments by climate, migrants' access to and availability of seasonal ranges face additional threats. Direct processes such as infrastructure development and harvest may inhibit access by animals to seasonal ranges, influence population dynamics, and drive microevolutionary change in vertical migrants (Pecl et al. 2009, Pigeon et al. 2016, McInturff et al. 2020). Because migrants have more expansive annual ranges than nonmigratory animals, more opportunities arise for anthropogenic processes to disrupt their life history. Management of systems of vertical migration should account for the multifaceted spatiotemporal requirements of migrants.

Seasonal landscapes that actively face direct human-induced change such as deforestation and destructive harvest are likely to be immediate concerns for vertical migrants. For example, due to rapid and accelerating global deforestation (Hansen et al. 2013, Kim et al. 2015), habitat fragmentation is of particular concern for migrants that specialize on forests for at least part of their life history. The Eastern Arc Mountains of Tanzania house a large proportion of forest-dependent birds, but also face a high degree of deforestation (Buchanan et al. 2011). Such loss of forest habitat is concerning for both the numerous endemic tree species (Hall et al. 2009) and avian altitudinal migrants that live there (Burgess and Mlingwa 2000). One such species is the Banded green sunbird (*Anthreptes rubritorques*), a forest-dependent altitudinal migrant endemic to the Eastern Arc Mountains, which is now listed as a Threatened species due to habitat loss through deforestation (BirdLife International 2017). Conservation efforts must prioritize areas of rapidly vanishing habitat, especially where these intersect with

forecasts of climate change impacts on habitat availability, and particularly in instances where highly endemic species face extinction (Post and Brodie 2015).

Parallel to habitat destruction, movement barriers limit the realized availability of seasonal ranges to migratory animals. Human infrastructure, including fencing, roads, and bridges, interrupt directed movement, thereby preventing migrants from accessing seasonal ranges. Because anthropogenic delineations between land designations rarely fall along ecological boundaries, fences bar passage across otherwise continuous niche space. Semi-permeable solutions, such as wildlife-friendly fencing, increase connectivity between seasonal ranges, while still fulfilling the original intention of the infrastructure (Paige 2008, Sawyer et al. 2013). Barrier permeability may be similarly important in marine settings. For example, many crabs undergo seasonal movements between shallow estuarine and deeper ocean waters (e.g. Bigford 1979). The construction of bridges connecting capes at the mouth of estuaries may present temporary or permanent barriers to crab migration: project scheduling and design permeability must be considerations if the conservation of marine-estuarine bathymetric migrants is a priority.

Effectively managing for the future will rely on focused consideration of the seasonal role humans play in the systems vertical migrants occupy, and the sensitivity of niche space to a changing climate. One such example lies in a climate change hotspot, the East Australian Current (EAC), which has faced changes in the strength and seasonality of its flow and poleward shifts in the distribution of species that inhabit it (Johnson et al. 2011, Champion et al. 2018). The southern rock lobster (*Jasus edwardsii*) is an economically important species that undergoes seasonal bathymetric movements to shallow water for molting (MacDiarmid 1991).

Jasus sp. lobsters face seasonal fishery pressure in Tasmania, which is also highest in shallow waters near the coast. Lobster recruitment is expected to fall in the coming decades as sea temperature rises (Pecl et al. 2009), but they face the added threat of invading sea urchins that arrived in response to overfishing (Johnson et al. 2011). Accounting for spatiotemporal variation in lobster abundance, and determining whether effects of climate and harvest are additive or synergistic, are crucial to the success of fishery management there.

While systems of vertical transhumant pastoralism may not fit neatly under some contemporary definitions of "migration," their seasonal structure of landscape use presents an opportunity to forecast dynamics and examine policy through analogy: transhumant pastoralism is the practice of leading livestock along seasonal routes to track pasture quality, and mountain ranges across the world have served as systems for vertical pastoralism throughout human history. A primary concern of shepherds is the condition of grazing and wintering lands; decisions about grazing timelines dictate forage quality for livestock, and frequently incite conflict (Beck 1991). Shifts in predictable forage phenology may be difficult to match by pastoralists due to the often-rigid transit schedules imposed on them through political avenues. Nepalese herders have reported earlier snowmelt and advanced plant phenology in the Himalaya, where they undergo seasonal vertical movements to maintain yaks and other ungulates (Aryal et al. 2016). Added to shifting social and cultural landscapes, environmental change amplifies the expected decline of vertical transhumant pastoralism in the coming decades (Hock et al. 2019). Protection of the routes that connect seasonal ranges, and flexibility by officials to account for changes in ecosystem dynamics, will be central to the conservation of this imperiled lifestyle.

Conclusions

The evolution of analogous patterns across ecosystems lends insight to both basic and applied research questions (Burkepile et al. 2020). One such pattern is the seasonal movement between vertically separated habitats: vertical migration. Seasonal vertical migrations have evolved not only within marine and terrestrial habitats, but in some cases they involve transit between these inherently stratified ecosystems. Vertical migrants can be found throughout the animal kingdom, including among arthropods, birds, and even human-ecological systems. The heightened environmental variation generated by landscapes of relief allows animals to exploit or mediate the seasonality of their environment in order to facilitate growth and reproduction. However, the historic pattern of variation may be sensitive to adjustment by climate and accessibility by other anthropogenic impacts. Migrants' capacity to manage seasonal niche space by navigating biotopic space may underlie their ability to persist under climate and land use change, but well-planned conservation action and policy can help ensure the longevity of vertical migrants.

Figures
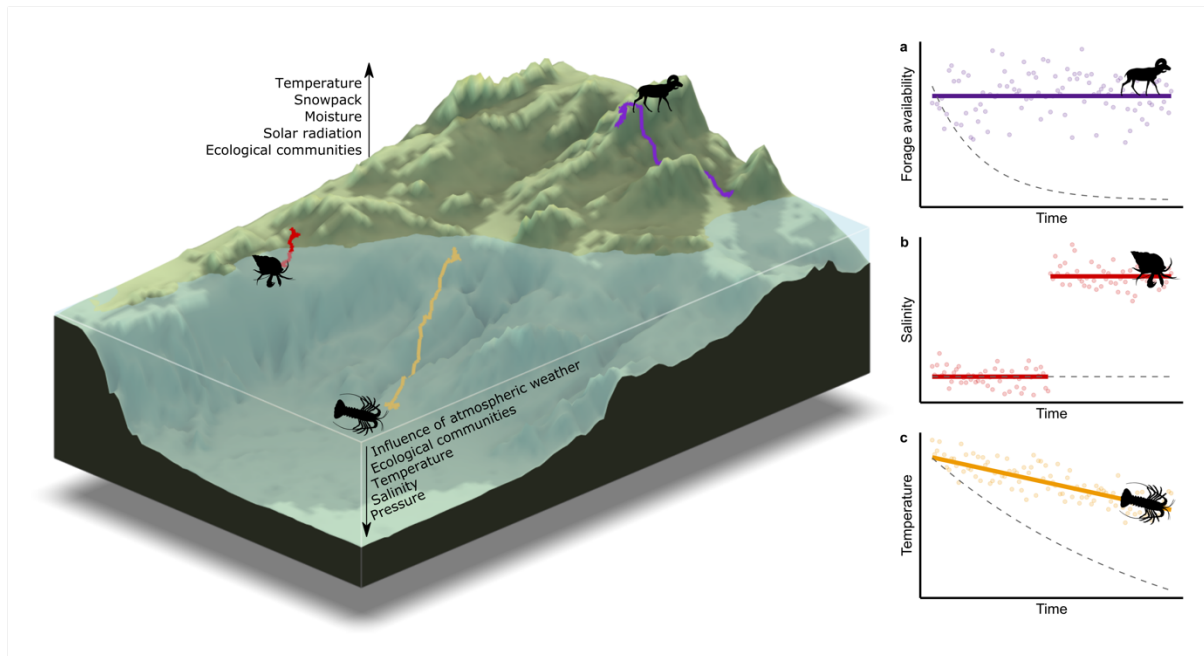
Figure 1.1. Landscapes of relief introduce multiple axes of environmental variation over short distances, which can be exploited by mobile organisms. In this conceptual illustration, exemplar species are shown at the destination end of their seasonal movement path in both the perspective landscape plot and niche panels (a-c). Environmental factors that vary vertically are indicated along arrows in the perspective plot. In a-c, one axis of niche space is plotted against time, with environmental conditions realized by seasonal migration shown in color, and environmental conditions realized by non-migration shown by a dashed line. Bighorn sheep track springtime plant growth as vegetation green-up progresses uphill ("niche tracking", a). Soldier hermit crabs face a massive shift in realized salinity when they move from their terrestrial non-reproductive environment to their marine reproductive and developmental environment ("niche switching", b). Other decapod crustaceans, such as some lobsters, dampen wintertime shifts in temperature by migrating to deeper waters ("dampened niche tracking", c). Data are for illustrative purposes only; terrain data from ETOPO1 (Amante and Eakins 2009), movement paths generated using directed random steps, and niche space generated using normal distributions with shifting center across time (R version 3.6.1). Animal silhouettes adapted from [phylopic]; illustrated by Scott Harmon, Ekaterina Kopeykina, and Joanna Wolf; and under public domain and creative commons licenses [CC0 1.0] and [CC 3.0].
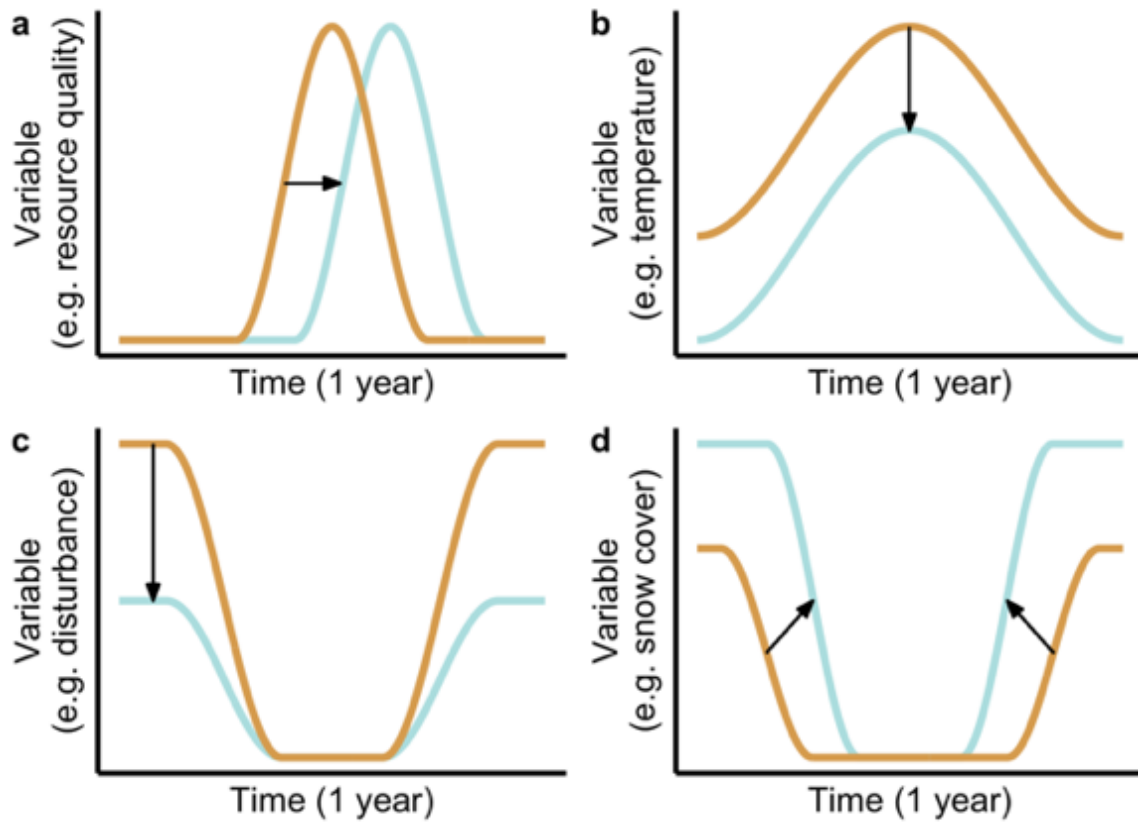
Figure 1.2. Landscapes of relief shape the spatiotemporal environmental variation through seasonal transformations across strata (tan and blue lines correspond to two environments of different elevation or depth). Phase *shifts* (a) involve a temporal advance or delay in the seasonal cycle without change in the intercept or magnitude of the cycle. Phase *differences* (b) arise when the cycle's intercept changes but without changing the amplitude of the cycle. Phase *products* occur where the same baseline conditions exist across space, but the magnitude of the cycle varies in the form of amplification or attenuation (c). Further spatiotemporal complexities may arise through a combination of these phase changes (d). The primary axes of phase variability are illustrated with black arrows.
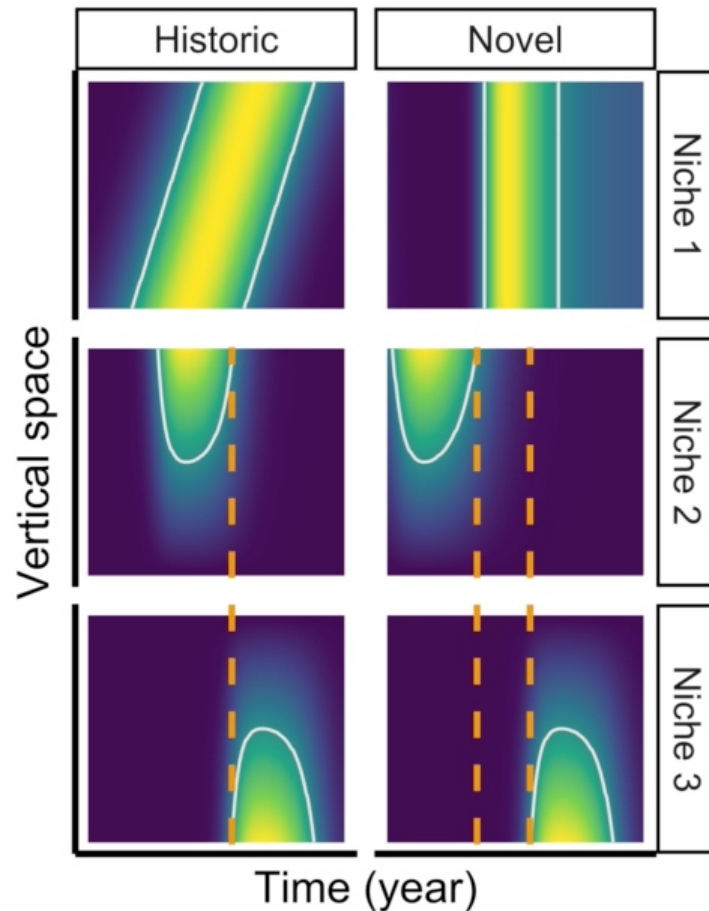
Figure 1.3. Inconsistent seasonal transformations across biotopic and niche axes precludes effective niche tracking and niche switching. Each panel illustrates the vertical gradient (y-axis) in niche value (color intensity) across the course of a year (x-axis). The left column of panels represents an historic climate regime, while the right column represents novel climatic conditions. Each row represents a different niche axis which may be tracked or differentially prioritized. Grey contour lines indicate an arbitrary threshold value within niche space that migrants seek out. For Niche 1, novel conditions lead to a more synchronous season across biotopic space. A tracking migrant may have historically migrated vertically to follow the spatiotemporal progression of Niche Variable 1, but under novel conditions more synchronous emergence of threshold niche access may reduce incentives to relocate in a coherent vertical pattern. For Niches 2 and 3, an advance in the timing of Niche 2 relative to Niche 3 leads to a temporal window where suitable space is not available along either niche axis under novel conditions (delineated with orange dashed lines). If a niche switcher depends on the historical synchrony of senescence in Niche Variable 2 and emergence of Niche Variable 3 during its migration, inconsistent change in the onset and termination of these factors will disrupt the pattern of environmental variation under which migration was adaptive.

Box 1.1. Seasonal variation is not universally predictable in landscapes of relief.

Migration is an adaptive life history strategy when seasonal variation follows a predictable schedule (high "contingency"; Colwell 1974, Shaw and Couzin 2013, Riotte-Lambert and Matthiopoulos 2020). In mountain and coastal regions, contingency of a given factor may vary across space (a). For example, although snow cover is highly contingent in the northern Canadian Rocky Mountains, reliable seasonal cycles are diminished toward the south (NDSI, a). However, seasonal variation may become more or less predictable over time (b) as factors individually respond to cascading effects of climate change. For example, sea surface temperature variation in numerous areas throughout the Malay Archipelago became less predictable in the 2010's compared to the 2000's, but the same pattern was not observed for chlorophyll concentration. In (a), contingency was calculated following Colwell (1974) for MODIS Terra NDVI and NDSI, and MODIS Aqua L3SMI Chlorophyll a and Sea surface temperature products aggregated to 10km pixel resolution. In (b), contingency of each factor during 2010-2019 was compared against contingency during 2000-2009 to identify change, with |ΔContingency | < 0.025 considered "Negligible."
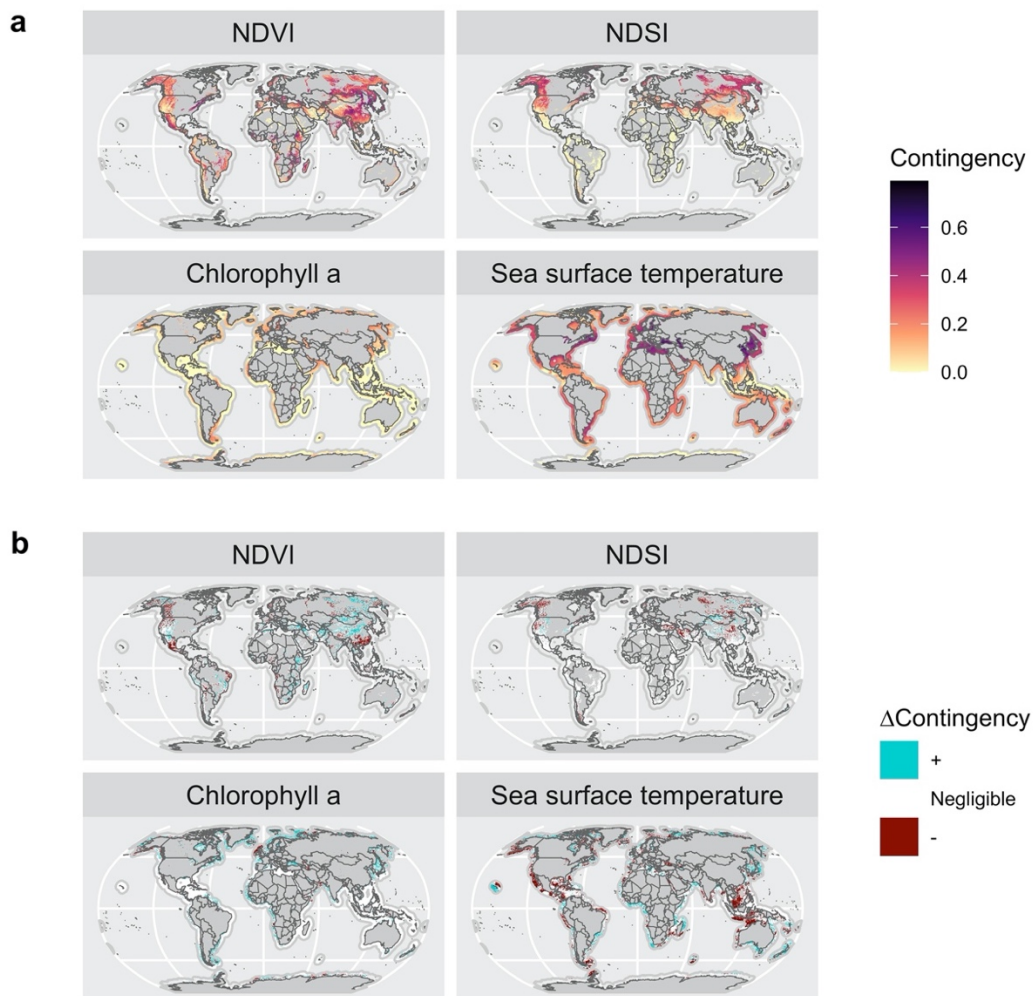
References

Aguzzi, J. et al. 2013. Seasonal bathymetric migrations of deep-sea fishes and decapod
    crustaceans in the NW Mediterranean Sea. - Prog. Oceanogr. 118: 210–221.
Aikens, E. O. et al. 2020. Wave-like Patterns of Plant Phenology Determine Ungulate Movement
    Tactics. - Curr. Biol.: S0960982220308484.
Albon, S. D. and Langvatn, R. 1992. Plant Phenology and the Benefits of Migration in a
    Temperate Ungulate. - Oikos 65: 502–513.
Alerstam, T. et al. 2003. Long-Distance Migration: Evolution and Determinants. - Oikos 103:
    247–260.
Amante, C. and Eakins, B. W. 2009. ETOPO1 1 Arc-Minute Global Relief Model: Procedures,
    Data Sources and Analysis NESDIS NGDC-24. - National Geophysical Data Center.
Amorim, E. et al. 2016. Immigration and early life stages recruitment of the European flounder
    (Platichthys flesus) to an estuarine nursery: The influence of environmental factors. - J.
    Sea Res. 107: 56–66.
Aryal, S. et al. 2016. Perceived changes in climatic variables and impacts on the transhumance
    system in the Himalayas. - Clim. Dev. 8: 435–446.
Assunção, V. A. et al. 2014. Floristics and Reproductive Phenology of Trees and Bushes in
    Central West Brazil. - An. Acad. Bras. Ciênc. 86: 785–800.
Bay, R. A. et al. 2021. Genetic variation reveals individual-level climate tracking across the
    annual cycle of a migratory bird. - Ecol. Lett. in press.
Beck, L. 1991. Nomad: A Year in the Life of a Qashqa'i Tribesman in Iran. - University of
    California Press.
Bigford, T. E. 1979. Synopsis of biological data on the rock crab, Cancer irroratus Say | Scientific
    Publications Office. - U.S. Department of Commerce, National Oceanic and Atmospheric
    Administration, National Marine Fisheries Service.
BirdLife International 2017. Anthreptes rubritorques. The IUCN Red List of Threatened Species
    2017: e.T22717663A118905827. - IUCN Red List Threat. Species
Blake, S. et al. 2013. Vegetation dynamics drive segregation by body size in Galapagos tortoises
    migrating across altitudinal gradients. - J. Anim. Ecol. 82: 310–321.
Boyle, W. A. 2008. Can variation in risk of nest predation explain altitudinal migration in tropical
    birds? - Oecologia 155: 397–403.
Boyle, W. A. 2017. Altitudinal bird migration in North America. - The Auk 134: 443–465.
Boyle, W. A. et al. 2010. Storms drive altitudinal migration in a tropical bird. - Proc. R. Soc. Lond.
    B Biol. Sci.: rspb20100344.
Brambilla, M. and Rubolini, D. 2009. Intra-seasonal changes in distribution and habitat
    associations of a multi-brooded bird species: implications for conservation planning. -
    Anim. Conserv. 12: 71–77.
Brown, A. and Thatje, S. 2011. Respiratory Response of the Deep-Sea Amphipod Stephonyx
    biscayensis Indicates Bathymetric Range Limitation by Temperature and Hydrostatic
    Pressure. - PLOS ONE 6: e28562.
Brown, A. and Thatje, S. 2015. The effects of changing climate on faunal depth distributions
    determine winners and losers. - Glob. Change Biol. 21: 173–180.

Brown, A. et al. 2017. Metabolic costs imposed by hydrostatic pressure constrain bathymetric range in the lithodid crab Lithodes maja. - J. Exp. Biol.: 11.

Buchanan, G. M. et al. 2011. Identifying Priority Areas for Conservation: A Global Assessment for Forest-Dependent Birds. - PLOS ONE 6: e29080.

Burgess, N. D. and Mlingwa, C. O. F. 2000. Evidence for altitudinal migration of forest birds between montane Eastern Arc and lowland forests in East Africa. - Ostrich 71: 184–190.

Burkepile, D. E. et al. 2020. Shared Insights across the Ecology of Coral Reefs and African Savannas: Are Parrotfish Wet Wildebeest? - BioScience 70: 647–658.

Capotondi, A. et al. 2012. Enhanced upper ocean stratification with climate change in the CMIP3 models. - J. Geophys. Res. Oceans in press.

Carney, R. 2005. Zonation of deep biota on continental margins. - In: Oceanography and Marine Biology: An Annual Review. pp. 211–278.

Ceresa, F. et al. 2020. Within-season movements of Alpine songbird distributions are driven by fine-scale environmental characteristics. - Sci. Rep. 10: 5747.

Champion, C. et al. 2018. Rapid shifts in distribution and high-latitude persistence of oceanographic habitat revealed using citizen science data from a climate change hotspot. - Glob. Change Biol. 24: 5440–5453.

Chapman, B. B. et al. 2011. The ecology and evolution of partial migration. - Oikos 120: 1764–1775.

Cleland, E. E. et al. 2007. Shifting plant phenology in response to global change. - Trends Ecol. Evol. 22: 357–365.

Colwell, R. K. 1974. Predictability, Constancy, and Contingency of Periodic Phenomena. - Ecology 55: 1148–1153.

Colwell, R. K. and Rangel, T. F. 2009. Hutchinson's duality: The once and future niche. - Proc. Natl. Acad. Sci. 106: 19651–19658.

Cooper, R. A. and Uzmann, J. R. 1971. Migrations and Growth of Deep-Sea Lobsters, Homarus americanus. - Science 171: 288–290.

Costello, M. J. et al. 2010. Surface Area and the Seabed Area, Volume, Depth, Slope, and Topographic Variation for the World's Seas, Oceans, and Countries. - Environ. Sci. Technol. 44: 8821–8828.

Crawford, J. A. and Pelren, E. C. 2001. Blue grouse winter movements, habitat, and survival in northeastern Oregon. in press.

Croll, D. A. et al. 2005. From wind to whales: trophic links in a coastal upwelling system. - Mar. Ecol. Prog. Ser. 289: 117–130.

Crossin, G. T. et al. 1998. Behavioral thermoregulation in the American lobster Homarus americanus. - J. Exp. Biol. 201: 365–374.

Delcroix, T. and Hénin, C. 1991. Seasonal and interannual variations of sea surface salinity in the tropical Pacific Ocean. - J. Geophys. Res. Oceans 96: 22135–22150.

Dennison, W. C. 1987. Effects of light on seagrass photosynthesis, growth and depth distribution. - Aquat. Bot. 27: 15–26.

Deutsch, C. et al. 2015. Climate change tightens a metabolic constraint on marine habitats. - Science 348: 1132–1135.

Dingle, H. and Drake, V. A. 2007. What Is Migration? - BioScience 57: 113–121.

Doi, W. et al. 2016. Larval Release and Associated Tree-Climbing Behavior of the Land Hermit Crab Coenobita Violascens (Anomura: Coenobitidae). - J. Crustac. Biol. 36: 279–286.

Elliott, M. et al. 2007. The guild approach to categorizing estuarine fish assemblages: a global review. - Fish Fish. 8: 241–268.

Elsen, P. R. and Tingley, M. W. 2015. Global mountain topography and the fate of montane species under climate change. - Nat. Clim. Change 5: 772–776.

French, S. P. et al. 1994. Grizzly Bear Use of Army Cutworm Moths in the Yellowstone Ecosystem. - Bears Their Biol. Manag. 9: 389–399.

Frey, S. J. K. et al. 2016. Microclimate predicts within-season distribution dynamics of montane forest birds. - Divers. Distrib. 22: 944–959.

Geroy, I. J. et al. 2011. Aspect influences on soil water retention and storage. - Hydrol. Process. 25: 3836–3842.

Gómez, J. M. 1993. Phenotypic Selection on Flowering Synchrony in a High Mountain Plant, Hormathophylla Spinosa (Cruciferae). - J. Ecol. 81: 605–613.

Gómez, C. et al. 2016. Niche-tracking migrants and niche-switching residents: evolution of climatic niches in New World warblers (Parulidae). - Proc. Biol. Sci. in press.

Grachev, Y. A. 1976. Distribution and quantity of brown bears in Kazakhstan. - IUCN Publ. New Ser. IUCN

Griffiths, R. P. et al. 2009. The effects of topography on forest soil characteristics in the Oregon Cascade Mountains (USA): Implications for the effects of climate change on soil properties. - For. Ecol. Manag. 257: 1–7.

Hahn, T. P. et al. 2004. Facultative Altitudinal Movements by Mountain White-Crowned Sparrows (Zonotrichia Leucophrys Oriantha) in the Sierra Nevada. - The Auk 121: 1269–1281.

Hall, J. et al. 2009. Conservation implications of deforestation across an elevational gradient in the Eastern Arc Mountains, Tanzania. - Biol. Conserv. 142: 2510–2521.

Hammond, J. C. et al. 2018. Global snow zone maps and trends in snow persistence 2001–2016. - Int. J. Climatol. 38: 4369–4383.

Hansen, M. C. et al. 2013. High-Resolution Global Maps of 21st-Century Forest Cover Change. - Science 342: 850–853.

Haroldson, M. A. et al. 2002. Grizzly Bear Denning Chronology and Movements in the Greater Yellowstone Ecosystem. - Ursus 13: 29–37.

Hock, R. et al. 2019. High Mountain Areas. - In: IPCC Special Report on the Ocean and Cryosphere in a Changing Climate [H.-O. Pörtner, D.C. Roberts, V. Masson-Delmotte, P. Zhai, M. Tignor, E. Poloczanska, K. Mintenbeck, A. Alegría, M. Nicolai, A. Okem, J. Petzold, B. Rama, N.M. Weyer (eds.)]. in press.

Hopkins, A. D. 1920. The Bioclimatic Law. - J. Wash. Acad. Sci. 10: 34–40.

Horvath, E. G. and Sullivan, K. A. 1988. Facultative Migration in Yellow-Eyed Juncos. - The Condor 90: 482–484.

Hsiung, A. C. et al. 2018. Altitudinal migration: ecological drivers, knowledge gaps, and conservation implications. - Biol. Rev. 93: 2049–2070.

Hunt, J. H. et al. 1999. Dry Season Migration by Costa Rican Lowland Paper Wasps to High Elevation Cold Dormancy Sites. - Biotropica 31: 192–196.

Huthnance, J. M. 1995. Circulation, exchange and water masses at the ocean margin: the role of physical processes at the shelf edge. - Prog. Oceanogr. 35: 353–431.

Inouye, D. W. et al. 2000. Climate change is affecting altitudinal migrants and hibernating species. - Proc. Natl. Acad. Sci. 97: 1630–1633.

Jackson, M. 1966. Effects of Microclimate on Spring Flowering Phenology. - Ecology 47: 407–415.

Jakoby, O. et al. 2019. Climate change alters elevational phenology patterns of the European spruce bark beetle (Ips typographus). - Glob. Change Biol. 25: 4048–4063.

Janzen, D. H. 1967. Why Mountain Passes are Higher in the Tropics. - Am. Nat. 101: 233–249.

Janzen, D. 2004. Ecology of dry-forest wildland insects in the Area de Conservación Guanacaste. - In: Biodiversity Conservation in Costa RicaLearning the Lessons in a Seasonal Dry Forest. University of California Press, in press.

Johnson, C. R. et al. 2011. Climate change cascades: Shifts in oceanography, species' ranges and subtidal marine community dynamics in eastern Tasmania. - J. Exp. Mar. Biol. Ecol. 400: 17–32.

Karagulle, D. et al. 2017. Modeling global Hammond landform regions from 250-m elevation data. - Trans. GIS 21: 1040–1060.

Kerby, J. and Post, E. 2013. Capital and income breeding traits differentiate trophic match–mismatch dynamics in large herbivores. - Philos. Trans. R. Soc. B Biol. Sci. 368: 20120484.

Kim, D.-H. et al. 2015. Accelerated deforestation in the humid tropics from the 1990s to the 2000s. - Geophys. Res. Lett. 42: 3495–3501.

Klemp, S. 2003. Altitudinal dispersal within the breeding season in the Grey Wagtail Motacilla cinerea. - Ibis 145: 509–511.

Klinges, D. H. and Scheffers, B. R. 2020. Microgeography, Not Just Latitude, Drives Climate Overlap on Mountains from Tropical to Polar Ecosystems. - Am. Nat. 197: 75–92.

Körner, C. 2004. Mountain Biodiversity, Its Causes and Function. - AMBIO J. Hum. Environ. 33: 11–17.

Körner, C. 2007. The use of 'altitude' in ecological research. - Trends Ecol. Evol. 22: 569–574.

Körner, C. and Paulsen, J. 2004. A world-wide study of high altitude treeline temperatures. - J. Biogeogr. 31: 713–732.

Lapp, S. et al. 2005. Climate warming impacts on snowpack accumulation in an alpine watershed. - Int. J. Climatol. 25: 521–536.

Largier, J. L. 2020. Upwelling Bays: How Coastal Upwelling Controls Circulation, Habitat, and Productivity in Bays. - Annu. Rev. Mar. Sci. 12: 415–447.

Laube, I. et al. 2015. Niche availability in space and time: migration in Sylvia warblers. - J. Biogeogr. 42: 1896–1906.

Loiselle, B. A. and Blake, J. G. 1991. Temporal Variation in Birds and Fruits Along an Elevational Gradient in Costa Rica. - Ecology 72: 180–193.

MacDiarmid, A. B. 1991. Seasonal changes in depth distribution, sex ratio and size frequency of spiny lobster Jasus edwardsii on a coastal reef in northern New Zealand. - Mar. Ecol. Prog. Ser. 70: 129–141.

Martínez-Meyer, E. et al. 2004. Evolution of seasonal ecological niches in the Passerina buntings (Aves: Cardinalidae). - Proc. Biol. Sci. 271: 1151–1157.

McInturff, A. et al. 2020. Fence Ecology: Frameworks for Understanding the Ecological Effects of Fences. - BioScience 70: 971–985.

Merkle, J. A. et al. 2016. Large herbivores surf waves of green-up during spring. - Proc R Soc B 283: 20160456.

Middleton, A. D. et al. 2018. Green-wave surfing increases fat gain in a migratory ungulate. - Oikos in press.

Mussehl, T. W. 1960. Blue Grouse Production, Movements, and Populations in the Bridger Mountains, Montana. - J. Wildl. Manag. 24: 60–68.

Mysterud, A. et al. 2001. Plant Phenology, Migration and Geographical Variation in Body Weight of a Large Herbivore: The Effect of a Variable Topography. - J. Anim. Ecol. 70: 915–923.

Nelson, R. A. et al. 1983. Behavior, Biochemistry, and Hibernation in Black, Grizzly, and Polar Bears. - Bears Their Biol. Manag. 5: 284–290.

Neubaum, D. J. et al. 2006. Autumn Migration and Selection of Rock Crevices as Hibernacula by Big Brown Bats in Colorado. - J. Mammal. 87: 470–479.

Nieves-Rivera, Á. and Williams, E. 2003. Annual migrations and spawning of Coenobita clypeatus (Herbst) on Mona Island (Puerto Rico) and notes on inland crustaceans. - Crustaceana 76: 547–558.

Nio, T. et al. 2019. Seaward migration and larval release of the land hermit crab Coenobita brevimanus Dana, 1852 (Anomura: Coenobitidae) on Iriomote Island, Japan. - Crustac. Res. 48: 67–80.

Paige, C. 2008. A Landowner's Guide to Wildlife Friendly Fences. - Montana Fish, Wildlife, and Parks.

Parmesan, C. 2006. Ecological and evolutionary responses to recent climate change. - In: Annual Review of Ecology Evolution and Systematics. Annual Reviews, pp. 637–669.

Paulmier, A. and Ruiz-Pino, D. 2009. Oxygen minimum zones (OMZs) in the modern ocean. - Prog. Oceanogr. 80: 113–128.

Pecl, G. T. et al. 2009. The east coast Tasmanian rock lobster fishery – vulnerability to climate change impacts and adaptation response options.

Philippart, C. J. M. et al. 2014. Reproductive phenology of coastal marine bivalves in a seasonal environment. - J. Plankton Res. 36: 1512–1527.

Pigeon, G. et al. 2016. Intense selective hunting leads to artificial evolution in horn size. - Evol. Appl. 9: 521–530.

Pinsky, M. L. et al. 2013. Marine Taxa Track Local Climate Velocities. - Science 341: 1239–1242.

Ponti, R. et al. 2020. Seasonal climatic niches diverge in migratory birds. - Ibis 162: 318–330.

Post, E. 2019. Time in Ecology: A Theoretical Framework. - Princeton University Press.

Post, E. and Brodie, J. 2015. Anticipating novel conservation risks of increased human access to remote regions with warming. - Clim. Change Responses 2: 2.

Pruess, K. P. 1967. Migration of the Army Cutworm, Chorizagrotis auxiliaris (Lepidoptera: Noctuidae). I. Evidence for a Migration. - Ann. Entomol. Soc. Am.: 11.

Rehnus, M. and Bollmann, K. 2020. Mountain hares Lepus timidus follow the green-up wave in the pursuit of high-quality food. - Wildl. Biol. in press.

Rehnus, M. et al. 2020. Advancing plant phenology causes an increasing trophic mismatch in an income breeder across a wide elevational range. - Ecosphere 11: e03144.

Rice, C. G. 2008. Seasonal Altitudinal Movements of Mountain Goats. - J. Wildl. Manag. 72: 1706–1716.

Riotte-Lambert, L. and Matthiopoulos, J. 2020. Environmental Predictability as a Cause and Consequence of Animal Movement. - Trends Ecol. Evol. 35: 163–174.

Robertson, C. et al. 2020. Submarine canyons influence macrofaunal diversity and density patterns in the deep-sea benthos. - Deep Sea Res. Part Oceanogr. Res. Pap. 159: 103249.

Sawyer, H. et al. 2013. A framework for understanding semi-permeable barrier effects on migratory ungulates. - J. Appl. Ecol. 50: 68–78.

Servheen, C. 1983. Grizzly Bear Food Habits, Movements, and Habitat Selection in the Mission Mountains, Montana. - J. Wildl. Manag. 47: 1026–1035.

Shadwick, E. H. et al. 2015. Seasonality of biological and physical controls on surface ocean CO2 from hourly observations at the Southern Ocean Time Series site south of Australia. - Glob. Biogeochem. Cycles 29: 223–238.

Shapiro, G. I. et al. 2003. Dense water cascading off the continental shelf. - J. Geophys. Res. Oceans in press.

Shaw, A. K. and Couzin, I. D. 2013. Migration or Residency? The Evolution of Movement Behavior and Information Usage in Seasonal Environments. - Am. Nat. 181: 114–124.

Smith, K. L. et al. 2013. Deep ocean communities impacted by changing climate over 24 y in the abyssal northeast Pacific Ocean. - Proc. Natl. Acad. Sci. 110: 19838–19841.

Somveille, M. et al. 2019. Where the wild birds go: explaining the differences in migratory destinations across terrestrial bird species. - Ecography 42: 225–236.

Spence, A. R. and Tingley, M. W. 2020. The challenge of novel abiotic conditions for species undergoing climate-induced range shifts. - Ecography 43: 1–20.

Spitz, D. B. et al. 2020. Habitat predicts local prevalence of migratory behaviour in an alpine ungulate. - J. Anim. Ecol. 89: 1032–1044.

Sprintall, J. and Cronin, M. F. 2001. Upper Ocean Vertical Structure. - In: Encyclopedia of Ocean Sciences. Elsevier, pp. 3120–3128.

Thompson, P. A. et al. 2015. Precipitation as a driver of phytoplankton ecology in coastal waters: A climatic perspective. - Estuar. Coast. Shelf Sci. 162: 119–129.

Vitasse, Y. et al. 2018. Global warming leads to more uniform spring phenology across elevations. - Proc. Natl. Acad. Sci. 115: 1004–1008.

White, Jr., Don et al. 1998. Grizzly bear feeding activity at alpine army cutworm moth aggregation sites in northwest Montana. - Can. J. Zool. 76: 221–227.

Whittaker, R. H. 1970. Communities and ecosystems. - Communities Ecosyst. in press.

Whittaker, R. H. and Niering, W. A. 1968. Vegetation of the Santa Catalina Mountains, Arizona: IV. Limestone and Acid Soils. - J. Ecol. 56: 523–544.

Winger, B. M. et al. 2019. A long winter for the Red Queen: rethinking the evolution of seasonal migration. - Biol. Rev. 94: 737–752.

Zwickel, F. C. and Bendell, J. F. 2003. Blue Grouse: Their Biology and Natural History. - NRC Research Press.

Chapter 2: drpToolkit: An automated workflow for aligning and analyzing vegetation and ground surface time series imagery

Abstract

1. Analysis of ecological data from digital repeat photography requires consistent image alignment across the time series of data collection. Current open-source methods facilitate the detection of frame shifts, but require manual adjustments by the user to reassign regions of interest when shifts occur.

2. We introduce `drpToolkit`, an open-source Python package that automates data management, image alignment, and data extraction from time series image sets. The toolkit operates on a folder of images and generates an aligned image time series using a user-defined keyframe, and extracts derived greenness and snow indices from user-defined regions of interest.

3. Imagery alignment improves the spatial consistency of repeated measures in an image set. Particularly among small regions of interest, data extracted from aligned imagery reflects observed changes in greenness compared to unaligned imagery.

4. This software simplifies the process of converting raw imagery stored on an SD card to useful ecological data. It automatically refiles imagery using a standardized format used in other applications, increasing the opportunity for cross-study comparisons of

phenology, and collaboration among researchers and agencies to improve

understanding of fine-scale ecological response to climate change.

Keywords

digital repeat photography, open source software, phenology, photogrammetry, time-lapse

photography

Introduction

Remote sensing data inform research and drive policy surrounding conservation of

biodiversity and ecosystem function (Skidmore et al., 2021). Scale gaps in remote sensing data,

such as those arising in measurements of landscape phenology, complicate the problem of

pairing in-situ measurements with coarsely resolved satellite data for modeling and forecasting

effects of climate change (Park et al., 2021). Improvements in the consistency, reliability, and

resolution of remote sensing measurements across scales of detection reduce error accrued

through modeling processes, and refine our understanding of scaling relationships between

individuals, species, communities, and ecosystems.

Digital repeat photography is the iterative measurement of a plot or site using imagery.

Repeated photogrammetric measures are common in ecology, for applications including

phenological monitoring, change detection, and occupancy modeling (Burton et al., 2015;

Crimmins & Crimmins, 2008; Farinotti et al., 2010; Nichols et al., 2016). Temporally constant

image collection protocols ("time-lapse" photography) are a special case of highly controlled

data collection, where imagery is collected on a pre-defined interval. In particular, derived

image bands from time-lapse data are useful for detecting changes in plant greenness and snow

cover at fine scales (Ide & Oguma, 2013; Xie et al., 2018). Although common indices generated

from satellite data (such as the Normalized Difference Vegetation Index, "NDVI" or Normalized

Difference Snow Index, "NDSI") rely on radiometric measurements that are not available on

most consumer-grade cameras, alternative data generated at the ground level can also be

informative about plant growth and snow presence.

Over the course of deployment of a time-lapse camera, variation among image scenes

may result from undesired camera shifting. Thus, a region of interest defined in image

coordinate space will not consistently represent an area of the physical scene unless imagery is

aligned prior to data extraction. Therefore, in order to obtain meaningful data from digital

repeat imagery, regions of interest must be constantly updated to accommodate shifting

scenes, or images must be aligned to a common reference image prior to data extraction.

Data management is an additional bottleneck in analysis of digital repeat photography.

Numerous software pipelines exist for management and analysis of time series imagery, but

most are interactive and require considerable user input (e.g. Niedballa et al., 2016;

Seyednasrollah et al., 2019). Consistent directory structure, file-naming conventions, and

metadata libraries improve not only reproducibility of analysis and results, but also cross-study

comparisons and meta-analyses.

To solve the problem of shifting image scenes due to fine rotations by fixed cameras, we

introduce `drpToolkit`, an open source Python library for estimating image transformations and

aligning imagery from automated time-lapse photography. For vegetation phenology studies,

the tool also estimates vegetation greenness from aligned images. This software facilitates the

data pipeline that connects raw imagery to useful image time series. `drpToolkit` scripts,

installation instructions, and sample data are available at

https://github.com/JepsonNomad/drpToolkit.

Methods

Image alignment

Image alignment can be achieved by solving for the best transformation between sets of keypoint pairs that link two images, a reference image and a novel image. Keypoints are first identified using a feature transform which describes points in image coordinate space. The SIFT feature transform is useful for identifying points in scenes with illumination variability (Lowe, 2004). Because some image regions may contain recurrent structural variation irrelevant to frame shifts and thus may impact alignment, it may be necessary to disqualify certain image regions from keypoint detection. `drpToolkit` combines SIFT features with an optional keypoint mask assigned to the reference image in order to identify a selection of high-quality keypoints in the reference image, and each novel image. Keypoint pairs are then filtered using RANSAC thresholding and Lowe's ratio to identify the best pairs.

`drpToolkit` simplifies the image alignment process by treating image scenes as 2-dimensional surfaces that can be linked by either an affine or homography transformation. Although fewer parameters must be identified for affine transformations, homography (perspective) transformations may improve alignment. After high-quality keypoint pairs are identified, a transformation matrix that describes the relationship between the novel image and reference image is estimated. The novel image can then be warped to align to the reference image by finding the product of novel image pixel coordinates and the transformation matrix.

In this toolkit, we assume that camera orientation among images is highly

autocorrelated, with shifts in the image scene leading to a new temporarily stable orientation.

Further, the transformation matrix is sequentially estimated across a time series of imagery.

This approach has two benefits: First, if too few keypoint pairs are detected to generate a

reliable transformation matrix, the algorithm can default to the last estimated transformation

matrix. Similarly, if keypoint pairs are detected but the estimated transformation matrix would

produce a highly warped image (e.g. if the determinant of the matrix is different from 1), the

algorithm can default to the last reasonable transformation matrix.

Derived image indices

Digital repeat photography is commonly employed for monitoring plant and snow

phenology (Ide & Oguma, 2013; Xie et al., 2018). The Normalized Difference Vegetation Index

(NDVI) and Normalized Difference Snow Index (NDSI) are two derived image bands that are

commonly used as proxies for vegetation rigor and snow presence, respectively. Calculation of

both of these indices requires a measurement of nonvisible wavelengths, which are available

on most publicly accessible satellite imagery. However, because standard consumer-grade

cameras do not produce imagery with nonvisible wavelengths, alternative approaches to NDVI

and NDSI are required. The Green Chromatic Coordinate (GCC) is a measure of relative

greenness in an image, and may be useful even under variable lighting conditions (Reid et al.,

2016). GCC is calculated using equation 1:

GCC = (G) / (R + G + B)   [1]

where R, G, and B are the values of red, green, and blue color channels, respectively. Whereas NDSI is calculated using the mid infrared band, an alternative approach allows digital camera operators to bypass that requirement by identifying the brightness of a pixel or image region relative to the total image (Hinkler et al., 2002). This generates a replacement infrared band (MIRrep), which can be substituted in to calculate a pseudo-NDSI based on RGB imagery (rgbNDSI) using equation 2:

rgbNDSI = (RGB - MIRrep) / (RGB + MIRrep)   [2]

where RGB is the mean value of red, green, and blue color channels for each image pixel. We found that at fine plot scales, lighting variation in the image scene often leads to an unacceptable rate of high rgbNDSI values in imagery with little or no snow. This stands in contrast to its utility for broader scenes (Buus-Hinkler et al., 2006; Fedorov et al., 2016). Because digital repeat photography is useful across multiple scales of inquiry, we include the rgbNDSI functionality in `drpToolkit` but caution users to closely inspect these results.

Example workflow

A typical workflow for digital repeat photography data management and data extraction will follow a scheme of: prepare imagery, align photos, and extract data (Figure 2.1). Because `drpToolkit` is modular, its three main workflow components can be called from the command line, or individual module functions can be called independently using Python. Here, we describe an example workflow for a year of imagery collected at one plot. Documentation is available for each module and can be accessed using (e.g.):

```
python3 prep.py --help
```

All imagery should contain valid EXIF metadata and be contained in a single folder. The toolkit avoids removing intermediate datasets, so users should be aware that running `drpToolkit` modules will use a comparable amount of storage as the folders of imagery with which they are working. Consumer-grade cameras frequently use uninformative filename conventions and multiple cameras may use identical filenames. Therefore, in the first step, imagery is copied from an existing directory (-i) to a new subdirectory, and renamed according to camera site and plot, and image timestamp information, following the conventions of the PhenoCam dataset (Richardson et al., 2018). In the following command line call, `drpToolkit` identifies imagery in the "data/img" directory (-i). These images can be cropped and resized using optional flags. Finally, renamed imagery is saved in a subdirectory defined by the -o flag.

```
python3 prep.py -i data/img -o prepped
```

Next, a directory of imagery (-i) is aligned to a common reference image (keyframe; -k). Each image is automatically loaded in sequence, the best transformation matrix is identified, and the image is remapped using that matrix and stored in the output directory (-o). A summary table with transformation matrix elements is stored in the output directory along with the aligned images, with the name "transTable.csv". By default, the transformation model is Homography. Users may wish to override this using the optional --transModel flag. Default parameters for RANSAC reprojection threshold and Lowe's ratio may also be overridden using the --rRT and --lRT flags.

```
python3 align.py -i data/img/prepped -k data/img/prepped/GB-
03_2018_08_14_120000.JPG -o aligned
```

Finally, GCC and rgbNDSI are calculated and extracted from each image in a directory (-i). If desired, indices can be extracted within a selection of regions of interest (optional -r flag). If no -r flag is included, the function will extract GCC and rgbNDSI for the entire image. Because use of the `align.py` module in advance of `extract.py` may lead to loss of representation by some regions of interest (Figure 2.2), the algorithm also summarizes the number of pixels in each region and the number of non-zero pixels in each region, for each image measurement.

```
python3 extract.py -i data/img/prepped/aligned -r
data/roi/ROIs.csv
```

If desired, a panelized series of summary images can be generated for inspection of results. Although not part of the data pipeline, we advocate for inspecting results before moving on to downstream analyses.

```
python3 panelize.py -i data/img/ prepped/aligned -t extract.csv
-r data/roi/ROIs.csv
```

Users should note that the data generated through this pipeline are raw values, and further processing will be required depending on the end goal of the study. For example, in some phenology applications, a 90th percentile moving window may reduce variation introduced by day-to-day variation in scene illumination (Sonnentag et al., 2012). However, many post-

alignment analytical methods are already widely available, such as the Python package

`vegindex` (Milliman, 2017/2021).

Limitations, solutions, and alternative approaches

Geometric constraints

This workflow assumes that the camera sensor did not move in geographical space, and

only shifts about its core in the three rotational axes of yaw, pitch, and roll. Complete loss of

scene overlap due to camera rotation will make alignment impossible. The degree of acceptable

overlap depends on the camera's angle of view and the distance from focal subject. Wide-angle

and fisheye lenses have increased radial distortion, leading to difficulty in identifying an

appropriate image transformation. Internal image distortion will also produce invalid results if

imagery is collected at a shallow angle with an extreme depth of field.

If the rotation of a camera results in only slight overlap across images, the calculated

homography is not likely to produce a realistic image. Significant shifts of the camera position

resulting in parallax within the dataset should also be avoided. In all of the above cases, it

would be inappropriate to use the `drpToolkit` workflow, necessitating more sophisticated

approaches with camera calibration and internal image geometry. For instance, the program

Hugin (http://hugin.sourceforge.net/) aligns images on the surface of a sphere to account for

camera calibration (rather than a plane as is the case with `drpToolkit`), however additional

manual intervention and computational requirements may be necessary in that environment.

Temporal considerations

The software was designed specifically to process time-lapse imagery, but it may be useful for some motion-triggered datasets as well. However, the keypoint matching algorithm does rely on some degree of consistency across images, which may not be met if photos are collected during both daytime and nighttime. Thus, camera trap datasets that include both daytime and nighttime images will be difficult to align using this algorithm. A solution to this issue is to split such datasets into a diurnal and nocturnal image set, identify a representative photo in both sets that are from matching camera orientations, and calculate homography for both sets separately.

Computational factors

Keypoint identification and homography estimation are computationally expensive tasks, and may be slow on some machines. We found that resizing imagery to smaller files was useful for speeding up the process of alignment and data extraction, but for our plot-scale imagery aggregation to ½ resolution imagery was not detrimental to our analyses. If the finest resolution imagery must be used, alignment and data extraction may use considerable computer resources. On a 2019 Macbook Pro with 16GB memory and 2.8 GHz Quad-Core Intel Core i7 processor, `prep.py` ran for about 1 minute, `align.py` for about 15 minutes, and `extract.py` about 3.5 minutes for a folder of 365 images.

Conclusions

Here, we presented a new open-source toolkit for preparing and aligning imagery generated through digital repeat photography, and for extracting ecologically relevant data

from that imagery. Alignment of images is a crucial step in the repeat photography workflow,

and treating unaligned photos as perfect repeated measures impacts the validity of

measurements in time-lapse studies. Although future work may improve measures of variation

in snow presence and vegetation rigor, our toolkit simplifies the data pipeline from images to

analysis-ready data for researchers, resource managers, and conservationists alike.
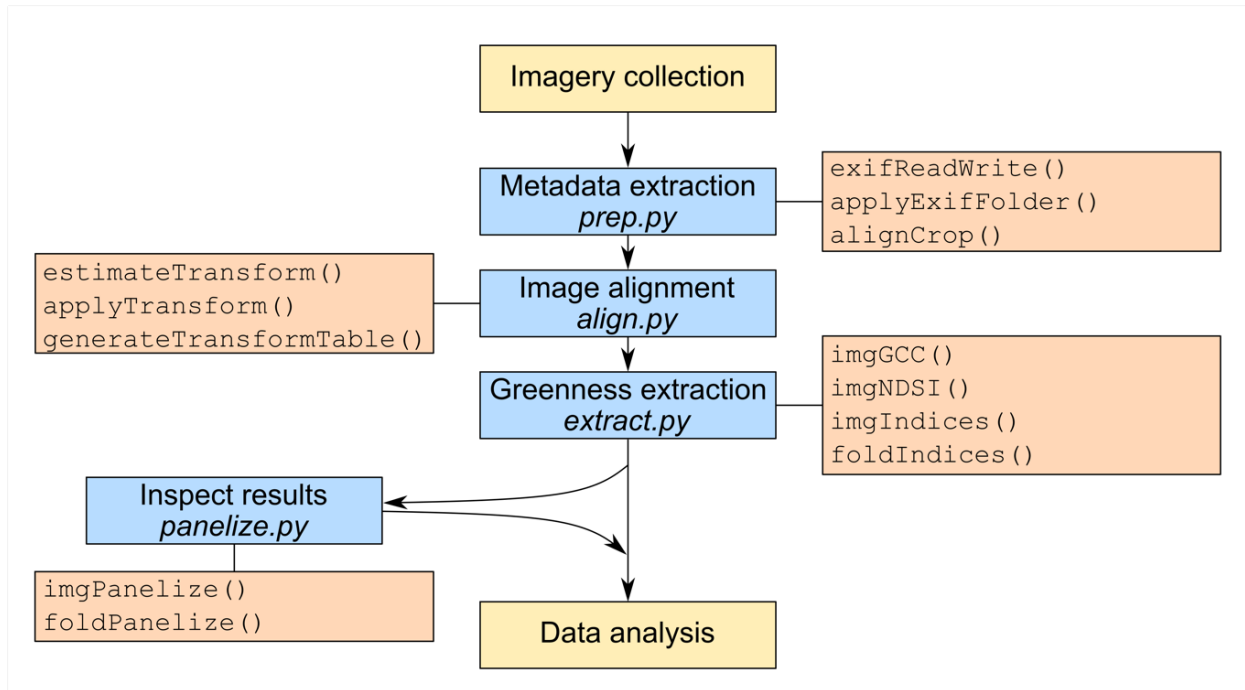
Figures

Figure 2.1. The `drpToolkit` workflow. The command-line interface (workflow steps and command line functions in blue boxes) operates at the folder level, however image-level functionality is available in the Python library (library functions in orange boxes).
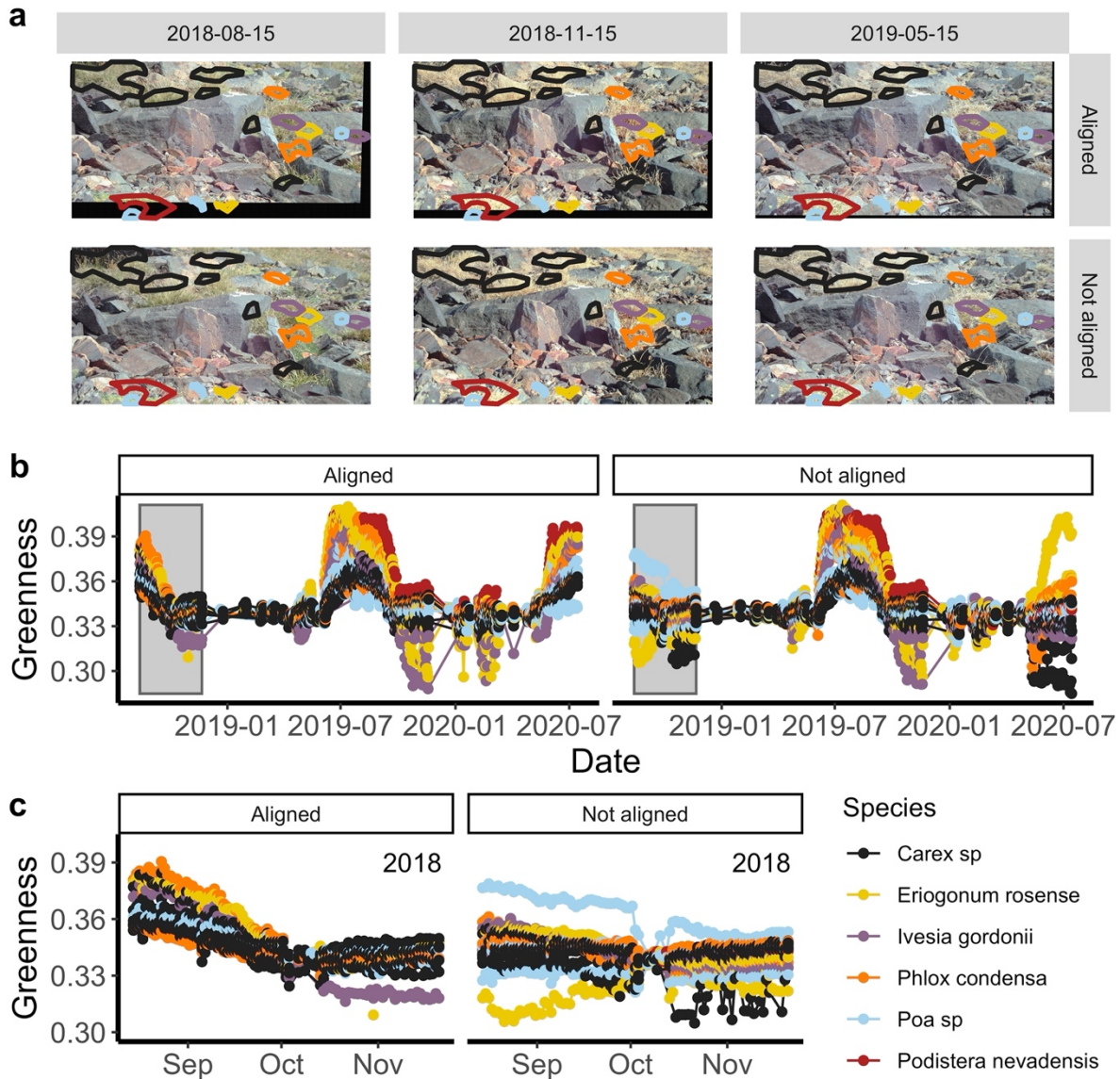
Figure 2.2. Comparison of ROI positioning in aligned and unaligned imagery. Constant ROI assignment across a time series of aligned imagery (a, top row) yields consistent measures in space. Constant ROI assignment across a time series of unaligned imagery (a, bottom row) leads to inconsistent measures in space. Derived image indices such as GCC (b) are sensitive to shifts in camera orientation if imagery is not aligned. For example, autumn browning in 2018 (b, grey window, and emphasized as a temporal subset in c) is not detected for most ROIs in unaligned imagery due to invalid ROI designation.

References

Burton, A. C., Neilson, E., Moreira, D., Ladle, A., Steenweg, R., Fisher, J. T., Bayne, E., & Boutin, S. (2015). REVIEW: Wildlife camera trapping: a review and recommendations for linking surveys to ecological processes. Journal of Applied Ecology, 52(3), 675–685. https://doi.org/10.1111/1365-2664.12432

Buus-Hinkler, J., Hansen, B. U., Tamstorf, M. P., & Pedersen, S. B. (2006). Snow-vegetation relations in a High Arctic ecosystem: Inter-annual variability inferred from new monitoring and modeling concepts. Remote Sensing of Environment, 105(3), 237–247. https://doi.org/10.1016/j.rse.2006.06.016

Crimmins, M. A., & Crimmins, T. M. (2008). Monitoring Plant Phenology Using Digital Repeat Photography. Environmental Management, 41(6), 949–958. https://doi.org/10.1007/s00267-008-9086-6

Farinotti, D., Magnusson, J., Huss, M., & Bauder, A. (2010). Snow accumulation distribution inferred from time-lapse photography and simple modelling. Hydrological Processes, 24(15), 2087–2097. https://doi.org/10.1002/hyp.7629

Fedorov, R., Camerada, A., Fraternali, P., & Tagliasacchi, M. (2016). Estimating Snow Cover From Publicly Available Images. IEEE Transactions on Multimedia, 18(6), 1187–1200. https://doi.org/10.1109/TMM.2016.2535356

Hinkler, J., Pedersen, S. B., Rasch, M., & Hansen, B. U. (2002). Automatic snow cover monitoring at high temporal and spatial resolution, using images taken by a standard digital camera. International Journal of Remote Sensing, 23(21), 4669–4682. https://doi.org/10.1080/01431160110113881

Ide, R., & Oguma, H. (2013). A cost-effective monitoring method using digital time-lapse cameras for detecting temporal and spatial variations of snowmelt and vegetation phenology in alpine ecosystems. Ecological Informatics, 16, 25–34. https://doi.org/10.1016/j.ecoinf.2013.04.003

Lowe, D. G. (2004). Distinctive Image Features from Scale-Invariant Keypoints. International Journal of Computer Vision, 60(2), 91–110. https://doi.org/10.1023/B:VISI.0000029664.99615.94

Milliman, T. (2021). Tmilliman/python-vegindex [Python]. https://github.com/tmilliman/python-vegindex (Original work published 2017)

Nichols, M. H., Nearing, M., Hernandez, M., & Polyakov, V. O. (2016). Monitoring channel head erosion processes in response to an artificially induced abrupt base level change using time-lapse photography. Geomorphology, 265, 107–116. https://doi.org/10.1016/j.geomorph.2016.05.001

Niedballa, J., Sollmann, R., Courtiol, A., & Wilting, A. (2016). camtrapR: An R package for efficient camera trap data management. Methods in Ecology and Evolution, 7(12), 1457–1462. https://doi.org/10.1111/2041-210X.12600

Park, D. S., Newman, E. A., & Breckheimer, I. K. (2021). Scale gaps in landscape phenology: Challenges and opportunities. Trends in Ecology & Evolution. https://doi.org/10.1016/j.tree.2021.04.008

Reid, A. M., Chapman, W. K., Prescott, C. E., & Nijland, W. (2016). Using excess greenness and green chromatic coordinate colour indices from aerial images to assess lodgepole pine

vigour, mortality and disease occurrence. Forest Ecology and Management, 374, 146–153. https://doi.org/10.1016/j.foreco.2016.05.006

Richardson, A. D., Hufkens, K., Milliman, T., Aubrecht, D. M., Chen, M., Gray, J. M., Johnston, M. R., Keenan, T. F., Klosterman, S. T., Kosmala, M., Melaas, E. K., Friedl, M. A., & Frolking, S. (2018). Tracking vegetation phenology across diverse North American biomes using PhenoCam imagery. Scientific Data, 5(1), 180028. https://doi.org/10.1038/sdata.2018.28

Seyednasrollah, B., Milliman, T., & Richardson, A. D. (2019). Data extraction from digital repeat photography using xROI: An interactive framework to facilitate the process. ISPRS Journal of Photogrammetry and Remote Sensing, 152, 132–144. https://doi.org/10.1016/j.isprsjprs.2019.04.009

Skidmore, A. K., Coops, N. C., Neinavaz, E., Ali, A., Schaepman, M. E., Paganini, M., Kissling, W. D., Vihervaara, P., Darvishzadeh, R., Feilhauer, H., Fernandez, M., Fernández, N., Gorelick, N., Geizendorffer, I., Heiden, U., Heurich, M., Hobern, D., Holzwarth, S., Muller-Karger, F. E., … Wingate, V. (2021). Priority list of biodiversity metrics to observe from space. Nature Ecology & Evolution, 1–11. https://doi.org/10.1038/s41559-021-01451-x

Sonnentag, O., Hufkens, K., Teshera-Sterne, C., Young, A. M., Friedl, M., Braswell, B. H., Milliman, T., O'Keefe, J., & Richardson, A. D. (2012). Digital repeat photography for phenological research in forest ecosystems. Agricultural and Forest Meteorology, 152, 159–177. https://doi.org/10.1016/j.agrformet.2011.09.009

Xie, Y., Civco, D. L., & Silander, J. A. (2018). Species-specific spring and autumn leaf phenology captured by time-lapse digital cameras. Ecosphere, 9(1), e02089. https://doi.org/10.1002/ecs2.2089

Chapter 3: Consistency in spring landscape phenology revealed through time-lapse imagery: implications for conservation and management of an endangered migratory herbivore

Abstract

Climate change modifies plant phenology through shifts in seasonal temperature and precipitation. Because the timing of plant growth can limit herbivore population dynamics, climatic alteration of historical patterns of vegetation seasonality may alter population trajectories in such taxa. Spatial patterns in the seasonal onset and progression of plant growth timing may mediate effects of climate change on herbivore populations, either by extending or contracting the available window of foraging opportunities. Thus, sound management decisions may depend on understanding how plant growth varies across a landscape within and among distinct management units or protected areas. Yet, it is difficult to study patterns in plant phenology at a scale relevant to large herbivores, which may prefer certain forage species, move between disparate seasonal ranges, and potentially require management actions such as translocation to achieve conservation goals. Here, we examine spatial variation in the timing of spring plant growth, measured using a network of automated time-lapse cameras distributed across the range of endangered Sierra Nevada bighorn sheep (*Ovis canadensis sierrae*) in California, USA. We measured the elevational lapse rate in the timing of spring plant growth across distinct management units of Sierra bighorn. Daily time-lapse imagery revealed consistent variation in green-up timing across elevation, both among latitudinal zones and among individual plant species. Green-up timing was earlier in 2020 than in 2019, reflecting differences in the end of the snowy season. Because bighorn forage seasonally on alpine

species with a brief growing period, spring migration of bighorn may be linked to variation in snowmelt and plant growth across elevational gradients.

Keywords

Endangered species, remote sensing, digital repeat photography, phenology, migration, climate change

Introduction

Climate change drives shifts in the timing of plant growth (Walther et al. 2002, Cleland et al. 2007, Vitasse et al. 2022), but plant response to changing temperature and precipitation regimes is complex (Primack et al. 2009, Post et al. 2016, Rafferty et al. 2020) and phenological variation at fine scales may not translate to landscape-scale patterns (Piao et al. 2019, Park et al. 2021). Montane settings generate extreme ecoclimatic variation across a narrow geographical range (Körner 2007, Klinges and Scheffers 2020), leading to local variation in the timing of plant growth (Hopkins 1920; Richardson et al. 2019). Such variation is important for herbivores if they rely on tracking high-quality resources or switching between habitat types to fulfill annual life history requirements (John and Post 2022). Yet, climate change stands to disrupt historical patterns of vegetation phenology across mountain slopes (Shen et al. 2014, Vitasse et al. 2018, Misra et al. 2021).

Large herbivores can prolong the seasonal duration of access to high-quality forage by coordinating movements with spatiotemporal variation in plant growth onset and senescence (Albon and Langvatn 1992, Bischof et al. 2012, Kauffman et al. 2021). For many ungulates, seasonal movements typified by, for example, migration, are adaptive when plant growth

progresses predictably across spatial gradients (Teitelbaum and Mueller 2019, Aikens et al.

2020b, Abraham et al. 2022). Climate-induced change to spatial patterns of spring plant growth

can drive variation in herbivore movement (Rickbeil et al. 2019, Aikens et al. 2020a) and even

reproductive success (Post et al. 2008). Spatial variation in spring plant growth thus mediates

effects of climate change on herbivore populations, either by extending or contracting the

available window of foraging opportunities.

Because herbivores track vegetation over large scales, sound conservation planning for

herbivores depends on understanding how plant growth varies across landscapes (Morellato et

al. 2016). Management of migrants requires adequate protection of seasonal ranges and their

connections (Martin et al. 2007, Runge et al. 2015), so a crucial aspect of wildlife conservation

and management is identifying drivers, patterns and limitations on animal movements (Barton

et al. 2015, Allen and Singh 2016). The seasonal and sometimes unpredictable movements of

migratory and nomadic species make such connections particularly enigmatic (Runge et al.

2014). One such species, the Sierra Nevada bighorn sheep ("Sierra bighorn," *Ovis canadensis*

sierrae), is an endangered alpine specialist endemic to the Sierra Nevada mountains of

California, USA (Figure 3.1; U.S. Fish and Wildlife Service 2007). Sierra bighorn undertake a

partial, facultative altitudinal migration along an elevational gradient that approaches 3000m

(Spitz et al. 2020). Because migration and lambing in Sierra bighorn is roughly coincident with

the annual season of snowmelt and plant green-up, variation in the timing and spatial

progression of plant growth may be especially important for their movement and persistence.

Studies of plant phenology in mountain systems are made especially difficult due to variable vegetation cover. Although lower slopes may feature dense forests, alpine peaks are often only sparsely populated by small plants (Körner 2004). In areas where vegetation cover is less dense, the relative coverage of plant material is lower, and consequently plants are proportionately less represented in satellite measurements. However, barren and herbaceous alpine regions are especially important for bighorn sheep, which rely on keen eyesight and unobstructed vision to avoid predators while foraging on sparse vegetation (Geist 1974). Therefore, in order to understand the importance of plant phenology for the foraging ecology of bighorn sheep (and alpine ungulates more generally), alternative techniques for tracking plant growth are required. One approach to overcoming limitations of both scale and accessibility in the study of plant phenology in montane systems is the use of time-lapse cameras (Ide and Oguma 2013). Time-lapse cameras offer an affordable and scalable means of monitoring plant growth across communities, elevations, and regions (Richardson 2018). Here, we use a network of time-lapse cameras to investigate variation in spatio-temporal patterns in the timing of plant growth across the range of Sierra Nevada bighorn sheep. We examine associations among terrain, snow cover, and vegetation phenology, in order to inform conservation and management decisions about Sierra bighorn, and compare our results to satellite remote sensing data to evaluate the extent to which green-up estimates transfer to novel settings.

Materials and Methods

Study system

Sierra bighorn are managed at the "herd unit" level, which approximately describes discrete populations, although some dispersal among herd units has been documented (U.S. Fish and Wildlife Service 2007). Since the 1970's, translocation efforts have expanded populations from three isolated groups to include fourteen currently occupied herd units (primarily ranging along the east slope of the Sierra, indicated by solid lines in Figure 3.1). Other potential areas of reintroduction have been identified and are under consideration for further translocation, and are included for context in maps (indicated by dashed lines in Figure 3.1).

The Sierra lies along the western edge of the American Cordillera, and features elevational relief in some places exceeding 2.5km. Mid-to-high elevation areas are characterized by heavy snowfall during winter; in some regions of the eastern Sierra, snow depth exceeds 5m in heavy snowfall years (Bair et al. 2018). In the alpine zone, sparse plant communities of predominantly herbaceous perennial species dot the landscape (Barbour et al. 1997). Lower slopes in the eastern Sierra are arid due to the rain shadow effect, and feature Mojave and Great Basin desert scrublands. The altitudinal range of Sierra bighorn spans from the alpine to the base of the Sierra escarpment, which they traverse seasonally. Bighorn tend to prefer to remain close to cliffy areas to which they can escape in the event of a predator encounter, and specialize on the rugged terrain that characterizes the eastern Sierra (Spitz et al. 2020).

Time-lapse camera network

Time-lapse, or digital repeat photography, is the serial collection of imagery following a fixed temporal interval, and is increasingly used as a near-surface remote sensing technique to track seasonal plant growth (Crimmins and Crimmins 2008, Richardson et al. 2009, Bater et al. 2011, Brown et al. 2016, Richardson 2018). One hundred thirty-five Wingscapes TimelapseCam Pro cameras were deployed in the Sierra Nevada mountains of California during the summer of 2018 based on expert knowledge of habitat use by Sierra bighorn, site accessibility, and minimizing impacts on federally-designated Wilderness (Figure 3.1). Because the intent of this study was to focus on forage phenology for Sierra bighorn, cameras were positioned across their elevational and latitudinal range, with selection of individual plots based on the occurrence of plant species consumed by bighorn. The cameras were programmed to capture at least three photos daily (at 11am, noon, and 1pm), but only noontime images were used in this analysis. Nine of the fourteen occupied herd units were selected for this study in order to limit overlap among jurisdictional areas by the camera network.

Image analysis

For each camera plot, a "keyframe" image was selected as a reference point for the remainder of the analysis. All identifiable plant ramets were traced and labeled using the VGG Image Annotator (Dutta and Zisserman 2019). In cases of dense beds of mixed or undifferentiable plant species, an umbrella "Unidentified/mixed" label was used. When present in the keyframe image scene, polygons for several rocks were also annotated in order to track seasonal variation in image greenness not associated with plant growth.

The software `drpToolkit` v1.0.0 (John et al. 2022) was used to align imagery and extract pixel greenness for individual plants from the time series. For each camera, all images were aligned using the SIFT algorithm (Lowe 2004) to find shared features between each image and that camera's keyframe, and calculate the 3x3 matrix defining the transformation between the raw image and the target keyframe (homography matrix). With all aligned imagery sharing a common coordinate space, greenness was extracted from each plant polygon, described above. Greenness was calculated using the green chromatic coordinate (GCC), defined as the mean value on the green band divided by the sum of the mean of the green + red + blue bands (Klosterman et al. 2014, Reid et al. 2016). Snow cover was manually flagged, and when snow was present in the foreground of an image, greenness data were censored from the analyses.

Because the camera model used in this study only allows automatic exposure, we retained only imagery that was collected using the 10 most common exposure settings per camera-year. Therefore, a camera with a generally darker image scene might have a slower selection of acceptable shutter times than a camera with a lighter image scene (for example, WH-13 and WH-10, respectively, due to variation in terrain color; Supplementary materials S1). We also retained only camera-years containing fewer than 3 months of missing data within the year, and fewer than three consecutive weeks of missing data between March and September.

Derivation of plant phenology indices followed standard procedures (Beck et al. 2006, Bischof et al. 2012) applied to plant-specific greenness values. For each region in each plot and during each year, greenness was rescaled so that the 0.1 quantile was set to 0 and the 0.925 quantile was set to 1; the rescaled 0 value was also imputed as a winter baseline when images contained snow. Next, a 7-day moving window was used to smooth the time series with the

window's median value. Then, the greenness time series was fit to a double logistic function

with the form:

$$GCC = \frac{1}{1+\exp\left(\frac{xmidS-x}{scalS}\right)} - \frac{1}{1+\exp\left(\frac{xmidA-x}{scalA}\right)} \qquad [1]$$

where GCC is the green chromatic coordinate; x is the ordinal day of year; xmidS and xmidA are

the timing of the inflection points during the upward phase of spring growth and downward

phase of autumn senescence, respectively; and scalS and scalA are scaling parameters defining

the rate of the upward and downward phases of spring and autumn growth and senescence,

respectively (Beck et al. 2006, Bischof et al. 2012). GCC is an effective metric for tracking

changes in greenness while minimizing effects of changes in illumination (Sonnentag et al.

2012). The same approach was used for MOD13Q1 NDVI (Didan 2015) extracted at the location

of each camera plot.

Finally, for each camera plot and year, equation 1 was fit to the binary snow cover time

series to index the timing of seasonal snow cover retreat and onset at the camera level.

Replacing GCC with binary snow cover, we interpret the xmidS, xmidA , scalS, and scalA

parameters analogously to the above, but here in reference to snow season parameters.

Statistical analyses

To examine the effect of snowmelt timing on green-up timing, a Bayesian linear mixed-

effects model was fitted using green-up timing as the response variable, snowmelt timing and

plant growth form as fixed effects, and year and camera plot ID as random intercepts. A plant's

growth form is a coarse description of its stature and durability, and is likely to underlie how

physiological processes respond to variation in snow depth and soil moisture (Iversen et al.

2009). To examine variation in the elevational lapse rate in green-up timing across latitude, we compared two models, one with aspect, elevation, and latitude as fixed effects; and one with aspect, elevation, latitude, and the interaction between elevation and latitude as fixed effects. In both models, green-up timing was the response variable, and year and camera plot ID were used as random intercepts. Models were compared based on the estimated log predictive density (ELPD; i.e. predictive performance) in a leave-one-out cross-validation approach; when ΔELPD was less than 4, models were taken to be equivalent. To examine variation in the elevational lapse rate in green-up timing across species, we used only green-up data for species that were observed in at least five camera plots. Two models were compared, one with species, aspect, and elevation as fixed predictors; and one with species, aspect, elevation, and the interaction between species and elevation as fixed predictors. We applied the same model comparison approach as that used for the latitudinal models above. When elevation or latitude were used as predictor variables, they were centered and scaled to aid model fit and evaluation, and aspect was cosine-transformed so that -1 indicates south-facing slopes and 1 indicates north-facing slopes.

All statistical analyses used the model fitting library `brms` V2.16.3 in R version 4.1.2. All models were fit using a normal distribution, 2500 warmup samples, 5000 iterations, and 4 chains. Non-informative priors were selected (green-up date intercept: normal distribution, μ =100, σ = 100; sd: cauchy distribution, x =0, γ = 10; sigma: normal distribution, x =0, γ = 10). Model convergence was evaluated based on MCMC chain inspection, R-hat values, and effective sample sizes. Results are reported as mean±SE posterior distribution estimates, and where applicable, a 95% Bayesian credible interval is included.

Results

The raw dataset comprised 95,188 images generated by 118 cameras. After filtering the raw dataset, 32,481 images were used to compile 94 camera-years of imagery, including 1,136 region-years of greenness, spanning 1448m-3798m elevation (mean = 2906.5m; standard deviation = 610.2m). More cameras generated usable time series in 2020 (n = 79) than 2019 (n = 16). Because the winter of 2018-2019 was a comparably snowy year across the Sierra compared to the dry winter of 2019-2020 (United States Department of Agriculture 2022), we compare these years where possible, but all models described hereafter include year as a random effect to account for interannual differences while exploring intra-annual covariates of interest as fixed effects. Green-up was typically more rapid than senescence across the camera network, and varied across elevation and latitude (Figure 3.2). Variation in green-up timing was more coherent across elevation than it was across latitude.

Across plant growth forms, green-up was strongly related to snowmelt timing in both years of the study (Figure 3.3). In a linear mixed-effects model with green-up timing as the response variable, growth form and snowmelt timing as predictors, and year and camera as random effects, green-up was 0.45±0.03 days later per 1-day delay in snowmelt (95% CI: 0.40,0.51). Annual and perennial grasses were the first growth forms to undergo green-up, followed by herbs and mixed vegetation cover, followed by shrubs and trees. Although green-up timing was associated with snowmelt timing across growth forms, the mean posterior slope of the relationship was always less than 1, indicating that with later snowmelt timing the temporal lag between snowmelt timing and green-up timing diminished (Figure 3.3).

The elevational lapse rate in green-up timing was constant across latitude (Figure 3.4). A comparison of two models, one that included aspect, elevation and latitude (which were not correlated; Pearson's R = 0.39) as fixed predictor variables, and one that included aspect, elevation, latitude, and the interaction between elevation and latitude as predictor variables, did not lend strong support for either model over the other (cross-validated ΔELPD of no-interaction model = -0.5±0.4). In the simpler model (Bayesian R^2 = 0.845±0.005), green-up was delayed by 16.50±4.56 days on north-facing vs. south-facing slopes (95% CI: 7.36, 25.24), by 24.73±1.60 days per standard deviation in elevation (95% CI: 21.59, 27.83), and by 0.40±1.63 days per standard deviation in latitude (95% CI: -3.20, 3.98). In this model, the overall unscaled elevational lapse rate of 4.21 days per hundred meters of elevation scales to a difference of 98.9 days in green-up timing between the lowest-elevation and highest-elevation cameras. In the interactive model, green-up was delayed by 16.68±4.70 days on north-facing vs. south-facing slopes (95% CI: 7.36, 25.56), by 24.17±1.79 days per standard deviation in elevation (95% CI: 20.63, 27.70), and by 0.41±1.65 days per standard deviation in latitude (95% CI: -2.85, 3.70), and the estimated interaction overlapped 0 (-1.00 ±1.59; 95% CI: -4.13, 2.13), indicating that latitude did not affect the delay in green-up timing across elevation within the study extent.

Of the species that were present in more than five unique camera plots within a given year, the slope of green-up timing vs. elevation generally did not vary (Figure 3.5). One species, *Hulsea algida*, underwent green-up earliest at the highest-elevation sites in 2020 (Figure 3.5 main panel), but after including both years of data and accounting for terrain aspect, there was no detectable directional pattern in green-up timing across elevation (Figure 3.5 inset). Models with elevation and species as fixed effects and camera plot and year as random effects

59

explained over 85% of the variation in green-up timing (Bayesian R^2 = 0.854 when no interaction is present). A model that also included an interaction between species and elevation only marginally increased explanatory performance (Bayesian R^2 = 0.857), and the difference in expected log predictive density between the models was small (cross-validated ΔELPD = 4.5±3.9). Thus, as with latitude, there was not support for an interaction between species and elevation. In the model without an interaction, the mean scaled posterior estimate for elevation was 21.92±2.26 (95% CI: 17.58, 26.44) days per standard deviation in elevation.

Green-up timing detected at the satellite level broadly corresponded with green-up timing across all vegetation tracked at the camera plot level (Figure 3.6). However, the relationship between camera-derived green-up timing and satellite-derived green-up timing was mediated by land cover class, where inter-sensor correspondence was highest among shrub and forested areas (Pearson's R = 0.80 and 0.92, respectively), and lower among herbaceous and barren areas (Pearson's R = 0.05 and 0.32, respectively). Data from MOD13Q1 affirm an elevational delay in green-up timing (slope = 32.73±2.40 days per standard deviation in elevation; 95% CI = 28.03, 37.45).

Discussion

Our results reveal consistent patterns in the timing of spring plant growth across the range of Sierra Nevada bighorn sheep. Green-up occurred earlier during the drought year of 2020 than during the comparatively snowy year of 2019. Plant green-up timing was delayed with respect to snowmelt timing across plant growth forms in both years of the study. Although green-up timing was somewhat delayed with increasing latitude, elevation emerged as a more

important axis along which plant green-up timing varies. Among common species in the Sierra, the delay in green-up timing with respect to elevation was approximately constant.

These findings corroborate the results from other work identifying a pattern of delayed vegetation green-up timing with increasing elevation (Hopkins 1920, Albon and Langvatn 1992, Vitasse et al. 2018 but also see Wang et al. 2014). Terrain factors alone explained over 80% of variation in green-up timing in the eastern Sierra, and modeling results suggest that topography may drive differences in the magnitude and duration of the green-up season across herd units (Figure 3.7). Due to the extreme topographic relief of the Sierra, low-elevation sites may undergo green-up months before high-elevation sites that are only a few kilometers away.

Additional spatial and interspecific variation in predominant drivers of plant phenology are important for understanding how future climate change will impact the resource landscape (John et al. 2020). For example, a recent study using PhenoCam data found an important role of temperature in driving the elevational delay in deciduous forest phenology, but also uncovered intra- and interannual differences in the main factors driving green-up phenology in grasslands (Richardson et al. 2019). Disentangling how these factors structure landscape phenology will help refine ecological forecasts, a clear need in applied conservation settings.

Snowpack, snowmelt, and conditions during the snow-free season are central to alpine plants' life history and community composition (Winkler et al. 2018, Jerome et al. 2021). An increasingly severe drought across California is related in part to reductions in snowpack across the Sierra (Reich et al. 2018). However, model uncertainty around future drought conditions makes anticipating future change in snowpack across the Sierra difficult (Cook et al. 2018). Critically, the biggest losses in spring snowpack along the eastern Sierra occur at elevations

between 1500m and 2500m during drought years (Berg and Hall 2017); areas near the base of the escarpment around these elevations are where migratory Sierra bighorn overwinter (Spitz et al. 2017).

Notably, the lag between snowmelt timing and green-up timing was greatest when snowmelt was earlier. This occurred mainly at low elevations, presumably due to the relative importance of abiotic constraints on the plant growing season: While months of deep snow cover represents a predominant constraint for plant growth in the alpine, brief and scant snow cover offers increased sun exposure in a comparatively warmer environment for plants at lower elevations. Because moisture availability is limited to local snowmelt and rainfall for plants in xeric mountain sites (Williams et al. 2009), low-elevation plants in the eastern Sierra likely rely on local rain events unrelated to snowmelt for meeting moisture demands. Drought response is important in structuring vegetation communities in arid environments, underpinning phenological variation across elevation (Fallon and Cavender-Bares 2018). If the movements of bighorn relate to forage phenology (e.g. Merkle et al. 2016), elevation-dependent adjustment to the snowpack regime may modify habitat selection by bighorn, especially during the early spring and at low elevations.

In this study, species-specific plant green-up timing varied by approximately ten days at the median elevation, indicating that conspecific plants at similar elevations may exhibit different green-up timing, and conspecifics at different elevations may exhibit similar green-up timing. Spatial variation in plant green-up timing can be further explained by incorporating other terrain factors such as aspect; our models support including cosine-transformed terrain aspect (i.e. slope northness) as an explanatory variable for green-up timing. Phenological

variation within and across elevational ranges may help explain the vacillating movements

taken by some bighorn during their spring migration (Denryter et al. 2021).

Although green-up timing derived from the time-lapse camera network broadly

corresponded to green-up timing derived from satellite measurements, that relationship was

stronger for shrubland and forested areas; in plots with barren and herbaceous land cover, the

relationship was only weakly positive or nonsignificant (Figure 3.6). Other work has identified

relationships between satellite sensors and point estimates on the ground (Fontana et al. 2008,

Moon et al. 2021), but also shows that the correspondence between time-lapse and satellite-

derived measures of plant growth timing depend on the degree to which the camera scene

represents the broader local landscape (Hufkens et al. 2012, Browning et al. 2017). "Barren"

landscapes are notoriously difficult to monitor with coarse satellite measurements, and are

often excluded from analyses (e.g. Nijland et al. 2016, Bolton et al. 2020). It is likely that the

discrepancy we report here between time-lapse and satellite measurements among barren and

herbaceous landscapes relates not just to the resolution of satellite observations, but also to

the ramet-specific approach we applied to tracking image greenness. Notably, the closest

relationship between time-lapse and satellite-derived phenology estimates was apparent for

shrubland, a cover type that is both dense (and therefore conducive to high-quality satellite

estimates of landscape phenology) and common in the study area.

Because green-up timing on barren and herbaceous landscapes was poorly measured by

satellite data, conclusions drawn from satellite-derived measures of plant phenology should be

generated with caution. Rather than indexing the timing of plant growth, variation in coarse

measures of NDVI in these areas could instead relate to patterns in snow cover, soil moisture,

and terrain change (Sesnie et al. 2012, Huang et al. 2021). For example, in 2020 a single camera on barren terrain reported approximately median plant growth timing compared to other cameras on barren land, yet the satellite-derived measure of green-up timing at that location was delayed compared to other satellite-derived measures (Figure 3.6B, top-left panel). Coincidentally, a massive rockslide was observed at that site after a 5.8 magnitude earthquake struck near Lone Pine, CA in late June that summer. The "late" green-up date detected by satellite-derived NDVI could have been related not to delayed plant growth but instead to change in the spectral properties of landscape reflectance. Similarly, although there is general correspondence among time-lapse and satellite measures of green-up timing, satellite measures of senescence timing were often much later than measurements from the camera network, possibly related more to the onset of the snowy season than to senescence in biomass production. Because barren and herbaceous land cover are central to bighorn sheep habitat selection and foraging (Festa-Bianchet 1988), the results presented here suggest that more finely-resolved forms of remote sensing may uncover critical seasonal vegetation dynamics that are not captured at the satellite level.

Our results reveal that the elevational lapse rate in green-up timing is approximately constant across the range of Sierra bighorn. However, because of the varied structure of topographic relief across herd units, modeling results indicate that the duration of the green-up season may not be constant across herd units. Therefore, animals that undergo translocation to achieve conservation goals may not make optimal movement decisions in their new environment. Because climate change is expected to drive inconsistent change in future temperature and snow cover regimes across elevation in the Sierra (Reich et al. 2018), it is likely

that the historical pattern of landscape phenological change will be similarly disrupted.

Although translocated ungulates may require an adjustment period before effectively "surfing the green wave," the presence of experienced conspecifics, coupled with knowledge of local variation in spring phenology, facilitates that adjustment (Jesmer et al. 2018). In addition to social factors, knowledge and perception of available alternative conditions underlies migratory decision-making in Sierra bighorn (Berger et al. 2022). Thus, management decisions in response to and anticipation of environmental change should account for the multiple environmental novelties that translocated Sierra bighorn are likely to encounter.

Figures
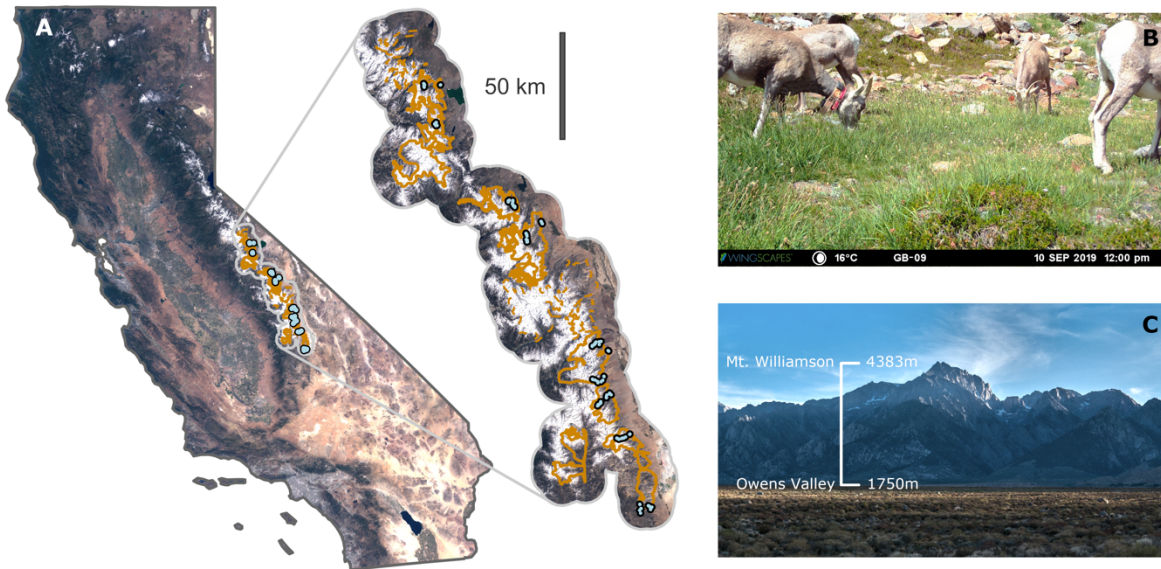
Figure 3.1. The time-lapse camera network (blue dots) spans the latitudinal range of Sierra Nevada bighorn sheep (A; currently occupied herd units designated by solid orange lines). Sierra bighorn captured by a time-lapse camera on Mt. Gibbs forage in a small meadow in late summer, 2019 (B). The east slope of the Sierra features dramatic escarpment with elevational relief in some places exceeding 2500m (C). Map of California compiled from Landsat 8 imagery courtesy of U.S. Geological Survey.
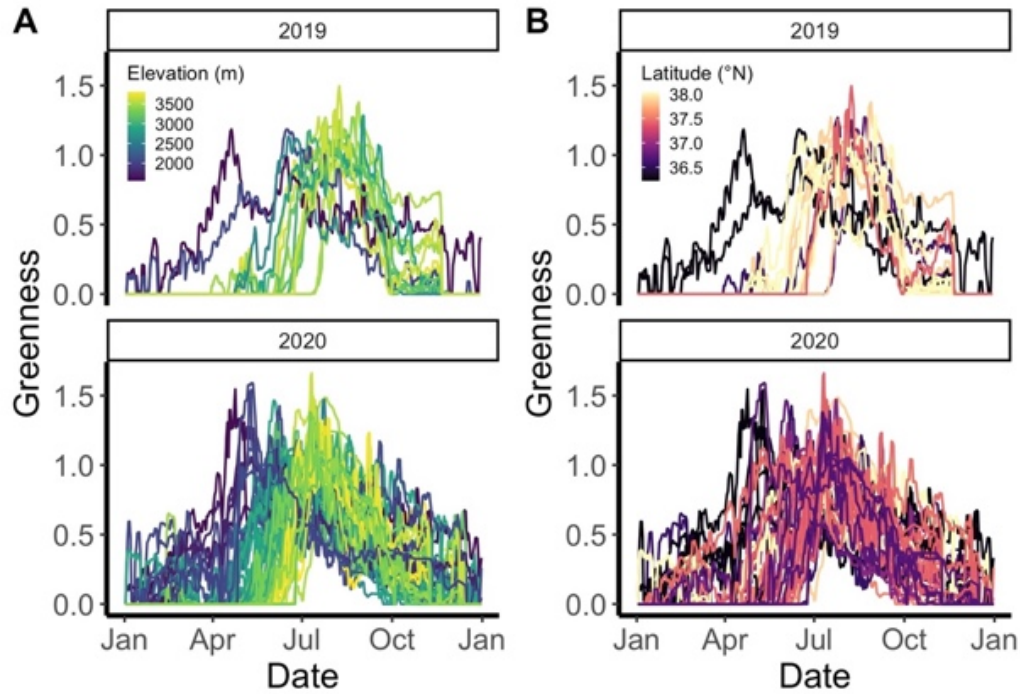
Figure 3.2. Seasonal variation in scaled greenness, aggregated by camera plot, follows a seasonal pattern of greening and senescing across elevation (A) and latitude (B). Although green-up occurred earlier in 2020 than 2019 (difference = 15.07±4.97 days, p < 0.001), senescence timing remained approximately constant across the two years (difference = 3.85±8.37 days, p > 0.1).
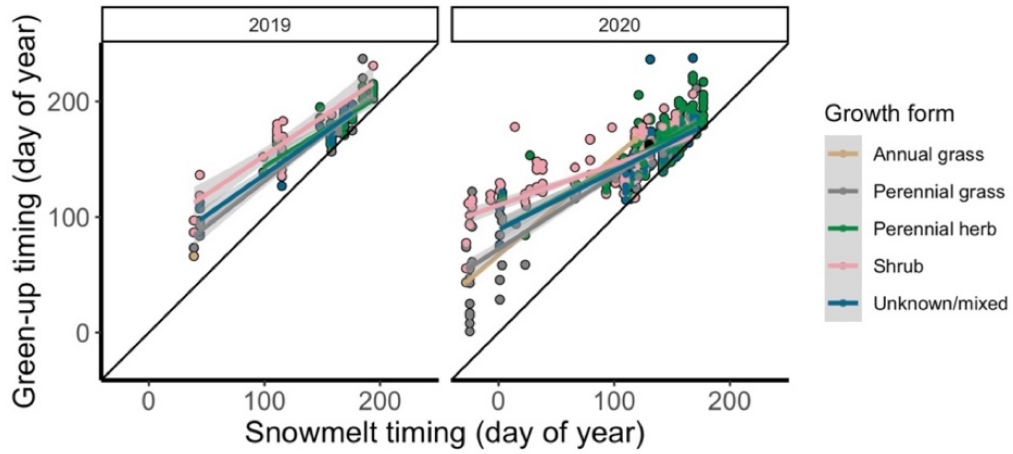
Figure 3.3. Green-up timing varies by over three months in the camera network, but is strongly correlated with local snowmelt timing in both years. Note that single deciduous tree species (*Cercocarpus ledifolius*) is shown with a black dot in 2020 and does not include a trend because it is the sole representative of that growth form.
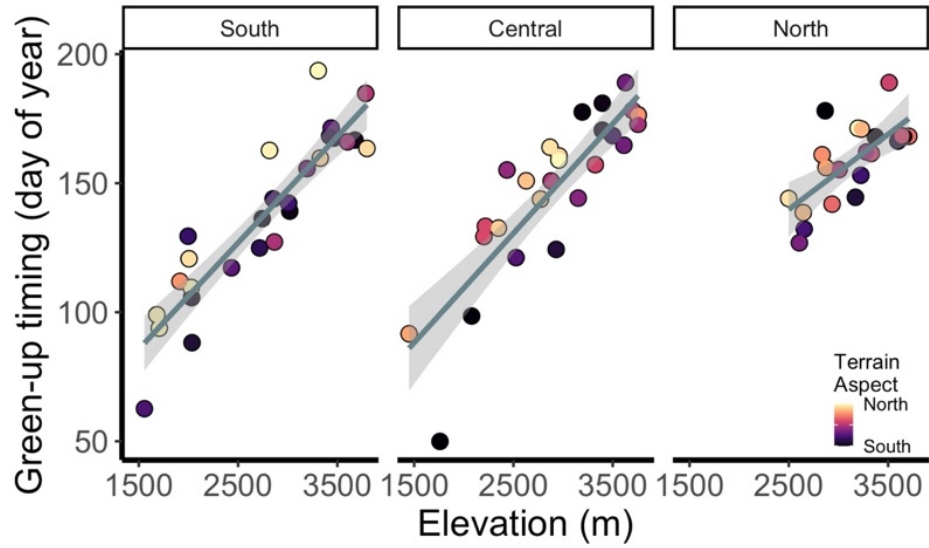
Figure 3.4. Timing of green-up in 2020, aggregated to the plot level, and binned equally into three latitudinal bins. The time-lapse camera network reveals a comparable elevational lapse rate in green-up timing across latitude.
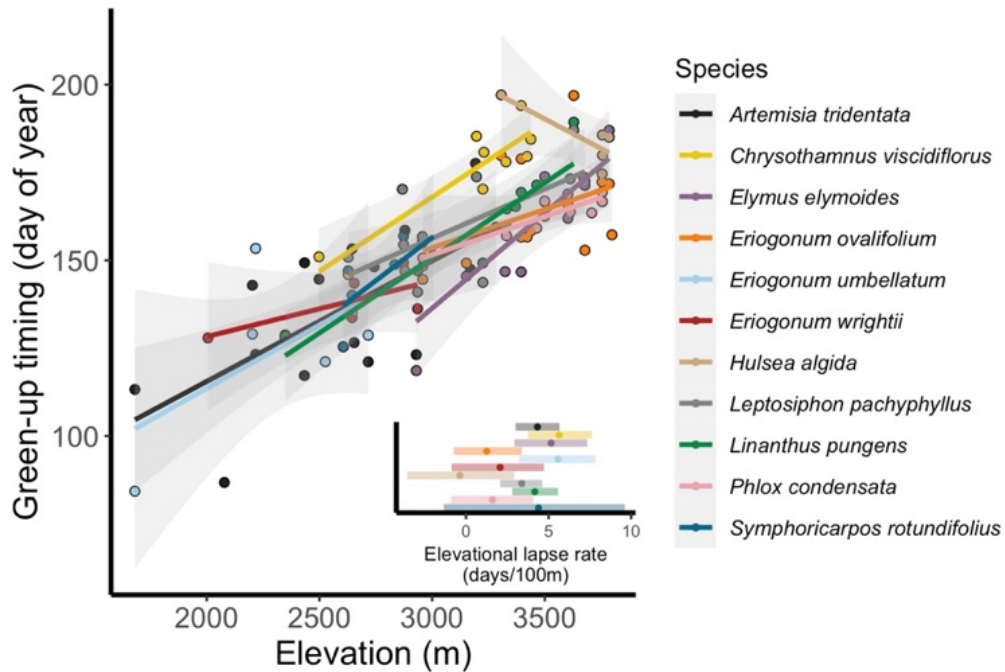
Figure 3.5. Timing of green-up in 2020 for species observed in at least five unique camera plots reveals variation in plant phenological response to increasing elevation. Contrast plot (inset) shows the elevational lapse rate (with 95% highest posterior density interval) for each species from a model including 2019 and 2020 data, with elevation and aspect as fixed effects and year and camera plot as random effects.
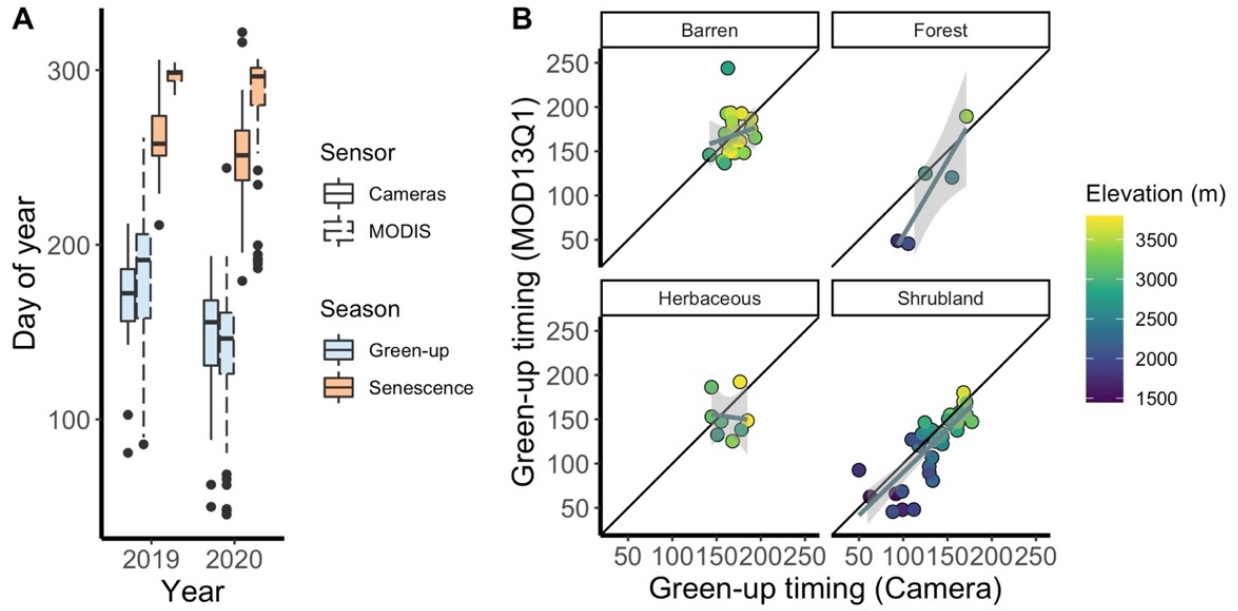
Figure 3.6. Green-up and senescence timing measured with MOD13Q1 NDVI in 2019 and 2020
(A), and comparison of 2020 green-up timing across the time-lapse camera network and
MOD13Q1-derived landscape phenology, faceted by land cover classification (B).
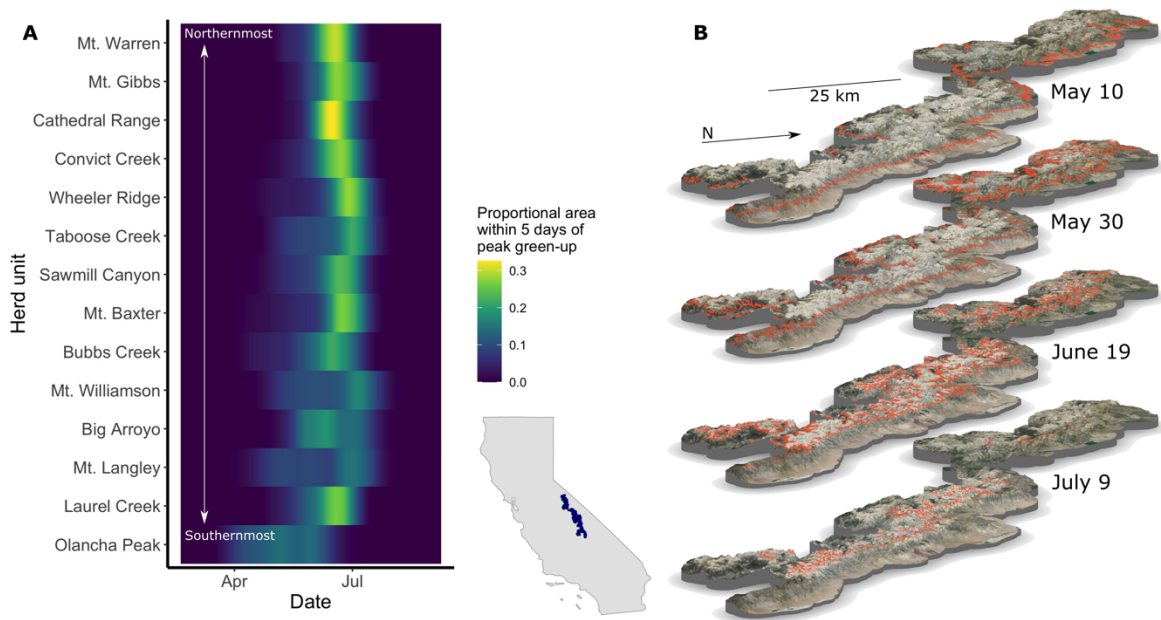
Figure 3.7. A terrain-only model (using elevation and cosine-transformed aspect as fixed predictors) explains 84.5% of variation in green-up timing across the time-lapse camera network. Model predictions reveal variation in the intensity of the green-up season across Sierra bighorn herd units (A). Throughout the region (B), the spatial window of areas at peak green-up (red) varies by elevation and time.

References

Abraham, J. O., N. S. Upham, A. Damian-Serrano, and B. R. Jesmer. 2022. Evolutionary causes and consequences of ungulate migration. Nature Ecology & Evolution:1–9.

Aikens, E. O., K. L. Monteith, J. A. Merkle, S. P. H. Dwinnell, G. L. Fralick, and M. J. Kauffman. 2020a. Drought reshuffles plant phenology and reduces the foraging benefit of green-wave surfing for a migratory ungulate. Global Change Biology 26:4215–4225.

Aikens, E. O., A. Mysterud, J. A. Merkle, F. Cagnacci, I. M. Rivrud, M. Hebblewhite, M. A. Hurley, W. Peters, S. Bergen, J. De Groeve, S. P. H. Dwinnell, B. Gehr, M. Heurich, A. J. M. Hewison, A. Jarnemo, P. Kjellander, M. Kröschel, A. Licoppe, J. D. C. Linnell, E. H. Merrill, A. D. Middleton, N. Morellet, L. Neufeld, A. C. Ortega, K. L. Parker, L. Pedrotti, K. M. Proffitt, S. Saïd, H. Sawyer, B. M. Scurlock, J. Signer, P. Stent, P. Šustr, T. Szkorupa, K. L. Monteith, and M. J. Kauffman. 2020b. Wave-like Patterns of Plant Phenology Determine Ungulate Movement Tactics. Current Biology:S0960982220308484.

Albon, S. D., and R. Langvatn. 1992. Plant Phenology and the Benefits of Migration in a Temperate Ungulate. Oikos 65:502–513.

Allen, A. M., and N. J. Singh. 2016. Linking Movement Ecology with Wildlife Management and Conservation. Frontiers in Ecology and Evolution 3.

Bair, E. H., R. E. Davis, and J. Dozier. 2018. Hourly mass and snow energy balance measurements from Mammoth Mountain, CA USA, 2011–2017. Earth System Science Data 10:549–563.

Barbour, M., B. Pavlik, F. Drysdale, and S. Lindstrom. 1997. California's changing landscapes: diversity and conservation of California vegetation. California Native Plant Society, Sacramento, Calif.

Barton, P. S., P. E. Lentini, E. Alacs, S. Bau, Y. M. Buckley, E. L. Burns, D. A. Driscoll, L. K. Guja, H. Kujala, J. J. Lahoz-Monfort, A. Mortelliti, R. Nathan, R. Rowe, and A. L. Smith. 2015. Guidelines for Using Movement Science to Inform Biodiversity Policy. Environmental Management 56:791–801.

Bater, C. W., N. C. Coops, M. A. Wulder, T. Hilker, S. E. Nielsen, G. McDermid, and G. B. Stenhouse. 2011. Using digital time-lapse cameras to monitor species-specific understorey and overstorey phenology in support of wildlife habitat assessment. Environmental Monitoring and Assessment 180:1–13.

Beck, P. S. A., C. Atzberger, K. A. Hogda, B. Johansen, and A. K. Skidmore. 2006. Improved monitoring of vegetation dynamics at very high latitudes: A new method using MODIS NDVI. Remote Sensing of Environment 100:321–334.

Berg, N., and A. Hall. 2017. Anthropogenic warming impacts on California snowpack during drought. Geophysical Research Letters 44:2511–2518.

Berger, D., D. German, C. John, R. Hart, T. Stephenson, and T. Avgar. 2022. Seeing Is Be-Leaving: Perception Informs Migratory Decisions in Sierra Nevada Bighorn Sheep (Ovis canadensis sierrae). Frontiers in Ecology and Evolution 10.

Bischof, R., L. E. Loe, E. L. Meisingset, B. Zimmermann, B. Van Moorter, and A. Mysterud. 2012. A Migratory Northern Ungulate in the Pursuit of Spring: Jumping or Surfing the Green Wave? American Naturalist 180:407–424.

Bolton, D. K., J. M. Gray, E. K. Melaas, M. Moon, L. Eklundh, and M. A. Friedl. 2020. Continental-scale land surface phenology from harmonized Landsat 8 and Sentinel-2 imagery. Remote Sensing of Environment 240:111685.

Brown, T. B., K. R. Hultine, H. Steltzer, E. G. Denny, M. W. Denslow, J. Granados, S. Henderson, D. Moore, S. Nagai, M. SanClements, A. Sánchez-Azofeifa, O. Sonnentag, D. Tazik, and A. D. Richardson. 2016. Using phenocams to monitor our changing Earth: toward a global phenocam network. Frontiers in Ecology and the Environment 14:84–93.

Browning, D. M., J. W. Karl, D. Morin, A. D. Richardson, and C. E. Tweedie. 2017. Phenocams Bridge the Gap between Field and Satellite Observations in an Arid Grassland Ecosystem. Remote Sensing 9:1071.

Cleland, E. E., I. Chuine, A. Menzel, H. A. Mooney, and M. D. Schwartz. 2007. Shifting plant phenology in response to global change. Trends in Ecology & Evolution 22:357–365.

Cook, B. I., J. S. Mankin, and K. J. Anchukaitis. 2018. Climate Change and Drought: From Past to Future. Current Climate Change Reports 4:164–179.

Crimmins, M. A., and T. M. Crimmins. 2008. Monitoring Plant Phenology Using Digital Repeat Photography. Environmental Management 41:949–958.

Denryter, K., T. R. Stephenson, and K. L. Monteith. 2021. Broadening the migratory portfolio of altitudinal migrants. Ecology 102:e03321.

Didan, K. 2015. MOD13Q1 MODIS/Terra Vegetation Indices 16-Day L3 Global 250m SIN Grid V006. NASA EOSDIS Land Processes DAAC.

Dutta, A., and A. Zisserman. 2019. The VIA Annotation Software for Images, Audio and Video. Pages 2276–2279 Proceedings of the 27th ACM International Conference on Multimedia. ACM, Nice France.

Fallon, B., and J. Cavender-Bares. 2018. Leaf-level trade-offs between drought avoidance and desiccation recovery drive elevation stratification in arid oaks. Ecosphere 9:e02149.

Festa-Bianchet, M. 1988. Seasonal range selection in bighorn sheep: conflicts between forage quality, forage quantity, and predator avoidance. Oecologia 75:580–586.

Fontana, F., C. Rixen, T. Jonas, G. Aberegg, and S. Wunderle. 2008. Alpine Grassland Phenology as Seen in AVHRR, VEGETATION, and MODIS NDVI Time Series - a Comparison with In Situ Measurements. Sensors 8:2833–2853.

Geist, V. 1974. Mountain Sheep: A Study in Behavior and Evolution. University of Chicago Press.

Hopkins, A. D. 1920. The Bioclimatic Law. Journal of the Washington Academy of Sciences 10:34–40.

Huang, K., Y. Zhang, T. Tagesson, M. Brandt, L. Wang, N. Chen, J. Zu, H. Jin, Z. Cai, X. Tong, N. Cong, and R. Fensholt. 2021. The confounding effect of snow cover on assessing spring phenology from space: A new look at trends on the Tibetan Plateau. Science of The Total Environment 756:144011.

Hufkens, K., M. Friedl, O. Sonnentag, B. H. Braswell, T. Milliman, and A. D. Richardson. 2012. Linking near-surface and satellite remote sensing measurements of deciduous broadleaf forest phenology. Remote Sensing of Environment 117:307–321.

Ide, R., and H. Oguma. 2013. A cost-effective monitoring method using digital time-lapse cameras for detecting temporal and spatial variations of snowmelt and vegetation phenology in alpine ecosystems. Ecological Informatics 16:25–34.

Iversen, M., K. A. Bråthen, N. G. Yoccoz, and R. A. Ims. 2009. Predictors of plant phenology in a diverse high-latitude alpine landscape: growth forms and topography. Journal of Vegetation Science 20:903–915.

Jerome, D. K., W. K. Petry, K. A. Mooney, and A. M. Iler. 2021. Snow melt timing acts independently and in conjunction with temperature accumulation to drive subalpine plant phenology. Global Change Biology 27:5054–5069.

Jesmer, B. R., J. A. Merkle, J. R. Goheen, E. O. Aikens, J. L. Beck, A. B. Courtemanch, M. A. Hurley, D. E. McWhirter, H. M. Miyasaki, K. L. Monteith, and M. J. Kauffman. 2018. Is ungulate migration culturally transmitted? Evidence of social learning from translocated animals. Science 361:1023–1025.

John, C., D. Miller, and E. Post. 2020. Regional variation in green-up timing along a caribou migratory corridor: Spatial associations with snowmelt and temperature. Arctic, Antarctic, and Alpine Research 52:416–423.

John, C., and E. Post. 2022. Seasonality, niche management and vertical migration in landscapes of relief. Ecography 2022:e05774.

John, C., F. Shilling, and E. Post. 2022. drpToolkit: An automated workflow for aligning and analysing vegetation and ground surface time-series imagery. Methods in Ecology and Evolution 13:54–59.

Kauffman, M. J., E. O. Aikens, S. Esmaeili, P. Kaczensky, A. Middleton, K. L. Monteith, T. A. Morrison, T. Mueller, H. Sawyer, and J. R. Goheen. 2021. Causes, Consequences, and Conservation of Ungulate Migration. Annual Review of Ecology, Evolution, and Systematics 52:null.

Klinges, D. H., and B. R. Scheffers. 2020. Microgeography, Not Just Latitude, Drives Climate Overlap on Mountains from Tropical to Polar Ecosystems. The American Naturalist 197:75–92.

Klosterman, S. T., K. Hufkens, J. M. Gray, E. Melaas, O. Sonnentag, I. Lavine, L. Mitchell, R. Norman, M. A. Friedl, and A. D. Richardson. 2014. Evaluating remote sensing of deciduous forest phenology at multiple spatial scales using PhenoCam imagery. Biogeosciences 11:4305–4320.

Körner, C. 2004. Mountain Biodiversity, Its Causes and Function. AMBIO: A Journal of the Human Environment 33:11–17.

Körner, C. 2007. The use of 'altitude' in ecological research. Trends in Ecology & Evolution 22:569–574.

Lowe, D. G. 2004. Distinctive Image Features from Scale-Invariant Keypoints. International Journal of Computer Vision 60:91–110.

Martin, T. G., I. Chadès, P. Arcese, P. P. Marra, H. P. Possingham, and D. R. Norris. 2007. Optimal Conservation of Migratory Species. PLOS ONE 2:e751.

Merkle, J. A., K. L. Monteith, E. O. Aikens, M. M. Hayes, K. R. Hersey, A. D. Middleton, B. A. Oates, H. Sawyer, B. M. Scurlock, and M. J. Kauffman. 2016. Large herbivores surf waves of green-up during spring. Proc. R. Soc. B 283:20160456.

Misra, G., S. Asam, and A. Menzel. 2021. Ground and satellite phenology in alpine forests are becoming more heterogeneous across higher elevations with warming. Agricultural and Forest Meteorology 303:108383.

Moon, M., A. D. Richardson, and M. A. Friedl. 2021. Multiscale assessment of land surface phenology from harmonized Landsat 8 and Sentinel-2, PlanetScope, and PhenoCam imagery. Remote Sensing of Environment 266:112716.

Morellato, L. P. C., B. Alberton, S. T. Alvarado, B. Borges, E. Buisson, M. G. G. Camargo, L. F. Cancian, D. W. Carstensen, D. F. E. Escobar, P. T. P. Leite, I. Mendoza, N. M. W. B. Rocha, N. C. Soares, T. S. F. Silva, V. G. Staggemeier, A. S. Streher, B. C. Vargas, and C. A. Peres. 2016. Linking plant phenology to conservation biology. Biological Conservation 195:60–72.

Nijland, W., D. K. Bolton, N. C. Coops, and G. Stenhouse. 2016. Imaging phenology; scaling from camera plots to landscapes. Remote Sensing of Environment 177:13–20.

Park, D. S., E. A. Newman, and I. K. Breckheimer. 2021. Scale gaps in landscape phenology: challenges and opportunities. Trends in Ecology & Evolution.

Piao, S., Q. Liu, A. Chen, I. A. Janssens, Y. Fu, J. Dai, L. Liu, X. Lian, M. Shen, and X. Zhu. 2019. Plant phenology and global climate change: Current progresses and challenges. Global Change Biology 25:1922–1940.

Post, E., J. Kerby, C. Pedersen, and H. Steltzer. 2016. Highly individualistic rates of plant phenological advance associated with arctic sea ice dynamics. Biology Letters 12:20160332.

Post, E., C. Pedersen, C. C. Wilmers, and M. C. Forchhammer. 2008. Warming, plant phenology and the spatial dimension of trophic mismatch for large herbivores. Proceedings of the Royal Society B-Biological Sciences 275:2005–2013.

Primack, R. B., I. Ibáñez, H. Higuchi, S. D. Lee, A. J. Miller-Rushing, A. M. Wilson, and J. A. Silander. 2009. Spatial and interspecific variability in phenological responses to warming temperatures. Biological Conservation 142:2569–2577.

Rafferty, N. E., J. M. Diez, and C. D. Bertelsen. 2020. Changing Climate Drives Divergent and Nonlinear Shifts in Flowering Phenology across Elevations. Current Biology 30:432-441.e3.

Reich, K. D., N. Berg, D. B. Walton, M. Schwartz, F. Sun, X. Huang, and A. Hall. 2018. Climate Change in the Sierra Nevada: California's Water Future. UCLA Center for Climate Science.

Reid, A. M., W. K. Chapman, C. E. Prescott, and W. Nijland. 2016. Using excess greenness and green chromatic coordinate colour indices from aerial images to assess lodgepole pine vigour, mortality and disease occurrence. Forest Ecology and Management 374:146–153.

Richardson, A. D. 2018. Tracking seasonal rhythms of plants in diverse ecosystems with digital camera imagery. New Phytologist 0.

Richardson, A. D., B. H. Braswell, D. Y. Hollinger, J. P. Jenkins, and S. V. Ollinger. 2009. Near-surface remote sensing of spatial and temporal variation in canopy phenology. Ecological Applications 19:1417–1428.

Richardson, A. D., K. Hufkens, X. Li, and T. R. Ault. 2019. Testing Hopkins' Bioclimatic Law with PhenoCam data. Applications in Plant Sciences 7.

Rickbeil, G. J. M., J. A. Merkle, G. Anderson, M. P. Atwood, J. P. Beckmann, E. K. Cole, A. B. Courtemanch, S. Dewey, D. D. Gustine, M. J. Kauffman, D. E. McWhirter, T. Mong, K.

Proffitt, P. J. White, and A. D. Middleton. 2019. Plasticity in elk migration timing is a response to changing environmental conditions. Global Change Biology 25:2368–2381.

Runge, C. A., T. G. Martin, H. P. Possingham, S. G. Willis, and R. A. Fuller. 2014. Conserving mobile species. Frontiers in Ecology and the Environment 12:395–402.

Runge, C. A., J. E. M. Watson, S. H. M. Butchart, J. O. Hanson, H. P. Possingham, and R. A. Fuller. 2015. Protected areas and global conservation of migratory birds. Science 350:1255–1258.

Sesnie, S. E., B. G. Dickson, S. S. Rosenstock, and J. M. Rundall. 2012. A comparison of Landsat TM and MODIS vegetation indices for estimating forage phenology in desert bighorn sheep (Ovis canadensis nelsoni) habitat in the Sonoran Desert, USA. International Journal of Remote Sensing 33:276–286.

Shen, M., G. Zhang, N. Cong, S. Wang, W. Kong, and S. Piao. 2014. Increasing altitudinal gradient of spring vegetation phenology during the last decade on the Qinghai–Tibetan Plateau. Agricultural and Forest Meteorology 189–190:71–80.

Sonnentag, O., K. Hufkens, C. Teshera-Sterne, A. M. Young, M. Friedl, B. H. Braswell, T. Milliman, J. O'Keefe, and A. D. Richardson. 2012. Digital repeat photography for phenological research in forest ecosystems. Agricultural and Forest Meteorology 152:159–177.

Spitz, D. B., M. Hebblewhite, and T. R. Stephenson. 2017. 'MigrateR': extending model-driven methods for classifying and quantifying animal movement behavior. Ecography 40:788–799.

Spitz, D. B., M. Hebblewhite, and T. R. Stephenson. 2020. Habitat predicts local prevalence of migratory behaviour in an alpine ungulate. Journal of Animal Ecology 89:1032–1044.

Teitelbaum, C. S., and T. Mueller. 2019. Beyond Migration: Causes and Consequences of Nomadic Animal Movements. Trends in Ecology & Evolution.

United States Department of Agriculture. 2022. SNOwpack TELemetry Network (SNOTEL). Natural Resources Conservation Service.

U.S. Fish and Wildlife Service. 2007. Recovery Plan for the Sierra Nevada Bighorn Sheep:1–199.

Vitasse, Y., F. Baumgarten, C. M. Zohner, T. Rutishauser, B. Pietragalla, R. Gehrig, J. Dai, H. Wang, Y. Aono, and T. H. Sparks. 2022. The great acceleration of plant phenological shifts. Nature Climate Change 12:300–302.

Vitasse, Y., C. Signarbieux, and Y. H. Fu. 2018. Global warming leads to more uniform spring phenology across elevations. Proceedings of the National Academy of Sciences 115:1004–1008.

Walther, G. R., E. Post, P. Convey, A. Menzel, C. Parmesan, T. J. C. Beebee, J. M. Fromentin, O. Hoegh-Guldberg, and F. Bairlein. 2002. Ecological responses to recent climate change. Nature 416:389–395.

Wang, S., C. Wang, J. Duan, X. Zhu, G. Xu, C. Luo, Z. Zhang, F. Meng, Y. Li, and M. Du. 2014. Timing and duration of phenological sequences of alpine plants along an elevation gradient on the Tibetan plateau. Agricultural and Forest Meteorology 189–190:220–228.

Williams, C. J., J. P. McNamara, and D. G. Chandler. 2009. Controls on the temporal and spatial variability of soil moisture in a mountainous landscape: the signature of snow and complex terrain. Hydrology and Earth System Sciences 13:1325–1336.

Winkler, D. E., R. J. Butz, M. J. Germino, K. Reinhardt, and L. M. Kueppers. 2018. Snowmelt Timing Regulates Community Composition, Phenology, and Physiological Performance of Alpine Plants. Frontiers in Plant Science 9.

Supplementary materials S3.1

BA-02	BA-05	BA-08	BA-09	BA-10	BA-11	BA-12

BA-13	BA-14	BA-15	CN-01	CN-02	CN-06	CN-07

CN-08	CN-09	CN-10	CN-13	CN-14	CN-15	GB-02

GB-03	GB-04	GB-05	GB-06	GB-10	GB-12	GB-13

GB-14	LN-02	LN-03	LN-04	LN-05	LN-08	LN-09

LN-13	LN-15	OL-01	OL-03	OL-04	OL-05	OL-06

OL-08	OL-09	OL-10	OL-15	SW-03	SW-04	SW-05

SW-06	SW-07	SW-08	SW-09	SW-12	SW-13	SW-15

WA-02	WA-03	WA-04	WA-08	WA-14	WA-15	WH-02

WH-05	WH-07	WH-08	WH-09	WH-10	WH-11	WH-12

WH-13	WH-14	WH-15	WL-04	WL-05	WL-08	WL-09

WL-10	WL-15

Chapter 4: Pursuit and escape drive fine-scale movement variation during migration in a temperate alpine ungulate

Abstract

Climate change reduces snowpack, advances snowmelt phenology, drives summer warming, alters precipitation regimes, and consequently modifies vegetation phenology in mountain systems. Altitudinal migrants cope with seasonal variation in such conditions by moving between seasonal ranges at different elevations, but vertical movements may be complex and are often not unidirectional during the spring migratory season. We uncover drivers of vertical movement variation in an endangered alpine specialist, Sierra Nevada bighorn sheep. We used step selection analysis to determine factors that promote vertical movements, and factors that drive selection of destinations after vertical movements. Our results reveal that high temperatures consistently drive uphill movements, and provide some evidence for the contribution of precipitation events to downhill movements. Furthermore, bighorn select destinations that have a high relative index of forage growth and an intermediate delay since snowmelt. These results indicate that although Sierra bighorn seek out foraging opportunities related to landscape phenology, they compensate for fine-scale environmental stressors by undertaking brief vertical movements. Future warming or increased storm intensity may therefore impact fine-scale vertical movements – and tradeoffs related to forage access – by migrants.

Introduction

Recent and ongoing climate change disrupt the spatiotemporal pattern of spring plant growth through modified precipitation and temperature regimes (Asam et al. 2018, Park et al. 2019). Because herbivores commonly track plant phenology during their spring migration (Abrahms et al. 2019, Kauffman et al. 2021, La Sorte and Graham 2021), climate change may affect spatiotemporal patterns of herbivore movement and migration (Seebacher and Post 2015). Forage tracking is a useful tactic for herbivores in landscapes with gradients in plant phenology, because access to highly digestible plant material is maintained or maximized through time (van der Graaf 2006, Aikens et al. 2017).

Many migratory ungulates track forage phenology across elevational gradients in a form of seasonal vertical migration (Albon and Langvatn 1992, Hebblewhite et al. 2008, Sawyer and Kauffman 2011). Although vertical migration in ungulates may emerge in a traditional, "undistracted" form of movement from one range to another, the geographical proximity of seasonal ranges separated by elevation allows migrants to use a broader portfolio of redistribution tactics that span a range of directedness (Denryter et al. 2021). Migrants may undergo several movements during a foraging season to maximize resource access across multiple sub-seasonal ranges (Couriot et al. 2018, van de Kerk et al. 2021).

However, fine-scale movements during the migratory season could be additionally influenced by factors other than foraging opportunities. Because landscapes of relief generate multiple axes of ecoclimatic variation, vertical movements enable herbivores to realize change in multiple environmental conditions (John and Post 2022). Vertical movements may allow migrants to alleviate or intensify realized environmental conditions through both static

landscape variation (ecological variability across space but not time) and dynamic landscape variation (variability across both space and time). Whereas seasonal variation in snow cover and forage availability may ultimately underlie seasonal redistribution of migrants, variation in exposure to high temperatures or severe storms can be mitigated by moving across elevation (Boyle et al. 2010, Semenzato et al. 2021). Because temperatures tend to decrease at higher elevations, upward movements can lead to a reduction experienced heat; conversely, dangers associated with rain and storms on alpine plateaus can be relieved by moving down slope faces into comparatively protected canyons.

The objective of this study was to evaluate the extent to which static and dynamic variation in environmental conditions leads to complex use of elevation in an herbivorous altitudinal migrant, Sierra Nevada bighorn sheep ("Sierra bighorn", *Ovis canadensis sierrae*). Sierra bighorn are a federally endangered subspecies of bighorn sheep endemic to the Sierra Nevada mountains of California (USA) that migrates between the Owens Valley and High Sierra each spring, but with substantial variation in day-to-day elevation use (Denryter et al. 2021). We expected that migration timing and habitat selection would broadly correspond with landscape phenology, but that fine-scale variation in elevation use during the migratory season would arise in response to fine-scale stressors such as high temperature and potentially dangerous precipitation events. To test this expectation, we used a three-part approach to explore Sierra bighorn movement responses to dynamic landscape variation: First, we determined whether upslope migration timing was related to green-up timing. Second, we tested the extent to which variation in environmental stressors and resources promoted

adjustments in elevation use. And third, we examined whether Sierra bighorn tracked

spatiotemporal variation in landscape phenology.

Methods

Study system

Sierra Nevada bighorn sheep are alpine specialists and partial, facultative, altitudinal

migrants in the Sierra Nevada mountains of California (Spitz et al. 2020; Figure 4.1). Sierra

bighorn that undergo uphill spring displacement typically follow one of two migratory patterns

(Denryter et al. 2021): In undistracted migrations, individuals undertake a single, uphill trip,

departing from low-elevation winter range and settling on high-elevation summer range. In

vacillating migrations, individuals undertake multiple up-and-down movements over a period of

days or weeks before settling on high-elevation summer range. Sierra bighorn occupy 14 "herd

units," a spatial delineation used for conservation metrics and management decisions, and

which approximately represent discrete bighorn populations (U.S. Fish and Wildlife Service

2007).

Movement data

Bighorn were fit with GPS collars (various models from Advanced Telemetry Systems,

North Star Science and Tech LLC, LOTEK Engineering Ltd., Televilt, VECTRONIC Aerospace

GmbH, Followit, and Sirtrack LTD; described in Anderson et al. 2022) during spring and fall

capture seasons (March and October) between 2004-2016. Animal handling was done under

veterinarian supervision and approved under the California Department of Fish and Wildlife

Animal Welfare Policy (2017-02). In total, 196 unique individuals were tracked for a total of 370

animal-years, with an average of 30.8±17.8 animals per year. Collars were deployed in 13 herd

units that span the full latitudinal, longitudinal, and elevational range of current Sierra bighorn

habitat. Collars were programmed to collect GPS locations at a minimum frequency of 1 fix per

12 hours.

Raster data

USGS 3DEP 10m National Map elevation data were acquired via Google Earth Engine

(Gorelick et al. 2017, U.S. Geological Survey 2022). Slope and aspect were calculated using the

4-neighbor rule, and escape terrain was classified using a 30° slope threshold. Distance from

escape terrain was calculated using the fasterraster v.0.6.0 R plugin for QGIS v.3.22 (Morelli et

al. 2020, QGIS.org 2022).

Forage vegetation production and phenology were indexed using MOD13Q1 NDVI

(Didan 2015). Landscape phenology was determined by rescaling NDVI values from the bottom

2.5 percentile and top 97.5 quartile to 0 and 1, respectively, and smoothing with a 3-day

median window (Bischof et al. 2012) before fitting to a double logistic function following the

form:

$$NDVI = \frac{1}{1+\exp\left(\frac{xmidS-x}{scalS}\right)} - \frac{1}{1+\exp\left(\frac{xmidA-x}{scalA}\right)} \tag{1}$$

where x is the ordinal day of year, xmidS and xmidA are the ordinal days of green-up and

senescence inflection points respectively, and scalS and scalA are scaling parameters describing

the rate of green-up and senescence, respectively (Beck et al. 2006). Scaled, interpolated NDVI

(siNDVI) was taken to represent forage production at the pixel level relative to production at

that pixel during other times of the year.

A modeled snow dataset was used to index fractional snow cover (FSC) and snowmelt timing (Rittger et al. 2021). This dataset was generated using a data fusion and machine learning approach that combines Landsat 5, Landsat 7, and MODIS satellite imagery to generate daily FSC estimates at 30m resolution. Independent validation reveals strong concurrence among FSC in this dataset and point estimates of snow cover throughout the range of Sierra bighorn (Supplementary materials S1). Snow cover was also fit to Equation 1 above by substituting FSC for NDVI and fitting the curve on a [0,100] interval rather than a [0,1] interval.

Daily temperatures and precipitation were extracted from the DAYMET V4 dataset at 1km resolution (Thornton et al. 2020). Because we were interested in temperature as a driver of uphill movement, we used daily maximum temperature to index potential heat stress across the eastern Sierra. Precipitation is infrequent in the Sierra outside winter, but is often associated with high winds and lightning, and causes terrain in the alpine zone to become wet and particularly unstable (Wieczorek and Jäger 1996).

Migration classification

Seasonal elevation use was determined by extracting elevation from the 3DEP National Map using the raw bighorn GPS location data. Migrants were classified using the migrateR package (Spitz et al. 2017). MigrateR uses an elevational analogue for measuring net squared displacement, and classifies individuals as "resident", "disperser", or "migrant" based on a model comparison approach between a consistent position through time, a single upward movement across time, or an up-and-down redistribution through time. We used minimum thresholds of 500m between elevational ranges and 21 days spent on each seasonal range when classifying individuals as residents, dispersers, and migrants (Spitz et al. 2017, 2018).

Because the focus of this study was on uphill spring migration, any uphill dispersers were combined into the migrant class.

Integrated step selection modeling

Habitat selection was examined using integrated step selection analysis (Avgar et al. 2016). A population-wide step selection framework was taken to incorporate the maximum information about movement variation during the spring migratory period. We chose a population-level model rather than individual-based assessment because minimal endpoint variance in predictor variables constrained our ability to resolve movement processes for animals that used short step lengths on terrain with poor-quality remote sensing data. A population-level model allowed us to include a greater number of individuals and test a greater number of candidate movement drivers simultaneously. To maintain sampling consistency across individuals, the three weeks centered on each migrant's migratory window was used for the analysis. For residents, the three weeks centered on the mean migration timing of that individual's herd unit in that year was used. If no migrants were detected in a resident's herd unit in a given year, the resident was excluded from the analysis. Only individuals with equal numbers of GPS observations were retained in order to avoid bias in the model design.

In cases where the GPS fix rate was more frequent than 12 hours, relocation data were temporally rarified to a 12-hour frequency. Each resampled fix was treated as a startpoint, with the following fix treated as a used endpoint. Thirty random destinations were used as available endpoints. Endpoints were drawn from gamma and von Mises distributions fitted to each individual's step length and turning angle history, respectively.

Environmental covariates were extracted at all start- and endpoints. Terrain features were treated as fixed across time. Snowmelt timing and green-up timing were fixed across time within years, while FSC, distance from snow, siNDVI, temperature, and precipitation all varied daily. Elevation, terrain slope, and temperature were normalized across the full extracted dataset to aid in model fitting. Aspect was cosine-transformed such that north-facing slopes were 1 and south-facing slopes were -1. Precipitation, distance from escape terrain, and distance from snow were transformed using log(value + 1).

Drivers of habitat selection during migration movements were evaluated using conditional logistic regression with case (positive endpoint = 1; negative endpoint = 0) as the response variable and habitat covariates as predictor variables. Two model families were built: First, a complete movement model included startpoint conditions as interactions with the endpoint elevation to identify drivers of movement (i.e., an impetus), as well as fixed endpoint conditions to identify drivers of habitat selection (i.e., an outcome). The second family included all of the same predictor variables except for interactive effects (i.e. startpoint values), in order to explore variation in relative selection strength along the quadratic terms (time since peak snowmelt)^2 and (time since peak green-up)^2.

Two applications of step selection modeling were used to understand the catalysts and outcomes of fine-scale elevational movement by bighorn sheep (Supplementary materials S2). In the first model family ("full movement model"), drivers and outcomes of bighorn movement were combined into a single model by including conditions at the beginning and end of each movement step. Startpoint conditions were allowed to interact with endpoint elevation in order to test hypotheses about drivers of elevational movements. Endpoint conditions were

included to evaluate factors important for destination selection. A model was constructed for

the full Sierra bighorn dataset, and four additional models were constructed for migrants only,

residents only, males only, and females only. In the second model family ("habitat selection

model"), no interaction terms were included, and instead only endpoint variables (i.e., variables

that are potentially important for habitat selection) were analyzed. These models were

constructed to evaluate relative selection strength along continuous variables, compared with

the mean condition of those variables. Specifically, snowmelt recency and green-up recency,

and their polynomials, may be important for selection because they index the relative

phenological status of the landscape.

All statistical analyses were done using R version 4.1.2 (R Core Team 2019).

Results

Across the study system, green-up timing was consistently later in years when snowmelt

timing was later (Figure 4.2A). In a mixed-effects model with green-up timing as the response

variable, snowmelt timing as the predictor variable, and year as a random intercept, green-up

was 6.2±0.20 days later per 10-day delay in snowmelt at the herd unit level (p < 0.001;

conditional R^2 = 0.86). Thus, years with especially early snowmelt were characterized by a

greater lag between the timing of peak snowmelt and peak green-up. The mean difference in

timing between peak snowmelt and peak green-up was 137.2±1.2 days.

Uphill migration timing covaried with green-up timing, and in years with later green-up

timing, migration timing was delayed as well (Figure 4.2B). Mean migration timing occurred

before mean green-up timing at the herd unit level in 81.4% of cases, however anomalously

late migrations were observed in several cases when bighorn moved uphill as late as mid-

September. The earliest migrant relative to green-up timing migrated 67 days prior to mean green-up timing at the herd unit level, while the latest migrant relative to green-up timing migrated 71 days after mean green-up timing at the herd unit level. A linear mixed-effects model that had migration timing as the response variable, green-up timing as a predictor, and herd unit identity and year as random intercepts, revealed that the midpoint of migration was 6.8±1.4 days later per 10-day delay in green-up timing ($p < 0.001$; conditional $R^2 = 0.53$).

Throughout the migratory season, bighorn selected steep, south-facing slopes that were close to escape terrain. Temperature at the onset of movement interacted with destination elevation, leading to selection toward higher elevations on days with warmer temperatures (Figure 4.3). However, males continued to select destinations with high temperatures, whereas females selected against destination temperature. Precipitation at the onset of movement interacted with destination elevation leading to downhill movements by bighorn on rainy days, but this relationship was restricted to migrants and females. When siNDVI was at its peak, it was 1.3 times as likely to be selected than when at its winter baseline, but females were more likely to select high-NDVI habitat than males.

In the no-interaction (habitat selection) model, bighorn avoided high temperature and minimized distance to snow, and selected steep, south-facing slopes near escape terrain with high siNDVI (Figure 4.4A). Snowmelt and green-up recency were both significant predictors of selection when used in isolation, but in a model containing both snowmelt recency, green-up recency, and their polynomials, only snowmelt recency was significant (Supplementary Materials S3). Although we show the results of the model including snowmelt recency, green-up recency and their polynomials, green-up recency and snowmelt recency were moderately

correlated (r = 0.41). Comparison by QIC revealed the strongest support for the model including all four terms (ΔQIC=0), but favored the snowmelt-only model (ΔQIC=13.48) over the green-up-only model (ΔQIC=1919.21). Importantly, across all three of the habitat selection models, the polynomial terms for snowmelt and green-up recency reveal that selection is strongest for destinations with an intermediate lag since fractional snow cover loss was at its fastest (Figure 4.4B). Although there was less support for including green-up recency, the relationship in both the full model and the green-up only model follows a pattern of diminishing selection strength with increasing time since peak green-up (Figure 4.4C).

Discussion

Sierra Nevada bighorn sheep undertake a partial, facultative vertical migration during the spring snowmelt and green-up season (Spitz et al. 2020), but vertical movements by Sierra bighorn are rarely unidirectional and often lead to complex use of elevation (Denryter et al. 2021). Although seasonal variation in space use leads to a general pattern of redistribution across elevation, our results indicate that fine-scale vertical movements during the migratory season might allow bighorn to realize multiple goals, including pursuing foraging opportunities, avoiding heat stress, and seeking refuge from storms.

Uphill migration timing by Sierra bighorn was broadly associated with green-up timing at the herd unit level, which was in turn associated with snowmelt timing. Coordinating migration timing with resource phenology is common among ungulates, presumably because foraging efficiency increases with access to highly digestible early-stage plant growth (Jesmer et al. 2018, Gurarie et al. 2019, Aikens et al. 2020). The Sierra Nevada mountains feature strong interannual variation in snow cover, snowmelt timing, and green-up timing, with over three months

between the earliest and latest green-up records over the course of this study. Although most uphill migrations occurred before mean green-up timing at the herd unit level, some individuals underwent comparatively late uphill movements, possibly related to intraspecific competition or social avoidance.

Our full movement model identified a positive interaction between startpoint temperature and endpoint elevation in driving step selection. This indicates that brief uphill forays were associated with high temperatures, presumably related to escape from heat stress. Heat stress in other ungulates drives similar behavioral responses, leading to selection toward higher elevation and modified daily foraging schedules during hot days (Semenzato et al. 2021). In the eastern Sierra Nevada, high spring temperatures accelerate snowmelt, and where snowmelt is earliest, the lag between snowmelt timing and green-up timing is greatest (Chapter 3 this dissertation). Therefore, higher spring temperatures may cause bighorn to spend increased time at high elevations while there is still high-quality forage below.

Conversely, we found a slight negative effect of precipitation on elevation selection, indicating that storms may drive downhill movements, presumably related to escape from either risk of lightning strike or rockslides. While downhill movements in response to storms are known in birds (Boyle et al. 2010), our study provides evidence of similar responses to storms by ungulates. Notably, this effect was driven mostly by migrants, whereas residents displayed less selection against elevation when precipitation was high, suggesting that migrants are more flexible in their response to dynamic environmental variation. If the frequency of spring and summer storms increases across the Sierra, bighorn sheep may sacrifice foraging opportunities

at high elevations in favor of seeking out protected combes and canyons further down mountainsides.

Because the migratory season of bighorn sheep generally corresponds with lambing, ewes must balance heightened nutritional requirements with selection of habitat that accommodates safe lamb rearing (Forshee 2018, Robinson et al. 2020). Movements toward steep terrain at high elevations by ewes may therefore reflect habitat selection for parturition and lamb rearing rather than habitat selection for foraging. Our full movement model results indicated that ewes were more responsive to abiotic stressors (high temperatures and precipitation) in their use of elevation than were rams, while simultaneously selecting for NDVI more strongly than rams. Other wild sheep species also exhibit sex-specific habitat selection, with ewes prioritizing areas that will facilitate lamb growth and survival, and rams prioritizing foraging opportunities at the expense of access to safe terrain (Marchand et al. 2015). While our model did not identify strong selection for siNDVI by rams, we suspect that rams pursued highly digestible, freshly emergent plant material which had not yet reached peak siNDVI.

Of the candidate habitat selection variables, bighorn followed expected patterns of selecting for steep slopes and against distance from escape terrain (Spitz et al. 2020). Bighorn also selected against cosine-transformed aspect, possibly related to foraging opportunities, which are abundant on south-facing slopes during spring. Endpoint precipitation varied only marginally across space, and therefore could not be included as a habitat selection variable (Supplementary materials S4). However, endpoint temperature was highly variable and by moving across elevation, bighorn achieved considerable change in realized heat. In the habitat

selection models, bighorn selected strongly against endpoint temperature; a 1-standard

deviation increase in temperature was associated with a 59.6% likelihood of selecting that step.

Model comparison revealed that snowmelt timing was more important than green-up

timing for habitat selection by bighorn. Notably, however, we analyzed snowmelt using a daily

30m modeled fractional snow cover product (Rittger et al. 2021), whereas we analyzed green-

up using 16-day 250m MOD13Q1 satellite imagery (Didan 2015). We suspect the snow model

was selected over the green-up model due to the comparatively fine spatial and temporal

resolution of the snow product, coupled with spectral difficulties in determining vegetation

growth in high alpine barren landscapes using MODIS data. Combined, these factors could

result in the snow product revealing fine-scale landscape phenological variation that is masked

at coarser scales (Park et al. 2021). Because snowmelt and plant growth are so tightly linked in

alpine systems (e.g. Winkler et al. 2018, and Chapter 3 this dissertation), we attribute habitat

selection for snowmelt recency in this analysis to forage phenology and availability. Indeed, at

the coarse level, relative selection was strong for siNDVI (Figure 4.4A), suggesting that bighorn

selected for areas when NDVI at that site peaked. Further, selection for snowmelt recency

peaked at 106 days, just shorter than the average lag between peak snowmelt timing and peak

green-up timing.

The 3000m elevational gradient of the Sierra Nevada generates a broad ecoclimatic

window that bighorn sheep can use in response to both short- and long-term abiotic stressors.

Reduced future snowpack and higher temperatures at low-mid elevations along the Sierra

escarpment (Schwartz et al. 2017, Sun et al. 2019) will likely modify the historic pattern of

vegetation green-up, thereby complicating the balance between stress avoidance, forage

pursuit, and access to escape terrain. Since the delay between snowmelt and green-up timing is greatest at low elevations where snowmelt is earliest, increasingly early snowmelt at low-mid elevations may lead to a vertical contraction in the range of terrain where plant growth predictably and immediately follows snowmelt. Simultaneously, a higher frequency of hot days may drive bighorn away from areas at a peak phase of forage quality. Therefore, if abiotic stress avoidance and forage access are to be maintained, site visitation by bighorn during spring will likely shift toward higher elevations where escape terrain is nearby while maintaining a resource supply that is digestible and nutritious.

To better understand how movement responses to diel and seasonal environmental variation translate into nutritional and energetic outcomes, finer data on bighorn movement and landscape patterns in digestible nutrients are required. Work combining accelerometry and high-resolution remote sensing data could shed light on energy expenditure and intake, particularly if they are paired with measurements of bighorn body condition and plant nutrient concentration. Improving inference about individual survival and reproductive capacity, and ultimately carrying capacity at the level of management units, will facilitate conservation of existing Sierra bighorn populations and potentially inform site selection for future reintroductions.
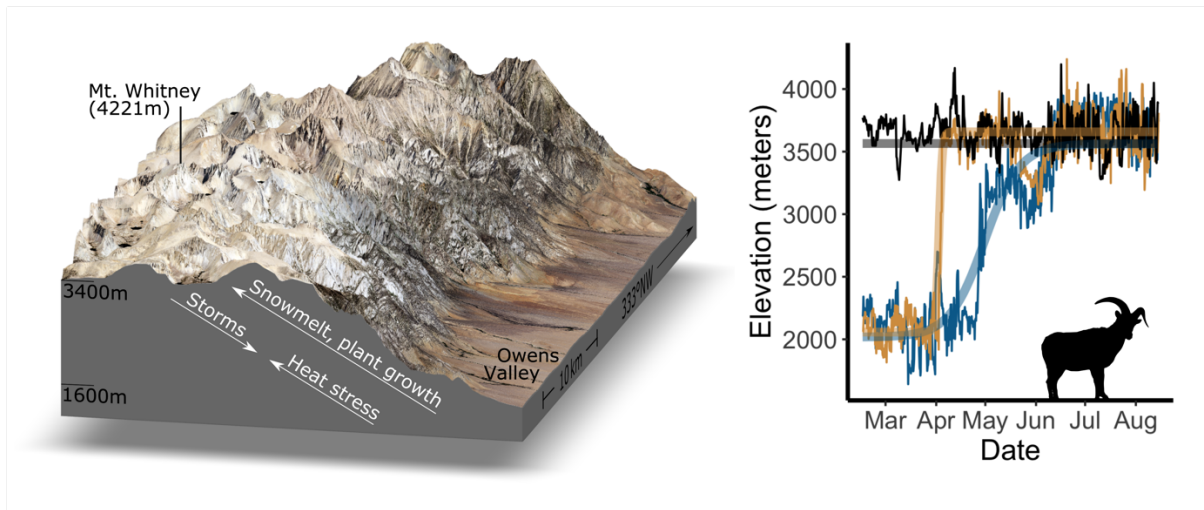
Figure 4.1. Sierra Nevada bighorn sheep confront variation in stressors and resources throughout spring migrations between low-elevation winter range and high-elevation summer range (left). For some individuals, spring migration follows a unidirectional, undistracted path (right, tan), whereas for others multiple up-and-down movements slow down the mean pace of vertical redistribution (blue). For yet other individuals, wintertime residency at high elevations leads to consistent use of a narrower range of elevational strata throughout the spring (black).
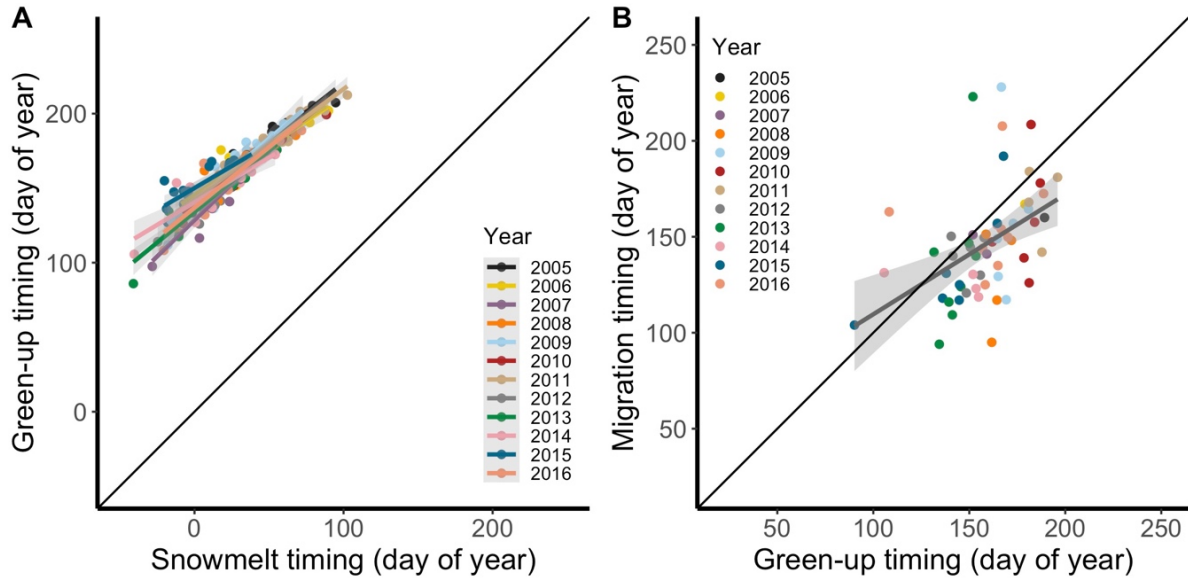
Figure 4.2. Green-up timing vs. snowmelt timing (A) and migration timing vs. green-up timing (B) aggregated at the herd unit level, 2005-2016.
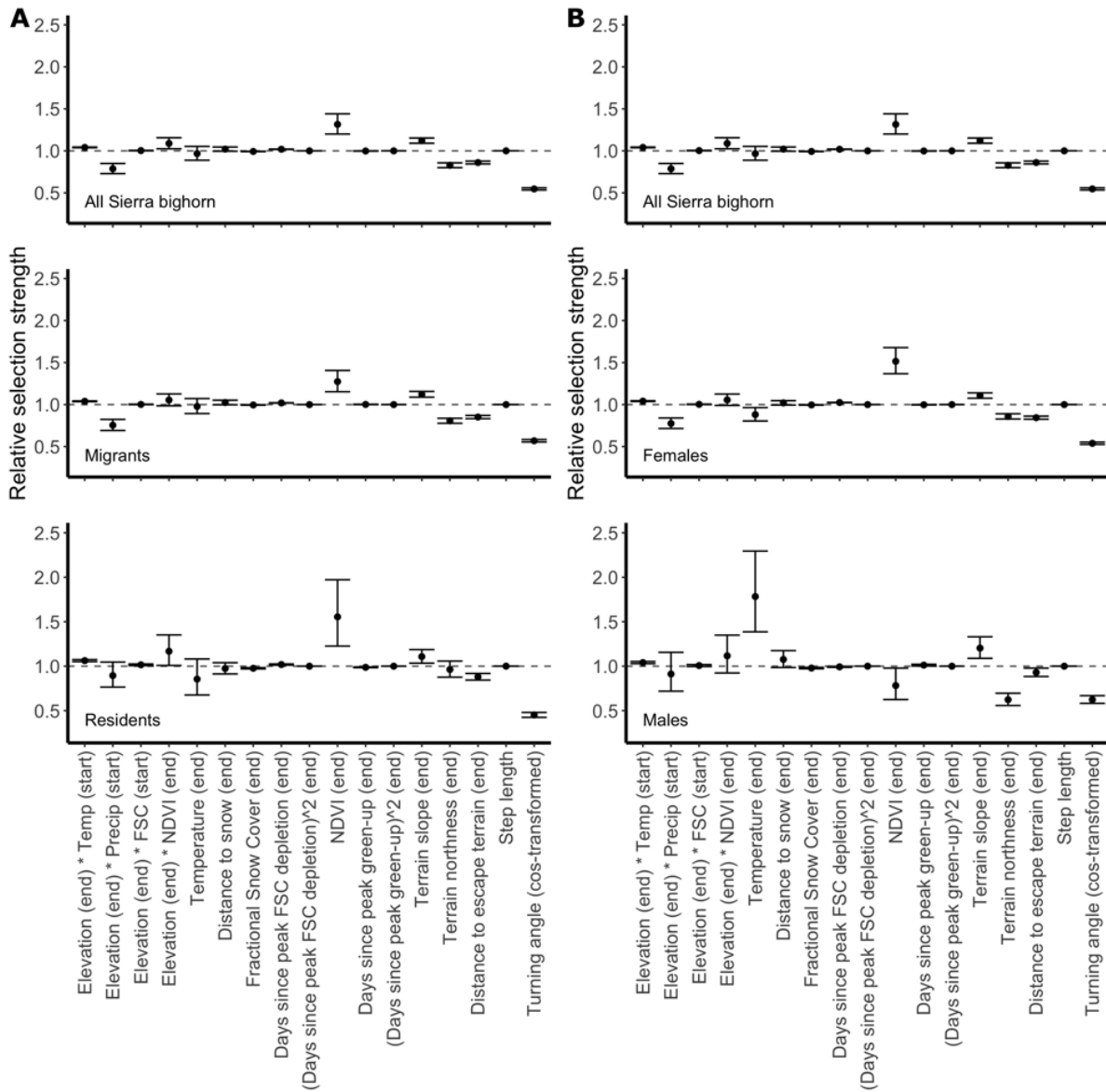
Figure 4.3. Full modeling results for population-level step selection analysis Sierra bighorn movement. Start and end parentheticals connote whether the value was collected at the initiation of a step or the terminus of a step, respectively.
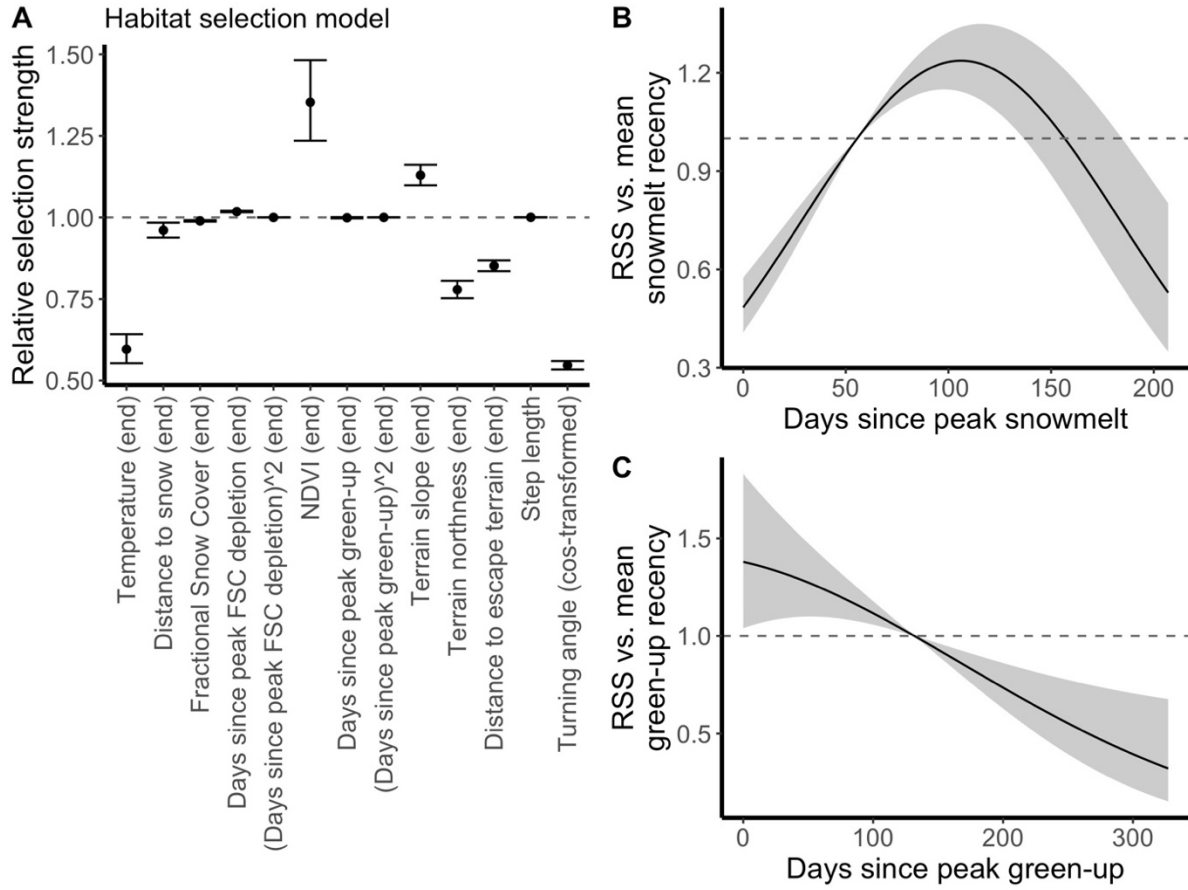
Figure 4.4. Relative selection strength (RSS) for Sierra bighorn in a habitat selection model (A) suggests selection for destination NDVI, steep terrain, and south-facing slopes during migration periods. Relative selection strength varies across snowmelt recency and green-up recency, including their polynomial terms (B, C, respectively).

References

Abrahms, B. et al. 2019. Memory and resource tracking drive blue whale migrations. - PNAS 116: 5582–5587.

Aikens, E. O. et al. 2017. The greenscape shapes surfing of resource waves in a large migratory herbivore. - Ecol Lett 20: 741–750.

Aikens, E. O. et al. 2020. Wave-like Patterns of Plant Phenology Determine Ungulate Movement Tactics. - Current Biology: S0960982220308484.

Albon, S. D. and Langvatn, R. 1992. Plant Phenology and the Benefits of Migration in a Temperate Ungulate. - Oikos 65: 502–513.

Anderson, K. et al. 2022. Cost distance models to predict contact between bighorn sheep and domestic sheep. - Wildlife Society Bulletin n/a: e1329.

Asam, S. et al. 2018. Relationship between Spatiotemporal Variations of Climate, Snow Cover and Plant Phenology over the Alps—An Earth Observation-Based Analysis. - Remote Sensing 10: 1757.

Avgar, T. et al. 2016. Integrated step selection analysis: bridging the gap between resource selection and animal movement. - Methods in Ecology and Evolution 7: 619–630.

Beck, P. S. A. et al. 2006. Improved monitoring of vegetation dynamics at very high latitudes: A new method using MODIS NDVI. - Remote Sens. Environ. 100: 321–334.

Bischof, R. et al. 2012. A Migratory Northern Ungulate in the Pursuit of Spring: Jumping or Surfing the Green Wave? - Am. Nat. 180: 407–424.

Boyle, W. A. et al. 2010. Storms drive altitudinal migration in a tropical bird. - Proceedings of the Royal Society of London B: Biological Sciences 277: 2511–2519.

Couriot, O. et al. 2018. Truly sedentary? The multi-range tactic as a response to resource heterogeneity and unpredictability in a large herbivore. - Oecologia in press.

Denryter, K. et al. 2021. Broadening the migratory portfolio of altitudinal migrants. - Ecology 102: e03321.

Didan, K. 2015. MOD13Q1 MODIS/Terra Vegetation Indices 16-Day L3 Global 250m SIN Grid V006.

Forshee, S. 2018. LIFE ON THE EDGE: RISK OF PREDATION DRIVES SELECTION OF HABITAT AND SURVIVAL OF NEONATES IN ENDANGERED SIERRA NEVADA BIGHORN SHEEP. - Graduate Student Theses, Dissertations, & Professional Papers in press.

Gorelick, N. et al. 2017. Google Earth Engine: Planetary-scale geospatial analysis for everyone. - Remote Sensing of Environment 202: 18–27.

Gurarie, E. et al. 2019. Tactical departures and strategic arrivals: Divergent effects of climate and weather on caribou spring migrations. - Ecosphere 10: e02971.

Hebblewhite, M. et al. 2008. A multi-scale test of the forage maturation hypothesis in a partially migratory ungulate population. - Ecological Monographs 78: 141–166.

Jesmer, B. R. et al. 2018. Is ungulate migration culturally transmitted? Evidence of social learning from translocated animals. - Science 361: 1023–1025.

John, C. and Post, E. 2022. Seasonality, niche management and vertical migration in landscapes of relief. - Ecography 2022: e05774.

Kauffman, M. J. et al. 2021. Causes, Consequences, and Conservation of Ungulate Migration. - Annual Review of Ecology, Evolution, and Systematics 52: 453–478.

La Sorte, F. A. and Graham, C. H. 2021. Phenological synchronization of seasonal bird migration with vegetation greenness across dietary guilds. - Journal of Animal Ecology 90: 343–355.

Marchand, P. et al. 2015. Coupling scale-specific habitat selection and activity reveals sex-specific food/cover trade-offs in a large herbivore. - Animal Behaviour 102: 169–187.

Morelli, T. L. et al. 2020. The fate of Madagascar's rainforest habitat. - Nat. Clim. Chang. 10: 89–96.

Park, D. S. et al. 2019. Herbarium specimens reveal substantial and unexpected variation in phenological sensitivity across the eastern United States. - Philosophical Transactions of the Royal Society B: Biological Sciences 374: 20170394.

Park, D. S. et al. 2021. Scale gaps in landscape phenology: challenges and opportunities. - Trends in Ecology & Evolution in press.

QGIS.org 2022. QGIS Geographic Information System.

R Core Team 2019. R: A Language and Environment for Statistical Computing.

Rittger, K. et al. 2021. Multi-sensor fusion using random forests for daily fractional snow cover at 30 m. - Remote Sensing of Environment 264: 112608.

Robinson, R. W. et al. 2020. Determining Timing of Births and Habitat Selection to Identify Lambing Period Habitat for Bighorn Sheep. - Frontiers in Ecology and Evolution in press.

Sawyer, H. and Kauffman, M. J. 2011. Stopover ecology of a migratory ungulate. - J. Anim. Ecol. 80: 1078–1087.

Schwartz, M. et al. 2017. Significant and Inevitable End-of-Twenty-First-Century Advances in Surface Runoff Timing in California's Sierra Nevada. - Journal of Hydrometeorology 18: 3181–3197.

Seebacher, F. and Post, E. 2015. Climate change impacts on animal migration. - Climate Change Responses in press.

Semenzato, P. et al. 2021. Behavioural heat-stress compensation in a cold-adapted ungulate: Forage-mediated responses to warming Alpine summers. - Ecology Letters 24: 1556–1568.

Spitz, D. B. et al. 2017. 'MigrateR': extending model-driven methods for classifying and quantifying animal movement behavior. - Ecography 40: 788–799.

Spitz, D. B. et al. 2018. How plastic is migratory behavior? Quantifying elevational movement in a partially migratory alpine ungulate, the Sierra Nevada bighorn sheep (Ovis canadensis sierrae). - Can. J. Zool. 96: 1385–1394.

Spitz, D. B. et al. 2020. Habitat predicts local prevalence of migratory behaviour in an alpine ungulate. - Journal of Animal Ecology 89: 1032–1044.

Sun, F. et al. 2019. Understanding End-of-Century Snowpack Changes Over California's Sierra Nevada. - Geophysical Research Letters 46: 933–943.

Thornton, M. M. et al. 2020. Daymet: Daily Surface Weather Data on a 1-km Grid for North America, Version 4. - ORNL DAAC in press.

U.S. Fish and Wildlife Service 2007. Recovery Plan for the Sierra Nevada Bighorn Sheep.: 1–199.

U.S. Geological Survey 2022. 10-Meter Resolution Digital Elevation Model.

van de Kerk, M. et al. 2021. Variation in movement patterns of mule deer: have we oversimplified migration? - Movement Ecology 9: 44.

van der Graaf, S. 2006. Surfing on a green wave - how plant growth drives spring migration in the Barnacle Goose Branta leucopsis. - Ardea 94: 567.

Wieczorek, G. F. and Jäger, S. 1996. Triggering mechanisms and depositional rates of postglacial slope-movement processes in the Yosemite Valley, California. - Geomorphology 15: 17–31.

Winkler, D. E. et al. 2018. Snowmelt Timing Regulates Community Composition, Phenology, and Physiological Performance of Alpine Plants. - Front Plant Sci in press.

Chapter 5: Projected bioclimatic distributions in Nearctic Bovidae signal the potential for reduced overlap with protected areas

Manuscript accepted for publication in *Ecology and Evolution*

Abstract

Assumptions about factors such as climate in shaping species' realized and potential

distributions underlie much of conservation planning and wildlife management. Climate and

climatic change lead to shifts in species distributions through both direct and indirect ecological

pressures. Distributional shifts may be particularly important if range overlap is altered

between interacting species, or between species and protected areas. The cattle family

(*Bovidae*) represents a culturally, economically, and ecologically important taxon that occupies

many of the world's rangelands. In contemporary North America, five wild bovid species inhabit

deserts, prairies, mountains, and tundra from Mexico to Greenland. Here, we aim to

understand how future climate change will modify environmental characteristics associated

with North American bovid species relative to the distribution of extant protected areas. We fit

species distribution models for each species to climate, topography, and land cover data using

observations from a citizen science dataset. We then projected modeled distributions to the

end of the 21st century for each bovid species under two scenarios of anticipated climate

change. Modeling results suggest that suitable habitat will shift inconsistently across species,

and that such shifts will lead to species-specific variation in overlap between potential habitat

and existing protected areas. Furthermore, projected overlap with protected areas was

sensitive to the warming scenario under consideration, with diminished realized protected area

under greater warming. Conservation priorities and designation of new protected areas should account for ecological consequences of climate change.

Keywords

Bovidae, Climate change, Conservation, Species distribution modeling, MaxEnt, Range shift

Introduction

Elevational and latitudinal shifts in species' ranges constitute widely documented ecological responses to climate change (Chen *et al.*, 2011; Büntgen *et al.*, 2017; Williams and Blois, 2018). Through both direct (e.g. thermal stress) and indirect (e.g. temperature-mediated natural enemy activity) mechanisms, climate shapes species distributions across local, regional, and global scales (Araújo and Luoto, 2007). As ongoing human pressure further shapes contemporary species distributions (Laliberte and Ripple, 2004; Faurby and Araújo, 2018), identifying factors associated with species presence and measuring how these factors will change lends insight on how potential species distributions may shift in the coming decades. Effective conservation planning therefore relies on well-defined forecasts of change in species distribution (Rodríguez *et al.*, 2007). Yet, for many species, the extent to which future distributions will overlap with existing protected areas remains unresolved (IPBES, 2019).

The designation of effective protected areas requires balancing the immediate needs of imperiled species with anticipated conditions decades or centuries into the future. Although the establishment of protected areas has increased dramatically over the past century (Watson *et al.*, 2014), the density, area, and governance of protected areas varies considerably across space (Bingham *et al.*, 2019; UNEP-WCMW and IUCN, 2021). As conserved spaces continue to

be planned and adopted, formal analyses of interactions among climate and geographical

factors governing species distributions and projected changes in them will aid in the

prioritization of areas to protect (Monzón, Moyer-Horner and Palamar, 2011; Scridel *et al.*,

2021; Sierra-Morales *et al.*, 2021). Biotic interactions may yet further control species

distributions, especially for herbivores that specialize on particular food resources (e.g. Beumer

et al., 2019). Thus, effective conservation planning will take into account not only future change

in temperature and precipitation, but also shifts in vegetation distributions and landcover

types.

In North America, the mammalian family *Bovidae* is represented by five extant species:

bighorn sheep (*Ovis canadensis*), thinhorn sheep (*Ovis dalli*), North American bison (*Bison

bison*), mountain goat (*Oreamnos americanus*), and muskox (*Ovibos moschatus*). These species

constitute a broad-ranging phylogeographic clade that survived marked warming at the end of

the Pleistocene. Today, they occupy deserts, prairies, tundra, and alpine zones across the

Nearctic (Castelló, 2016). The bovid species of North America accumulated a legacy of hunting,

introduced disease, and human development, leading to shifts in abundance, migratory

propensity, and distributions.

Here, we fit and project Ecological Niche Models (ENMs) for Nearctic bovid species

under two scenarios of anticipated climate change generated using occurrence data from a

public database of species observations. We relate modeled current and future species

distributions to existing protected areas, with the goals of identifying how environmental

parameters may shift in the coming decades, and how well current protected areas align with

modeled distributions. We discuss our modeling results in the context of other work on conservation and spatial variation in wild bovids.

Methods

Species presence data

Species presence data were downloaded from the Global Biodiversity Information Facility ("GBIF" (GBIF, 2022)). This database includes species presence observations from museum collections, university records, and citizen science contributions. Presence data were extracted using the `rgbif` library in R v.3.6.1 (Chamberlain *et al.*, 2021), with GBIF taxon key associated with each of the five North American bovids (*Ovis canadensis*, 2441119; *Ovis dalli*, 2441118; *Oreamnos americanus*, 2441151; *Ovibos moschatus*, 2441108; and *Bison bison*, 2441176), as well as the remaining North American members of Artiodactyla (*Antilocapra americana*, 2440902; *Odocoileus hemionus*, 2440974; *Odocoileus virginianus*, 2440965; *Cervus canadensis*, 8600904; *Alces alces*, 4262283; *Rangifer tarandus*, 5220114; and *Dicotyles tajacu*, 2440996). Occurrence data were sent through a cleaning process to remove biased, uninformative, or inappropriate observations (for a full description of removed observations see "Biodiversity data" in Supplementary materials S5.1). First, points with missing geographic information were censored. Next, observations outside of North America were removed, as were cases where observation locations did not correspond with observation country. Records with no associated observation date, and records with observation date prior to 1980, were removed. Finally, irrelevant observation locations (e.g. bighorn sheep at the Chicago Zoo) were removed.

Data generated through citizen science collection face concerns over validity and sampling bias (Yesson *et al.*, 2007; Beck *et al.*, 2013). The dataset we used constitutes a set of charismatic, easily-identified species, in a generally well-sampled geographic region (see supplementary materials S5.1, Biodiversity Data). Because presence-only species distribution models are sensitive to spatial biases in sampling effort (Phillips *et al.*, 2009), we used occurrence data from the full set of North American even-toed ungulates to generate a sampling bias grid, which was used during the background data generation (described below). Furthermore, we coarsened the resolution of the predictor dataset to accommodate uncertainty in observation location. However, our efforts to control for biases in species presence data limit the resolving power of species distribution, and we were thus unable to account for effects of microclimate (e.g. Lembrechts et al., 2019) in our models, or incorporate anticipated fine-scale change in our projections.

Climate, land cover, and topography data

Historical and projected Worldclim v. 2.1 data (Fick and Hijmans, 2017), present and future GCAM land cover data (Chen *et al.*, 2020), and North America Elevation GRID data (available at https://www.sciencebase.gov/catalog/item/4fb5495ee4b04cb937751d6d) were used as baseline environmental covariates. All predictors were coarsened to 6x6km pixels in an equal-area projection to accommodate spatial uncertainty and match the resolution of the coarsest predictor data product in species occurrence data using bilinear interpolation.

Current and future climate data were accessed from the Worldclim v. 2.1 dataset. We selected data generated from all eight available global climate models (GCMs; BCC-CSM2-MR, CanESM5, CNRM-CM6-1, CNRM-ESM2-1, IPSL-CM6A-LR, MIROC-ES2L, MIROC6, and MRI-ESM2-

0) under two shared socio-economic pathways (SSPs; SSP2-4.5 and SSP5-8.5) for the period

2081-2100. SSPs were adopted with the CMIP6 models, and incorporate socioeconomic growth

with the previously-used representative concentration pathways (Riahi *et al.*, 2017). SSP2

reflects a future with moderate development, on track with historical growth and inequality,

but with reduced dependence on fossil fuels; whereas SSP5 reflects a future with accelerating

socioeconomic development and reduced global inequality, but with a heavy reliance on fossil

fuels. SSP2-4.5 predicts about 3°C warming by the end of this century, while SSP5-8.5 predicts

about 5°C warming relative to the 1850-1900 average (Tebaldi *et al.*, 2021). Data on future

conditions were re-centered and transformed according to the approach described for

historical data above.

Current and future (2081-2100) land use/land cover data were accessed from the GCAM

Demeter land use dataset (Chen *et al.*, 2020). GCAM data are reported by cover type on a

fractional scale from 0-100, where 100 indicates the pixel is saturated by that type. We

aggregated each of the GCAM tree cover types into their respective biome (PFT4 and 6; 1, 5,

and 7; and 2, 3, and 8 representing tropical, temperate, and boreal trees, respectively), and

PFT15-30 into an umbrella category, "Agriculture", to reduce the size of the candidate predictor

pool. Thus, from the GCAM data we included 14 vegetation layers, an agriculture layer, a barren

layer, and an urban layer. We used the SSP1-2.6 2015 model to index current land cover

conditions. Because GCAM data are not available for the same CMIP6 models as Worldclim, we

condensed the five available models of land use futures into their respective SSP scenarios

(SSP2-4.5 and SSP5-8.5) by taking the mean value of each fractional land cover type for each

pixel across the five available models. The "current" SSP1-2.6 scenario was also condensed from the five available models.

To account for topographic constraints on species distribution, we included elevation and terrain ruggedness as predictors. Terrain ruggedness (TRI) was calculated following standard gdal protocols (GDAL/OGR contributors, 2021). Finally, elevation and TRI were centered by subtracting the mean layer value from all grid cells within each layer. Topography data were treated as static, and therefore the same topography products were used for present and future (2081-2100) datasets.

Vector spatial data

Land boundaries of North America were extracted from the rnaturalearth::ne_countries() dataset (South, 2017). The periphery of the Greenland Inland Ice Sheet was delineated by vectorizing all cells classified as "ice" in the raster version of the Circumpolar Arctic Vegetation Map (Raynolds *et al.*, 2019). Protected area boundaries were identified using the World Database of Protected Areas (UNEP-WCMW and IUCN, 2021), and filtered to include only polygons with area greater than 100km^2.

Statistical modeling

Complete details on overview, data, model design, assessment, and prediction (ODMAP; (Zurell *et al.*, 2020)) are available in Supplementary materials S5.1. MaxEnt v. 3.4.3 models (Phillips, Dudík and Schapire, 2021) were fit to presence and background locations for each bovid species. We used the `SDMtune` library (Vignali *et al.*, 2020) to fit, evaluate, and generate predictions with MaxEnt models. For each species, a MaxEnt model was constructed using the

following approach: Occurrence records were spatially thinned to a radius of 6km. A bias grid

was generated using occurrence data from all North American artiodactyl species to account for

sampling bias in occurrence data (Phillips *et al.*, 2009). We assumed that sampling bias was

equivalent across Artiodactyla, given that they are large, charismatic, and easily identifiable,

and therefore used one bias grid for the continent. The bias grid was calculated by generating a

continental raster with 6x6km pixel resolution, identifying all pixels containing artiodactyl

species occurrences, and applying a 2-dimensional kernel density estimator with a normal

reference bandwidth. Ten thousand background points were randomly sampled from the bias

grid in lieu of absence data for model fitting for each species. Occurrence and background data

were subdivided into 60% training, 20% validation, and 20% testing partitions. Naïve MaxEnt

models were fit with training data and spatial cross-validation using the checkerboard1 function

in the R package ENMeval (Kass *et al.*, 2021). To minimize model complexity and reduce the

likelihood of overfitting, we considered only linear and quadratic feature classes (Elith *et al.*,

2011). We assumed no *a priori* knowledge of factors associated with species presence and

therefore included all 19 bioclimatic variables, all topographic covariates, and all land cover

indices in the naïve models. A data-drive variable selection procedure was then employed to

remove highly correlated predictor variables, based on a Spearman correlation threshold of 0.7

(Vignali *et al.*, 2020). After removing correlated predictors, models were optimized for

complexity using a genetic algorithm to identify the most robust combination of model

hyperparameters. We considered regularization multipliers between 0.5 (most complex) and 10

(least complex) and linear as well as linear+quadratic feature classes. Finally, we removed non-

important variables from the optimized models to maximize parsimony using a leave-one-out

jackknife test. We refer to these optimized models with selected variables as the "final model"
for each species. Final model reports were generated for each species (summarized in
Supplementary materials S5.3).

Species distributions were predicted using final models and three raster stacks:
"current" conditions defined by the training data, and two future scenarios (SSP2-4.5 and SSP5-
8.5), both for the period spanning 2081-2100. Because MaxEnt models generate continuous
prediction surfaces, model-specific response thresholds were used to differentiate between
predicted "presence" and "absence". We used two thresholds (Liu, White and Newell, 2013):
one with equal model sensitivity and specificity (ESS), and one which maximized the sum of
sensitivity and specificity (MSS). For each future SSP scenario, model consensus was calculated
as the sum of the MaxEnt model predictions under each GCM that were above the MSS
threshold, based on a comparison between the two thresholds under current conditions
revealing few differences except for a more constrained bison range using MSS. Correlative
distribution modeling approaches such as MaxEnt are limited by uncertainty in future
conditions, non-analogue conditions, and exclusion of endogenous factors that may allow
species to adapt or tolerate future change (Dawson *et al.*, 2011). Uncertainty in climate
forecasts was accounted for by compositing modeled species distributions across
environmental covariates predicted under a suite of GCM models. To account for non-analogue
conditions, we applied a clamping procedure to prevent projecting results outside the range of
conditions present during model training. We also generated multivariate environmental
similarity surfaces ("MESS grids"), and limited predictions to areas with positive MESS values
(Elith, Kearney and Phillips, 2010). MESS grids were calculated using the R package dismo

instantiation of `mess()` with all continuous predictors in the dataset, and are shown in Supplementary materials S5.1. We were unable to account for species' adaptive potential, and thus limit our interpretation of the results below to anticipated change in distribution of environmental characteristics associated with bovid species presence, rather than distribution of bovid species themselves.

Comparisons among species of land area, range elevation, range latitude, and realized protected area, were calculated by taking the mean value of current and projected data layers grouped by species and SSP. Standard errors of mean projected range measurements were calculated by treating GCM as a replicate. All analyses were performed in R v. 4.1.2 (R Core Team, 2019).

Results

We accessed 32,999 North American bovid records from GBIF. We removed 14,514 observations during data quality checks and 14,927 during data thinning, leaving 3,558 records for model fitting. Within the cleaned, thinned dataset, bighorn sheep were represented by 1915 records, thinhorn sheep by 218 records, mountain goats by 659 records, muskoxen by 218 records, and North American bison by 519 records.

In general, modeled potential habitat shifted in response to projected climate change in 2081-2100 (Figure 5.1). Modeled future habitat covered less area under the SSP5-8.5 scenario than under the SSP2-4.5 scenario for all species except thinhorn sheep (Table 5.1). Projected change in the surface area of modeled habitat was inconsistent across species, but with a trend of increasing change at higher latitudes (Table 5.1). For example, over a quarter of modeled potential habitat space is expected to be lost for thinhorn sheep by 2100 regardless of the SSP,

while the projected change for bighorn sheep is less coherent. The total area of modeled

potential habitat was never consistently higher under both scenarios for any species (although

modeled potential habitat increased slightly under SSP2-4.5 for bighorn sheep and mountain

goats).

Projected elevational range shifts were variable among species (Supplementary

materials S5.2). Whereas projections for bighorn sheep featured marginal elevational change

(current mean elevation = 1527m; SSP2-4.5 mean elevation = 1537±5m; SSP5-8.5 mean

elevation = 1583±7m), stronger elevational contraction was evident for thinhorn sheep (current

mean elevation = 826m; SSP2-4.5 mean elevation = 932±17m; SSP5-8.5 mean elevation =

934±44m). Projected latitudinal range shifts were similarly variable among species. For

example, modeled muskox habitat faces a significant northward contraction due to limited

available land area further north (current mean latitude = 68.1°N; SSP2-4.5 mean latitude =

71.7±0.4°N; SSP5-8.5 mean latitude = 74.5±0.5°N), while modeled mountain goat habitat shifts

slightly southward (current mean latitude = 53.1°N; SSP2-4.5 mean latitude = 52.2±0.4°N; SSP5-

8.5 mean latitude = 51.8±0.9°N).

Overlap between ENM projections and current protected areas varied among species,

and future overlap is expected to vary by species as well (Figure 5.2). Whereas habitat of

southerly montane species with minimal projected range shifts (bighorn sheep and mountain

goats) is not projected to face significant change in potential protected area, habitat of

northerly species such as thinhorn sheep and muskoxen is projected to face a considerable

reduction in potential protected area (38.6% and 43.1% of protected area for thinhorn sheep

and muskoxen, respectively, under SSP2-4.5, and 30.5% and 62.9% under SSP5-8.5). Projected

loss of potential protected area for bison followed a similar pattern (55.3% and 59.3% for SSP2-4.5 and SSP5-8.5 respectively). For the only obligate Arctic species, muskoxen, the projected reduction in potential protected area is considerably greater under the SSP5-8.5 scenario than under SSP2-4.5 (nearly 20% greater reduction in potential protected area under SSP5-8.5).

The proportion of potential species distributions that overlaps with protected area, and the proportion of protected area that overlaps with potential distributions, reveal different patterns in potential protected area among the bovid species (Figure 5.3). Although approximately proportional loss of protected area relative to potential species distributions is projected across the five North American bovid species (indicated by overlapping current and projected estimates in Figure 5.3a), the percentage of currently protected area that is projected to feature environments characterized by bovid presence is projected to drop across SSP's for thinhorn sheep, muskox, and American bison (indicated by the marked reduction in fraction of protected area estimated for these species in Figure 5.3b).

Discussion

We identified discordant projections by Maxent distribution models across Nearctic bovids. Inconsistent projections among species arose through two processes: unequal response by species to different topographic, land cover, and bioclimatic variables, and uneven projected environmental change across space. Projected potential habitat shifts in response to anticipated climate change are greatest for species at high latitudes, where observed warming outpaced change at lower latitudes, and is expected to continue to do so (Post, Steinman and Mann, 2018; Post *et al.*, 2019). Furthermore, for some species, the total area of potential protected space is projected to decrease more dramatically under the higher emissions

scenario, SSP5-8.5. Shifts in climatically suitable habitat seem likely for other high latitude

species, where effects of climate change are amplified.

Other species distribution modeling efforts corroborate the importance of human

impacts, terrain, and land cover characteristics for ungulate distributions (Kuemmerle *et al.*,

2012; Herrera-Sánchez *et al.*, 2020; Jenkins *et al.*, 2020). To our knowledge this is the first study

to simultaneously explore future distributions of multiple North American bovids in the context

of protected areas. However, modeling studies that employ different data sources and different

scales of analysis have uncovered important relationships between bovid species and their

environment that help contextualize our findings.

In a recent study, a MaxEnt model for desert bighorn sheep (*Ovis canadensis nelsoni*)

was hindcast to investigate range dynamics during the mid-Holocene (Gámez-Brunswick and

Rojas-Soto, 2020). Although this subspecies occupies only a portion of the total range of

bighorn sheep, the modeled current potential distribution of desert bighorn in that study

largely mirrors the current potential distribution of bighorn sheep across the southwest United

States predicted by our models. Importantly, our results suggest that potential habitat extends

further northward along the American cordillera than either the hindcast model of desert

bighorn or the actual current distribution of bighorn sheep (Brewer *et al.*, 2014). The predicted

presence of bighorn sheep through Yukon and Alaska likely relates to the similar life history

requirements of the closely related thinhorn sheep (*Ovis dalli*), which inhabits these higher

latitude regions of the cordillera. Indeed, among the selected predictor variables that were

shared among bighorn and thinhorn sheep Maxent models, most univariate response curves

were approximately comparable with shifted centers. Furthermore, a comparison of the two

species' modeled distributions reveals considerable overlap north of British Colombia. It is possible that the lack of bighorn sheep at high latitudes stems from competitive exclusion by thinhorn sheep, or through fine-scale environmental variation that was not evident at the scale of our study.

Maxent distribution models have also been used to examine spatial dynamics of muskoxen at local to regional, but not continental scales (Beumer *et al.*, 2019; Jenkins *et al.*, 2020; van Beest *et al.*, 2021). In those applications, GPS collars and systematic human observations were used to identify environmental covariates underlying muskox distribution in Northeast Greenland and the Canadian Arctic. Across levels of analysis, elevation emerged as an important covariate of muskox distribution, following the same tendency of selection toward low elevations we found here (Beumer *et al.*, 2019; Jenkins *et al.*, 2020). Notably, our variable selection and model optimization process did not retain the same bioclimatic variables that were selected in one study using Worldclim2 data (van Beest *et al.*, 2021), but that work included a subset of candidate predictor variables, used a coarser covariate resolution (20km), and the study extent was limited to northeast Greenland, as opposed to our 6km analysis of North America.

The results of this modeling study suggest a broader spatial range of present potential habitat than is realized for any of these five bovid species (Meagher, 1986; Côté and Festa-Bianchet, 2003; Demarchi and Hartwig, 2004; Brewer *et al.*, 2014; Cuyler *et al.*, 2020). For example, predictions from the muskox model indicate that Southampton and Baffin Islands are within the potential distribution of muskox, yet that species is not known to live there. Overprediction of actual distributions may have resulted from the coarse nature of our

predictor data (6x6km pixels), limiting factors that we were not able to account for (e.g. predation, important forage species, or habitat fragmentation by non-permeable barriers), or more complex responses to environmental variables than we allowed in our modeling design (such as absolute thermal tolerance thresholds or interactions among variables). Thus, the modeling results should be interpreted in the context of predicted change in environmental factors associated with bovid presence, rather than spatial redistribution of bovid species themselves.

The predictive ability of species distribution models is limited by the extent to which current predictor variables relate to the environment at the time of occurrence data collection, and the degree to which covariate forecasts represent future conditions. Worldclim data are least reliable in mountainous terrain, where fine-scale complexity overwhelms broad geographic variation and in remote areas where only sparse meteorological records were available for model training (Hijmans *et al.*, 2005; Fick and Hijmans, 2017). Furthermore, species distribution forecasts may be sensitive to inconsistent variation among modeled bioclimatological futures (Cerasoli, D'Alessandro and Biondi, 2022), and uncertainty related to the underlying GCMs (Foley, 2010; Bedia, Herrera and Gutiérrez, 2013). Finally, predicted future distributions rest upon assumptions about future change; for example, GCAM land use data incorporates no developments in urbanization through the end of the century, and modeled vegetation change stems only from land use impacts, as opposed to vegetation response to warming (Chen *et al.*, 2020), which is complex (Myers-Smith *et al.*, 2020) and important for spatial dynamics of large herbivores (Tape *et al.*, 2016).

Our model projections are based on relationships between observations of bovids and environmental factors where they were observed. In reality, drivers of range dynamics in large herbivores are complex and unlikely to relate directly to climatological variability. Instead, indirect effects of climate such as forage distribution and phenology, distribution of competitors and natural enemies, and frequency and severity of extreme weather events are likely to play important roles in changes in species distributions related to climate change (Parmesan, Root and Willig, 2000; Creel *et al.*, 2005; Winnie, Cross and Getz, 2008; Ponti and Sannolo, 2022). Historical relationships among humans and megafauna may drive patterns in species distribution, particularly if species are refugees from human exploitation (Cromsigt, Kerley and Kowalczyk, 2012). The importance of human impacts was evident for several of the species we investigated; for example, fractional agriculture and urban cover were the second- and third-most important variables in the thinhorn sheep model, which revealed strong patterns of selection against both cover types. Agriculture was the fifth-most important variable in the bison model, which showed a weaker pattern of selection against urban cover. While agriculture and urban land cover did not emerge as important factors in other models, it is likely that a more precise land cover data product (both in terms of spatial resolution and cover type) would reveal significant human effects. For example, the Human Footprint Index (1km resolution) may uncover fine-scale impacts of light and infrastructure on current bovid distributions that we could not explore here (Venter *et al.*, 2016), but a comparable forecast product is not currently available. Further, the ability of bovid populations to redistribute in the future will be limited by not only available destination space, but also by barriers to movement (Sawyer *et al.*, 2013; McInturff *et al.*, 2020).

Conservation planning is sensitive to biases in species distribution models (Wilson *et al.*, 2005), and we emphasize the need to incorporate multiple approaches and lines of evidence in planning future protected areas. Furthermore, although spatial priorities for protected areas increasingly rely on species distribution projections under climate change, they often ignore human response to climate change (Post and Brodie, 2015; Jones *et al.*, 2016). Human influence on the landscape limits movements by animals, which may ultimately lead to the local exclusion of broad-ranging migrants (Tucker *et al.*, 2018). Other work on large bovids has emphasized the importance of anthropogenic influence on habitat suitability (Epps *et al.*, 2005; Kuemmerle *et al.*, 2010). We were unable to include movement barriers and some human impacts on species ranges, such as roads and fencing, tourism, and recreation. More precise estimates of future suitable habitat for large herbivores will become possible as forecasts of anthropogenic change across the landscape become clearer.

Most immediately, North American bovids contend with alteration of existing suitable habitat (Krausman and Bleich, 2013), limitations on movement between seasonal ranges (Courtemanch *et al.*, 2017; Stoellinger *et al.*, 2020), and introduction of zoonotic disease (Clifford *et al.*, 2009). These threats are difficult to predict, and changes in their distribution and magnitude should be considered while crafting management and conservation plans. Of the protected areas that are already home to wild bovids, those which are expected to retain ecological and climatic characteristics that are associated with bovid presence may become especially important in the coming decades. As conservation planners make decisions about designation of new protected areas, it will be imperative to consider not just the future distribution of Nearctic bovids, but also future conditions for ecosystem services and human

response to change (IPBES, 2019). Protected areas conserve ecosystem function, culturally

important settings, recreational hotspots, and natural resources. However, if biodiversity, or

the longevity of a particular species is the goal, future climatological conditions and their

implication for the focal species and increased human access to remote regions should be a top

consideration in the prioritization of protected lands.
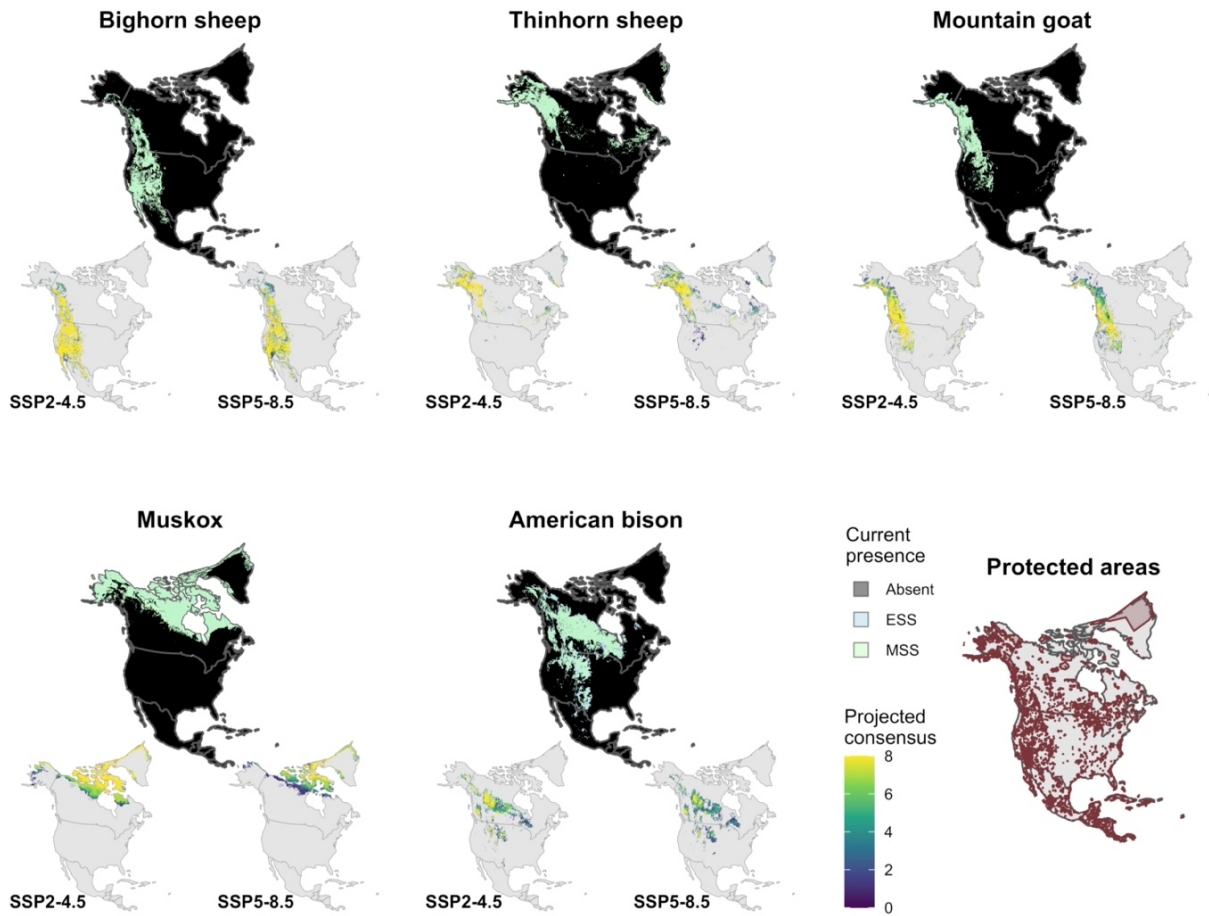
Figure 5.1. Predicted current potential habitat (top subplots) and consensus future potential habitat under future conditions in 2081-2100 modeled using two SSPs (bottom subplots) for each Nearctic bovid species. For the current plots, predicted potential habitat is indicated by pale blue (for the ESS threshold) and pale green (for the MSS threshold). For the consensus plots, the fill value increases in intensity with increasing predicted suitability across GCMs (using the MSS threshold). Protected areas indicated by merlot polygons, data from (UNEP-WCMW and IUCN, 2021).
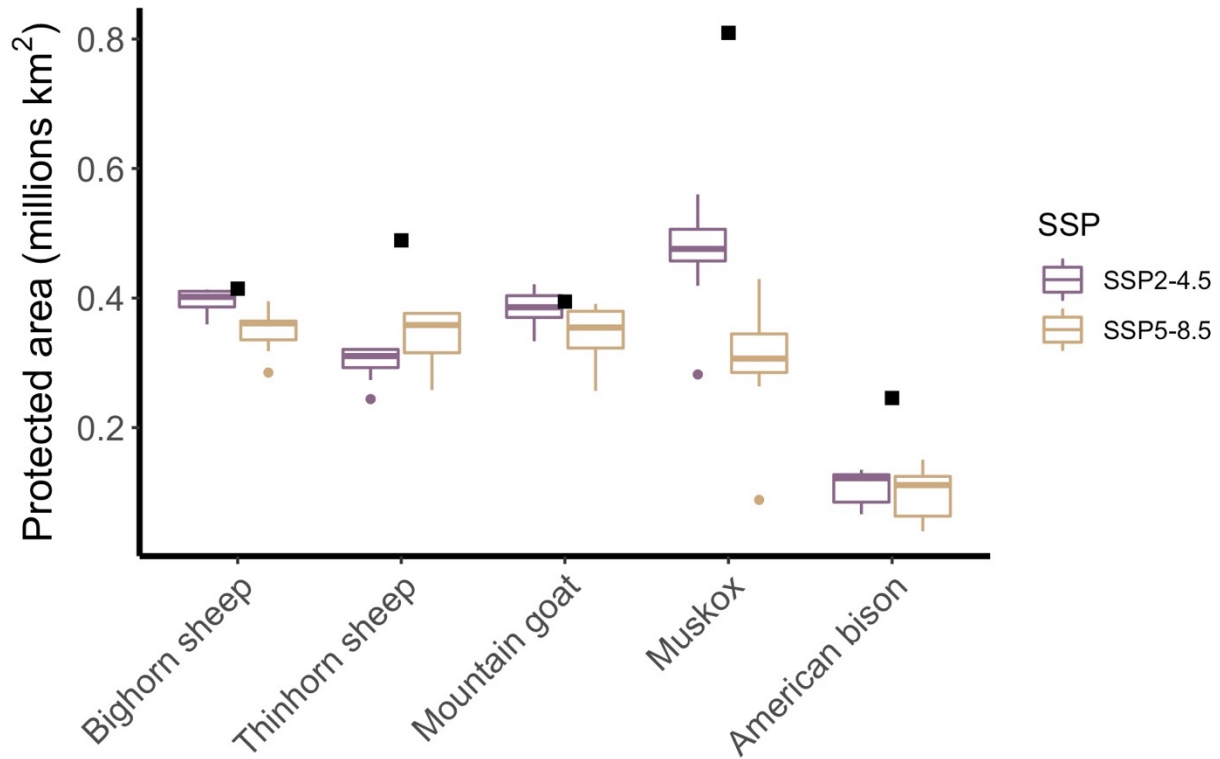
Figure 5.2. Protected area of modeled species distributions in millions of km^2. Squares indicate the land area of modeled current distributions that fall within protected areas, and boxes illustrate land area for modeled future distributions within protected areas under projected conditions for 2081-2100 under SSP2-4.5 (purple) and SSP5-8.5 (tan).
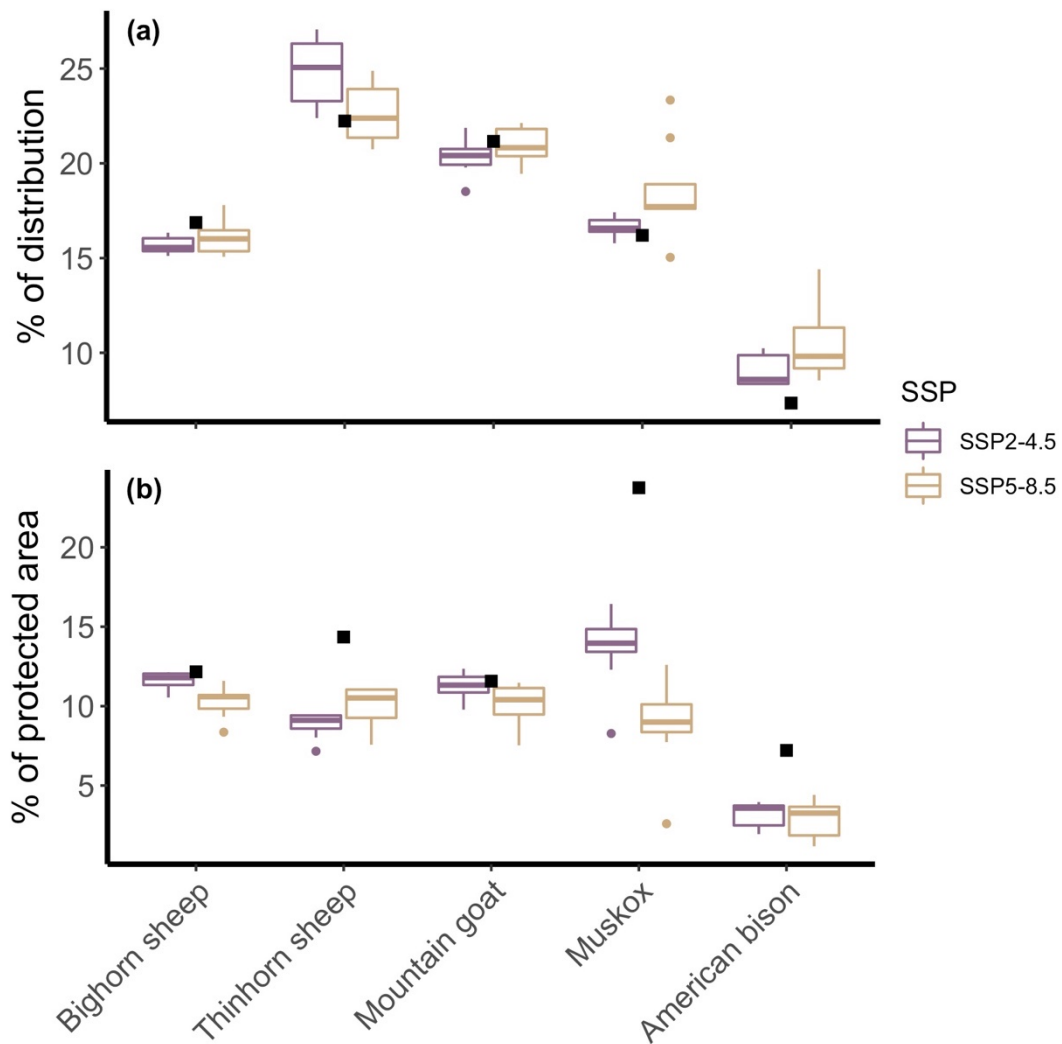
Figure 5.3. Potential protected area expressed as a percentage of potential species distributions (a) and as a percentage of currently protected area (b). In a, the proportion is calculated based on the percentage of each species, GCM, and SSP-specific potential distribution that overlaps with protected areas. In b, the proportion is calculated based on the percentage of currently protected areas that overlap with each species, GCM, and SSP-specific potential distribution. Black dots indicate current potential distribution estimates, purple boxes show variation in SSP2-4.5 scenarios across GCMs, and tan boxes show variation in SSP5-8.5 scenarios across GCMs.

Tables

Table 5.1. Surface area of modeled species distributions under current (1970-2000) and projected future (2081-2100) conditions, expressed in millions of km^2.

Species	Current	SSP2-4.5	SSP5-8.5
Bighorn sheep	2.46	2.53 ± 0.04	2.18 ± 0.09
Thinhorn sheep	2.20	1.21 ± 0.04	1.50 ± 0.09
Mountain goat	1.86	1.89 ± 0.04	1.65 ± 0.08
Muskox	5.00	2.77 ± 0.16	1.62 ± 0.21
American bison	3.34	1.22 ± 0.14	1.01 ± 0.18

References

Araújo, M.B. and Luoto, M. (2007) 'The importance of biotic interactions for modelling species distributions under climate change', Global Ecology and Biogeography, 16(6), pp. 743–753. doi:https://doi.org/10.1111/j.1466-8238.2007.00359.x.

Beck, J. et al. (2013) 'Online solutions and the "Wallacean shortfall": what does GBIF contribute to our knowledge of species' ranges?', Diversity and Distributions, 19(8), pp. 1043–1050. doi:https://doi.org/10.1111/ddi.12083.

Bedia, J., Herrera, S. and Gutiérrez, J.M. (2013) 'Dangers of using global bioclimatic datasets for ecological niche modeling. Limitations for future climate projections', Global and Planetary Change, 107, pp. 1–12. doi:10.1016/j.gloplacha.2013.04.005.

van Beest, F.M. et al. (2021) 'Rapid shifts in Arctic tundra species' distributions and inter-specific range overlap under future climate change', Diversity and Distributions, 27(9), pp. 1706–1718. doi:10.1111/ddi.13362.

Beumer, L.T. et al. (2019) 'Spatiotemporal dynamics in habitat suitability of a large Arctic herbivore: Environmental heterogeneity is key to a sedentary lifestyle', Global Ecology and Conservation, 18, p. e00647. doi:10.1016/j.gecco.2019.e00647.

Bingham, H.C. et al. (2019) 'Sixty years of tracking conservation progress using the World Database on Protected Areas', Nature Ecology & Evolution, 3(5), pp. 737–743. doi:10.1038/s41559-019-0869-3.

Brewer, C.E. et al. (2014) 'Bighorn Sheep: Conservation Challenges and Management Strategies for the 21st Century', Wild Sheep Working Group, Western Association of Fish and Wildlife Agencies, Cheyenne, Wyoming, USA [Preprint]. Available at: https://wafwa.org/wpdm-package/bighorn-sheep-conservation-challenges-management-strategies-for-the-21st-century/ (Accessed: 4 May 2022).

Büntgen, U. et al. (2017) 'Elevational range shifts in four mountain ungulate species from the Swiss Alps', Ecosphere, 8(4), p. e01761. doi:10.1002/ecs2.1761.

Castelló, J.R. (2016) Bovids of the World. Princeton, New Jersey (USA): Princeton University Press. Available at: https://press.princeton.edu/books/paperback/9780691167176/bovids-of-the-world (Accessed: 4 March 2021).

Cerasoli, F., D'Alessandro, P. and Biondi, M. (2022) 'Worldclim 2.1 versus Worldclim 1.4: Climatic niche and grid resolution affect between-version mismatches in Habitat Suitability Models predictions across Europe', Ecology and Evolution, 12(2), p. e8430. doi:10.1002/ece3.8430.

Chamberlain, S. et al. (2021) rgbif: Interface to the Global 'Biodiversity' Information Facility API. Available at: https://CRAN.R-project.org/package=rgbif (Accessed: 26 July 2021).

Chen, I.-C. et al. (2011) 'Rapid Range Shifts of Species Associated with High Levels of Climate Warming', Science, 333(6045), pp. 1024–1026. doi:10.1126/science.1206432.

Chen, M. et al. (2020) 'Global land use for 2015–2100 at 0.05° resolution under diverse socioeconomic and climate scenarios', Scientific Data, 7(1), p. 320. doi:10.1038/s41597-020-00669-x.

Clifford, D.L. et al. (2009) 'Assessing disease risk at the wildlife–livestock interface: A study of Sierra Nevada bighorn sheep', Biological Conservation, 142(11), pp. 2559–2568.

Côté, S. and Festa-Bianchet, M. (2003) 'Mountain goat', in Wild Mammals of North America: Biology, Management, Conservation, pp. 1061–1075.

Courtemanch, A.B. et al. (2017) 'Alternative foraging strategies enable a mountain ungulate to persist after migration loss', Ecosphere, 8(6), p. e01855. doi:10.1002/ecs2.1855.

Creel, S. et al. (2005) 'Elk Alter Habitat Selection as an Antipredator Response to Wolves', Ecology, 86(12), pp. 3387–3397. doi:https://doi.org/10.1890/05-0032.

Cromsigt, J.P.G.M., Kerley, G.I.H. and Kowalczyk, R. (2012) 'The difficulty of using species distribution modelling for the conservation of refugee species – the example of European bison', Diversity and Distributions, 18(12), pp. 1253–1257. doi:https://doi.org/10.1111/j.1472-4642.2012.00927.x.

Cuyler, C. et al. (2020) 'Muskox status, recent variation, and uncertain future', Ambio, 49(3), pp. 805–819. doi:10.1007/s13280-019-01205-x.

Dawson, T.P. et al. (2011) 'Beyond Predictions: Biodiversity Conservation in a Changing Climate', Science, 332(6025), pp. 53–58. doi:10.1126/science.1200303.

Demarchi, R.A. and Hartwig, C. (2004) Status of Thinhorn Sheep in British Columbia. Wildlife Bulletin B-119. Victoria, B.C.: British Columbia Ministry of Water, Land, and Air Protection. Available at: https://www.semanticscholar.org/paper/Status-of-Thinhorn-Sheep-in-British-Columbia-Demarchi-Hartwig/bb3dc28b96755c3cd9ad432d288c33760b00987f (Accessed: 2 June 2022).

Elith, J. et al. (2011) 'A statistical explanation of MaxEnt for ecologists', Diversity and Distributions, 17(1), pp. 43–57. doi:10.1111/j.1472-4642.2010.00725.x.

Elith, J., Kearney, M. and Phillips, S. (2010) 'The art of modelling range-shifting species', Methods in Ecology and Evolution, 1(4), pp. 330–342. doi:10.1111/j.2041-210X.2010.00036.x.

Epps, C.W. et al. (2005) 'Highways block gene flow and cause a rapid decline in genetic diversity of desert bighorn sheep', Ecology Letters, 8(10), pp. 1029–1038. doi:https://doi.org/10.1111/j.1461-0248.2005.00804.x.

Faurby, S. and Araújo, M.B. (2018) 'Anthropogenic range contractions bias species climate change forecasts', Nature Climate Change, 8(3), pp. 252–256. doi:10.1038/s41558-018-0089-x.

Fick, S.E. and Hijmans, R.J. (2017) 'WorldClim 2: new 1-km spatial resolution climate surfaces for global land areas', International Journal of Climatology, 37(12), pp. 4302–4315. doi:10.1002/joc.5086.

Foley, A.M. (2010) 'Uncertainty in regional climate modelling: A review', Progress in Physical Geography: Earth and Environment, 34(5), pp. 647–670. doi:10.1177/0309133310375654.

Gámez-Brunswick, C. and Rojas-Soto, O. (2020) 'New insights into palaeo-distributions based on Holocene rock art', Journal of Biogeography, 47(12), pp. 2543–2553. doi:https://doi.org/10.1111/jbi.13975.

GBIF (2022) 'GBIF Occurrence Download', Global Biodiversity Information Facility [Preprint]. doi:https://doi.org/10.15468/dl.burd8t.

GDAL/OGR contributors (2021) GDAL/OGR Geospatial Data Abstraction software Library. Open Source Geospatial Foundation. Available at: https://gdal.org.

Herrera-Sánchez, F.J. et al. (2020) 'Identifying priority conservation areas in a Saharan environment by highlighting the endangered Cuvier's Gazelle as a flagship species', Scientific Reports, 10(1), p. 8241. doi:10.1038/s41598-020-65188-6.

Hijmans, R.J. et al. (2005) 'Very high resolution interpolated climate surfaces for global land areas', International Journal of Climatology, 25(15), pp. 1965–1978. doi:10.1002/joc.1276.

IPBES (2019) Global assessment report on biodiversity and ecosystem services of the Intergovernmental Science-Policy Platform on Biodiversity and Ecosystem Services. E. S. Brondizio, J. Settele, S. Díaz, and H. T. Ngo (editors). Bonn, Germany: IPBES secretariat.

Jenkins, D.A. et al. (2020) 'Biotic interactions govern the distribution of coexisting ungulates in the Arctic Archipelago – A case for conservation planning', Global Ecology and Conservation, 24, p. e01239. doi:10.1016/j.gecco.2020.e01239.

Jones, K.R. et al. (2016) 'Incorporating climate change into spatial conservation prioritisation: A review', Biological Conservation, 194, pp. 121–130. doi:10.1016/j.biocon.2015.12.008.

Kass, J.M. et al. (2021) 'ENMeval 2.0: Redesigned for customizable and reproducible modeling of species' niches and distributions', Methods in Ecology and Evolution, 12(9), pp. 1602–1608. doi:10.1111/2041-210X.13628.

Krausman, P.R. and Bleich, V.C. (2013) 'Conservation and management of ungulates in North America', International Journal of Environmental Studies, 70(3), pp. 372–382. doi:10.1080/00207233.2013.804748.

Kuemmerle, T. et al. (2010) 'European Bison habitat in the Carpathian Mountains', Biological Conservation, 143(4), pp. 908–916. doi:10.1016/j.biocon.2009.12.038.

Kuemmerle, T. et al. (2012) 'Reconstructing range dynamics and range fragmentation of European bison for the last 8000 years', Diversity and Distributions, 18(1), pp. 47–59. doi:https://doi.org/10.1111/j.1472-4642.2011.00849.x.

Laliberte, A.S. and Ripple, W.J. (2004) 'Range Contractions of North American Carnivores and Ungulates', BioScience, 54(2), pp. 123–138. doi:10.1641/0006-3568(2004)054[0123:RCONAC]2.0.CO;2.

Lembrechts, J.J., Nijs, I. and Lenoir, J. (2019) 'Incorporating microclimate into species distribution models', Ecography, 42(7), pp. 1267–1279. doi:https://doi.org/10.1111/ecog.03947.

Liu, C., White, M. and Newell, G. (2013) 'Selecting thresholds for the prediction of species occurrence with presence-only data', Journal of Biogeography, 40(4), pp. 778–789. doi:10.1111/jbi.12058.

McInturff, A. et al. (2020) 'Fence Ecology: Frameworks for Understanding the Ecological Effects of Fences', BioScience, 70(11), pp. 971–985. doi:10.1093/biosci/biaa103.

Meagher, M. (1986) 'Bison bison', Mammalian Species, (266), pp. 1–8.

Monzón, J., Moyer-Horner, L. and Palamar, M.B. (2011) 'Climate Change and Species Range Dynamics in Protected Areas', BioScience, 61(10), pp. 752–761. doi:10.1525/bio.2011.61.10.5.

Myers-Smith, I.H. et al. (2020) 'Complexity revealed in the greening of the Arctic', Nature Climate Change, 10(2), pp. 106–117. doi:10.1038/s41558-019-0688-1.

Parmesan, C., Root, T.L. and Willig, M.R. (2000) 'Impacts of Extreme Weather and Climate on Terrestrial Biota', Bulletin of the American Meteorological Society, 81(3), pp. 443–450. doi:10.1175/1520-0477(2000)081<0443:IOEWAC>2.3.CO;2.

Phillips, S.J. et al. (2009) 'Sample selection bias and presence-only distribution models: implications for background and pseudo-absence data', Ecological Applications, 19(1), pp. 181–197. doi:10.1890/07-2153.1.

Phillips, S.J., Dudík, M. and Schapire, R.E. (2021) Maxent software for modeling species niches and distributions. Internet. Available at: https://biodiversityinformatics.amnh.org/open_source/maxent/ (Accessed: 28 February 2021).

Ponti, R. and Sannolo, M. (2022) 'The importance of including phenology when modelling species ecological niche', Ecography, n/a(n/a), p. e06143. doi:10.1111/ecog.06143.

Post, E. et al. (2019) 'The polar regions in a 2°C warmer world', Science Advances, 5(12), p. eaaw9883. doi:10.1126/sciadv.aaw9883.

Post, E. and Brodie, J. (2015) 'Anticipating novel conservation risks of increased human access to remote regions with warming', Climate Change Responses, 2(1), p. 2. doi:10.1186/s40665-015-0011-y.

Post, E., Steinman, B.A. and Mann, M.E. (2018) 'Acceleration of phenological advance and warming with latitude over the past century', Scientific Reports, 8(1), p. 3927. doi:10.1038/s41598-018-22258-0.

R Core Team (2019) 'R: A Language and Environment for Statistical Computing'. R Foundation for Statistical Computing. Available at: http://www.R-project.org/.

Raynolds, M.K. et al. (2019) 'A raster version of the Circumpolar Arctic Vegetation Map (CAVM)', Remote Sensing of Environment, 232, p. 111297. doi:10.1016/j.rse.2019.111297.

Riahi, K. et al. (2017) 'The Shared Socioeconomic Pathways and their energy, land use, and greenhouse gas emissions implications: An overview', Global Environmental Change, 42, pp. 153–168. doi:10.1016/j.gloenvcha.2016.05.009.

Rodríguez, J.P. et al. (2007) 'The Application of Predictive Modelling of Species Distribution to Biodiversity Conservation', Diversity and Distributions, 13(3), pp. 243–251.

Sawyer, H. et al. (2013) 'A framework for understanding semi-permeable barrier effects on migratory ungulates', Journal of Applied Ecology, 50(1), pp. 68–78. doi:10.1111/1365-2664.12013.

Scridel, D. et al. (2021) 'A genus at risk: Predicted current and future distribution of all three Lagopus species reveal sensitivity to climate change and efficacy of protected areas', Diversity and Distributions, 27(9), pp. 1759–1774. doi:10.1111/ddi.13366.

Sierra-Morales, P. et al. (2021) 'Climate change projections suggest severe decreases in the geographic ranges of bird species restricted to Mexican humid mountain forests', Global Ecology and Conservation, p. e01794. doi:10.1016/j.gecco.2021.e01794.

South, A. (2017) rnaturalearth: World map data from Natural Earth. The R Foundation. Available at: https://CRAN. R-project. org/package= rnaturalearth.

Stoellinger, T. et al. (2020) 'Where the Deer and The Antelope Play:Conserving Big Game Migrations As an Endangered Phenomena', Duke Environmental Law & Policy Forum, p. 81.

Tape, K.D. et al. (2016) 'Range Expansion of Moose in Arctic Alaska Linked to Warming and Increased Shrub Habitat', PLOS ONE, 11(4), p. e0152636. doi:10.1371/journal.pone.0152636.

Tebaldi, C. et al. (2021) 'Climate model projections from the Scenario Model Intercomparison Project (ScenarioMIP) of CMIP6', Earth System Dynamics, 12(1), pp. 253–293. doi:10.5194/esd-12-253-2021.

Tucker, M.A. et al. (2018) 'Moving in the Anthropocene: Global reductions in terrestrial mammalian movements', Science, 359(6374), pp. 466–469. doi:10.1126/science.aam9712.

UNEP-WCMW and IUCN (2021) 'Protected Planet: The World Database on Protected Areas (WDPA)'. Cambridge, UK: UNEP-WCMC and IUCN. Available at: www.protectedplanet.net (Accessed: 5 March 2021).

Venter, O. et al. (2016) 'Sixteen years of change in the global terrestrial human footprint and implications for biodiversity conservation', Nature Communications, 7(1), p. 12558. doi:10.1038/ncomms12558.

Vignali, S. et al. (2020) 'SDMtune: An R package to tune and evaluate species distribution models', Ecology and Evolution, 10(20), pp. 11488–11506. doi:10.1002/ece3.6786.

Watson, J.E.M. et al. (2014) 'The performance and potential of protected areas', Nature, 515(7525), pp. 67–73. doi:10.1038/nature13947.

Williams, J.E. and Blois, J.L. (2018) 'Range shifts in response to past and future climate change: Can climate velocities and species' dispersal capabilities explain variation in mammalian range shifts?', Journal of Biogeography, 45(9), pp. 2175–2189. doi:10.1111/jbi.13395.

Wilson, K.A. et al. (2005) 'Sensitivity of conservation planning to different approaches to using predicted species distribution data', Biological Conservation, 122(1), pp. 99–112. doi:10.1016/j.biocon.2004.07.004.

Winnie, J.A., Cross, P. and Getz, W. (2008) 'Habitat Quality and Heterogeneity Influence Distribution and Behavior in African Buffalo (syncerus Caffer)', Ecology, 89(5), pp. 1457–1468. doi:https://doi.org/10.1890/07-0772.1.

Yesson, C. et al. (2007) 'How Global Is the Global Biodiversity Information Facility?', PLOS ONE, 2(11), p. e1124. doi:10.1371/journal.pone.0001124.

Zurell, D. et al. (2020) 'A standard protocol for reporting species distribution models', Ecography, 43(9), pp. 1261–1277. doi:10.1111/ecog.04960.
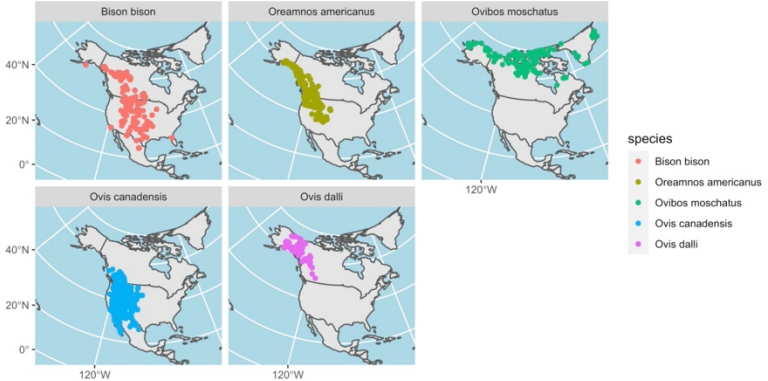
Supplementary materials S5.1

ODMAP protocol for ENM reporting:

ODMAP section	ODMAP subsection	ODMAP elements
Overview	**Authorship**	Christian John and Eric Post. Department of Wildlife, Fish, and Conservation Biology at the University of California, Davis. Contact: cjohn@ucdavis.edu. Projected bioclimatic distributions in Nearctic Bovidae signal the potential for reduced overlap with protected areas. doi available upon acceptance for publication.
	Model objective	Predict changes in overlap between North American bovid species and currently protected areas. The target output is forecasted species distributions for 5 North American bovid species
	Taxon	Bighorn sheep (*Ovis canadensis*), Thinhorn sheep (*Ovis dalli*), Mountain goat (*Oreamnos americanus*), Muskox (*Ovibos moschatus*), and American bison (*Bison bison*)
	Location	Terrestrial North America and its islands
	Scale of analysis	Spatial extent designed using political boundaries and includes Central and North America (xmin = 171.79°W; xmax = 12.20°W; ymin = 7.22°N; ymax = 83.65°N). Raster data were resampled to 6kmx6km pixels in Albers projection (+proj=aea +lat_0=40 +lon_0=-96 +lat_1=20 +lat_2=60 +x_0=0 +y_0=0 +datum=NAD83 +units=m +no_defs). "Present" climate data were from 1970-2000; Future climate data for 2081-2100.
	Biodiversity data overview	Observation data (presence-only) collected from GBIF records; predictor variables generated from WorldClim v2.1 (https://www.worldclim.org/), GCAM Demeter land use (https://data.pnnl.gov/group/nodes/dataset/13192), and North America Elevation 1-kilometer resolution GRID (https://www.sciencebase.gov/catalog/item/4fb5495ee4b04cb937751d6d). Topography data were treated as fixed, not varying between model fitting and prediction.
	Type of predictors	WorldClim bioclimatic variables, Demeter land use/land cover variables, and elevation/topography data.

	Hypotheses	We expected northward shifts and elevational contractions between historical and future modeled distributions, adjusting the representation of bioclimatic ranges in currently protected areas.
	Assumptions	We assume niche conservatism, error-free predictors, full knowledge of important predictors, observation independence, spp.-environment equilibrium, unbiased observations, and stationarity in model predictive ability.
	SDM algorithms	MaxEnt v3.4.3 was used with presence and 10000 background observations. Model results were compared with an identical procedure with 5000 background points and found to be in general agreement ($r > 0.7$ for all species).
	Model workflow	For each species, MaxEnt models were fit to a 60% training, 20% validation, and 20% testing subset of occurrence data using checkerboard cross-validation. Variable importance was assessed with permutation and jackknife tests. After cross-validation, full models were fit for each species. Full models were then used to project 2081-2100 suitable habitat using CMIP6 climate projections.
	Software, codes, and data	R version v3.6.1 "Action of the Toes", dismo v1.3.3, and Maxent v3.4.1 were used. Code for data access, cleaning, and model fit and predictions available at <https://github.com/JepsonNomad/NA_Bovidae_SDM>. Data available for bioclimatic data at <https://www.worldclim.org/>; for landuse data <https://data.pnnl.gov/group/nodes/dataset/13192>; for Elevation data <https://www.sciencebase.gov/catalog/item/4fb5495ee4b04cb937751d6d>; and for GBIF occurrences <https://doi.org/10.15468/dl.burd8t >

Data	Biodiversity data	Taxon names described above. Data were analyzed at the species level, using the GBIF system with species ID's 2441119, 2441118, 2441151, 2441108, 2441176 (respectively). GBIF occurrence data (<https://www.gbif.org/>) were accessed 5 May 2022 by way of the R package `rgbif` and the GBIF API. Data were filtered to retain only points on North America and Greenland, and to remove occurrences where latitude and longitude were not available, or where the listed observation coordinates were in a different country from the listed observation country. Points with observation dates prior to 1980 were also removed. Preserved specimens and fossil records were removed. Finally, several additional GBIF records were manually removed for other idiosyncratic reasons (Table 1). Occurrence records were thinned to a 6km radius, following the resolution of predictor data, to avoid duplicate sampling.

Table 1. GBIF records that were manually removed from the SDM analyses, and their reasons for removal.

Species	GBIF ID	Reason for removal
Bighorn sheep	922490545	Denali (probably thinhorn)
Bighorn sheep	1019041688	Recorded at zoo in Lansing Michigan
American bison	2596125567	Camp Pendleton, introduced
American bison	1850921137	Camp Pendleton, introduced
American bison	2381410738	Camp Pendleton, introduced
American bison	2269206648	Camp Pendleton, introduced
American bison	3079682696	Camp Pendleton, introduced
American bison	3415452210	Camp Pendleton, introduced
American bison	3457071522	Camp Pendleton, introduced
American bison	2631191303	San Fransisco Zoo
American bison	2631191308	San Fransisco Zoo
American bison	2631191306	Golden Gate Park
American bison	1893583451	Weird Mexico loc's
American bison	1893583408	Weird Mexico loc's
American bison	3456432067	Ranch near Santa Ysabel

		Occurrence map for the 5 North American bovid species:
	Data partitioning	We used a 60% subset of the original data to train the model for each species, and a 20% subset for validation. The remaining 20% were used for model testing. GBIF occurrence records, thinning, training, validation, and testing data partitioning can be recreated using the code on our GitHub repository <https://github.com/JepsonNomad/NA_Bovidae_SDM>.
	Predictor variables	Historic and future (CMIP6) bioclimatic variables were accessed at the WorldClim (v2.1) website (<https://worldclim.org/>) on 2 March 2021. We accessed 2.5m global data but cropped the dataset to North America and resampled to 6km pixels in an Albers Equal Area projection (see above) using bilinear interpolation with GDAL. GCAM Demeter data were accessed from the PNNL website (<https://data.pnnl.gov/group/nodes/dataset/13192>) on 3 June 2021 and resampled as above. Terrain data were accessed from <https://www.sciencebase.gov/catalog/item/4fb5495ee4b04cb937751d6d> on 26 July 2018 and resampled as above. Terrain ruggedness index (TRI) were also calculated using default GDAL settings.

	Transfer data for projection	All available CMIP6 model forecasts under SSP2-4.5 and SSP5-8.5 in the WorldClim v2 dataset were used for the period 2081-2100. Data were accessed at the WorldClim (v2.1) website <https://worldclim.org/>, and resampled following the same protocol as predictor variables used for model training. Differences between historical data and forecasts were visualized by converting temperature data to °C (original data in °C*10), centering based on historical data, and averaging across CMIP6 model projections.
Model	Variable pre-selection	All predictor variables were centered using the mean value of the resampled historic data. CMIP6 forecast data were centered according to the historic center values. GCAM Demeter data were condensed into single scenarios from CMIP6 models because the individual models available did not correspond with those from Worldclim. Elevation and terrain ruggedness index were also included. These variables remained unchanged between fitting the model on historic data and predicting with CMIP6 forecasts.
	Multicollinearity	Variables were removed through an iterative data-driven modeling process (Vignali et al 2020). For each species, Maxent models were fit with checkerboard1 cross-validation and allowing only linear and quadratic feature classes. When variables were highly correlated ($r > 0.7$), the variable with the most explanatory power (identified using a leave-one-out jackknife test) was retained. This process was repeated for the resulting model until correlations among predictor variables fell below 0.7. Model transfers were fit using CMIP6 forecasts for the bioclimatic layers, GCAM Demeter forecasts for the landcover data, and unchanged terrain data.
	Model settings	We used clamping and limited predictions to areas with positive MESS values (Elith et al 2010) to avoid extrapolation of conditions outside the range of the training data. 20% of input data were held for model testing. We allowed only linear and quadratic feature types to be used in model fitting, and then used a genetic algorithm to identify the best set of model hyperparameters (Vignali et al 2020).
	Model estimates	Variable importance was determined through data permutation and jackknife tests (Vignali et al 2020).
	Model selection	We did not use ensemble modeling to generate estimates, and instead relied on the final model generated after

		selection of model hyperparameters and variable reduction.
	Non-independence correction	Non-independence is an inherent feature of many citizen science datasets, and we acknowledge that points used to train the models described here likely feature both spatial and temporal autocorrelation. We used spatial thinning of occurrence to account for spatial autocorrelation and bias grids to generate background data.
	Threshold selection	Thresholding was used in order to translate the 8 CMIP model-based ENM projections into consensus plots, so that each model was equally weighted as 0=absent, 1=present. Sensitivity and specificity were maximized to determine the species-specific presence/absence threshold, although we compared this metric to a threshold based on equal sensitivity and specificity in Figure 5.1 (finding similar results). In preliminary modeling steps, we found this threshold selection technique related closely to the maximized true skill statistic.
Assessment	**Performance statistics**	Training and testing AUC were compared to assess model training. Models were evaluated using a 20% partition of fully-withheld testing data.
	Plausibility check	We performed plausibility checks for each species-specific model by plotting predicted presence for the baseline (1970-2000) predictor conditions, and found that models were generally predictive of known current species distributions (but see discussion on pattern of overprediction). Plausibility was also ascertained using marginal and sole-predictor response curves of important variables.
Prediction	**Prediction output**	Prediction outputs were defined using thresholding to differentiate potential presence (1) and absence (0), which we interpreted as "suitable" and "unsuitable" habitat, respectively. Across CMIP6 models, prediction outputs for future climate scenarios resulted in a discrete model consensus surface with the minimum possible value being 0 (no models predict presence) and maximum possible value being 8 (all models agree on presence).
	Uncertainty quantification	Uncertainty in future conditions was assessed using multi-model consensus, outlined above. Boundary conditions –

such as non-analogue climates – were accounted for using clamping and MESS grid during predictions, described above.

Future climate MESS grids (positive values only shown):

	SSP 2-4.5	SSP 5-8.5
BCC-CSM2-MR		
CanESM5		
CNRM-CM6-1		
CNRM-ESM2-1		
IPSL-CM6A-LR		
MIROC-ES2L		
MIROC6		
MRI-ESM2-0		

Supplementary materials S5.2

Table 1. Modeled current and projected mean elevation of each Nearctic bovid species, in meters above sea level.

Species	Current	SSP2-4.5	SSP5-8.5
Ovis canadensis	1526.61	1537.52 ± 4.75	1582.75 ± 6.72
Ovis dalli	826.38	932.04 ± 17.18	934.42 ± 44.29
Oreamnos americanus	1421.49	1401.15 ± 18.35	1443.50 ± 36.30
Ovibos moschatus	291.26	266.93 ± 1.98	313.72 ± 16.56
Bison bison	656.34	710.36 ± 31.23	778.33 ± 62.58

Table 2. Modeled current and projected mean latitude of each Nearctic bovid species, shown in degrees N.

Species	Current	SSP2-4.5	SSP5-8.5
Ovis canadensis	44.21	45.18 ± 0.23	45.80 ± 0.37
Ovis dalli	61.31	62.22 ± 0.18	61.21 ± 0.42
Oreamnos americanus	53.14	52.21 ± 0.36	51.83 ± 0.85
Ovibos moschatus	68.08	71.69 ± 0.36	74.47 ± 0.50
Bison bison	54.59	55.74 ± 0.29	54.47 ± 0.44

Supplementary materials S5.3. The following are Receiver-Operator Characteristic curves, variable importance tables, and univariate response curves for the 5 most important variables for each species. Univariate response curves can be interpreted as the response of habitat suitability to that variable on its own, without considering other variables.

Bighorn sheep
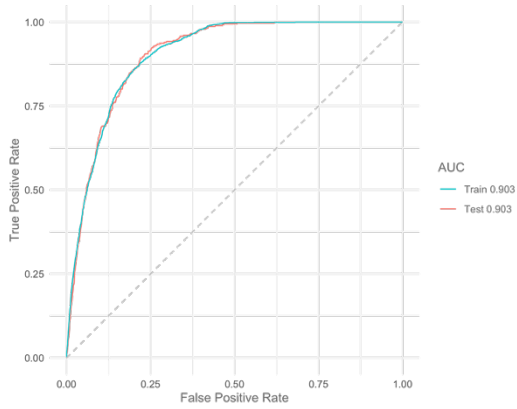
Variable	Permutation_importance	sd
TRI	41.0	0.003
Biocl_12	36.5	0.004
Biocl_04	11.6	0.004
C3_gra_arc	3.4	0.002
Biocl_08	2.1	0.001
treeTemperate	1.4	0.001
Biocl_15	1.1	0.001
treeBoreal	1.0	0.000
C4_gra	0.9	0.001
Biocl_02	0.7	0.001
C3_gra	0.2	0.000
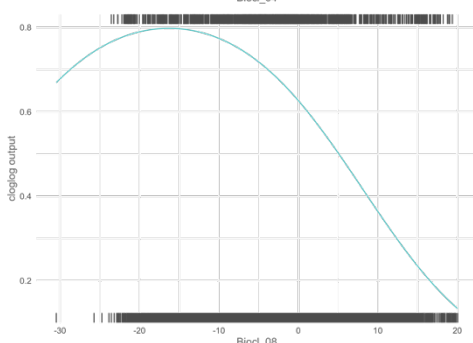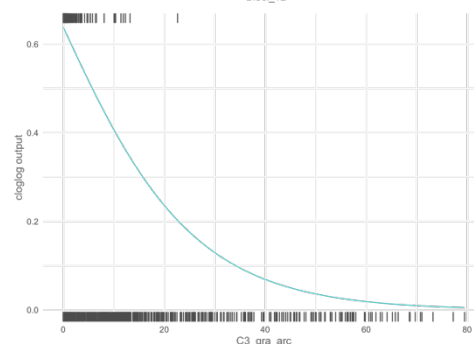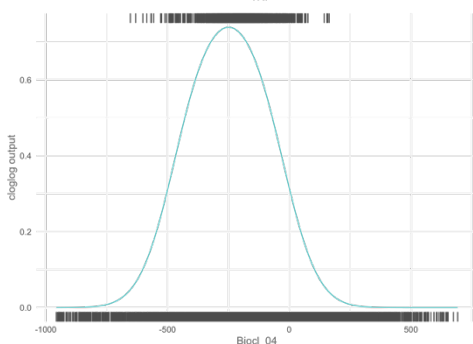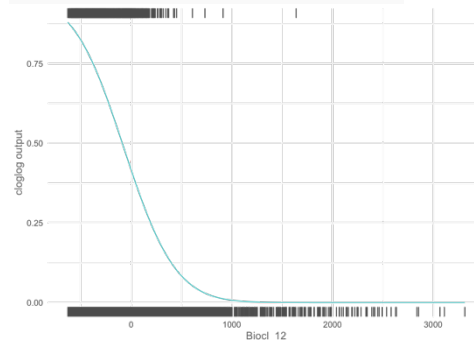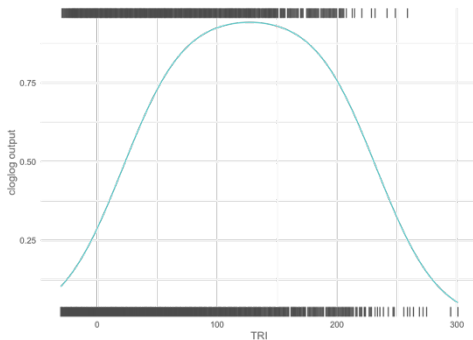
TRI: Terrain ruggedness index
Biocl_12: Annual precipitation
Biocl_04: Temperature seasonality
C3_gra_arc: C3 Arctic grasses fractional cover
Biocl_08: Mean temperature of wettest quarter

137

Thinhorn sheep
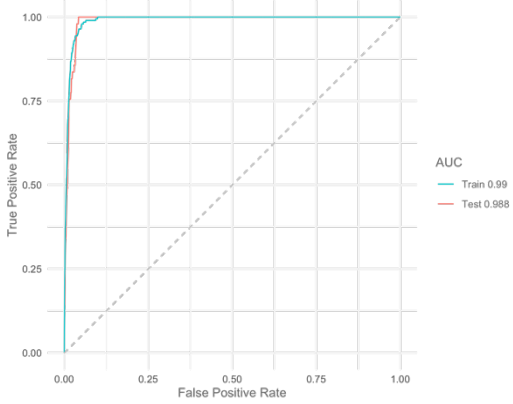
Variable	Permutation_importance	sd
Biocl_03	61.1	0.014
AGR	13.0	0.008
Urban	8.8	0.007
Biocl_19	6.8	0.010
treeTemperate	6.7	0.003
TRI	2.7	0.001
treeBoreal	0.5	0.000
C3_gra_arc	0.2	0.000
C3_gra	0.1	0.000
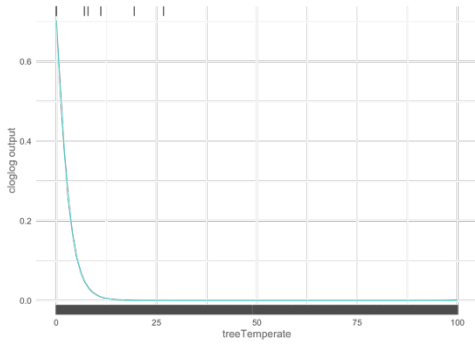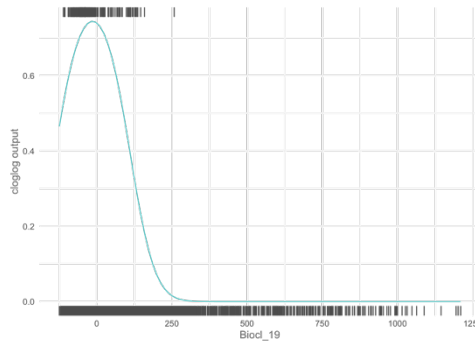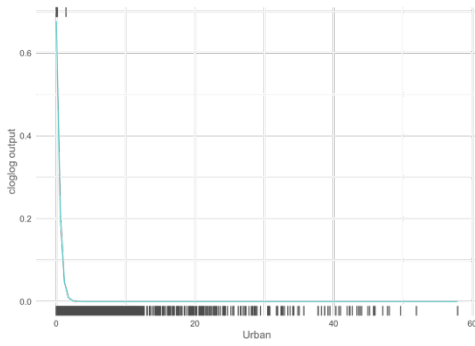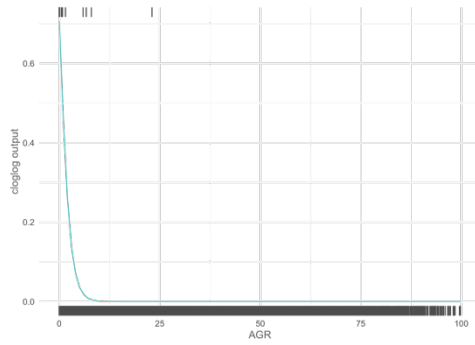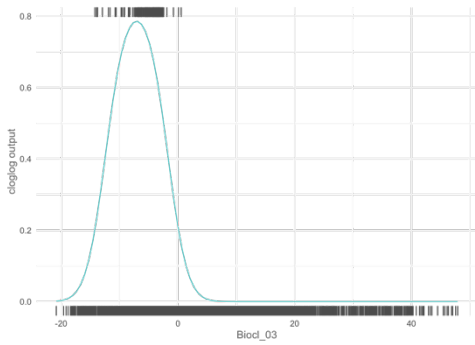
Biocl_03: Isothermality
AGR: Agriculture fractional cover
Urban: Urban fractional cover
Biocl_19: Precipitation of coldest quarter
treeTemperate: Temperate tree fractional cover

Mountain goat
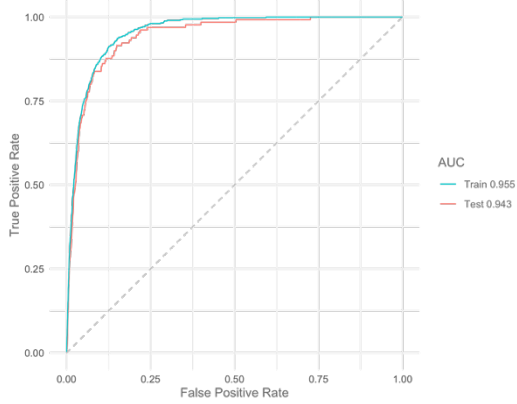
Variable	Permutation_importance	sd
TRI	63.6	0.005
Biocl_03	24.2	0.007
treeTemperate	3.8	0.001
BDS_tem	2.6	0.002
Biocl_18	2.0	0.001
C4_gra	1.3	0.001
DEM	0.9	0.000
treeBoreal	0.6	0.000
Biocl_15	0.4	0.000
C3_gra	0.4	0.000
Biocl_19	0.2	0.000
BDS_bor	0.1	0.000
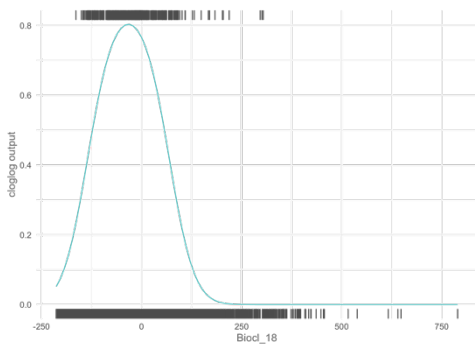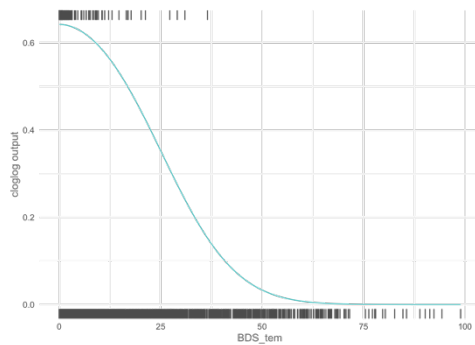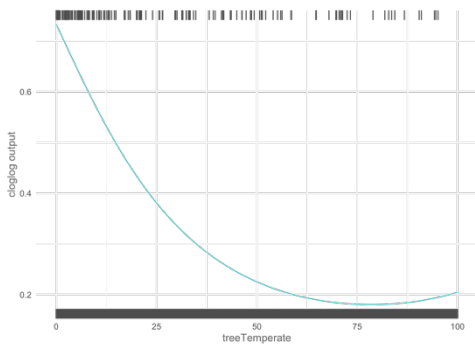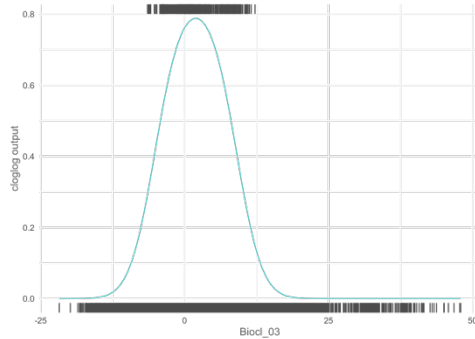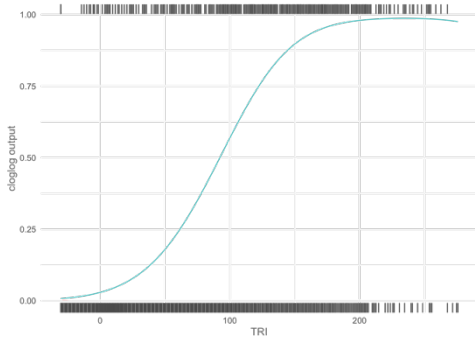
TRI: Terrain ruggedness index
Biocl_03: Isothermality
treeTemperate: Temperate tree fractional cover
BDS_tem: Broadleaf deciduous shrub fractional cover
Biocl_18: Precipitation of warmest quarter

Muskox
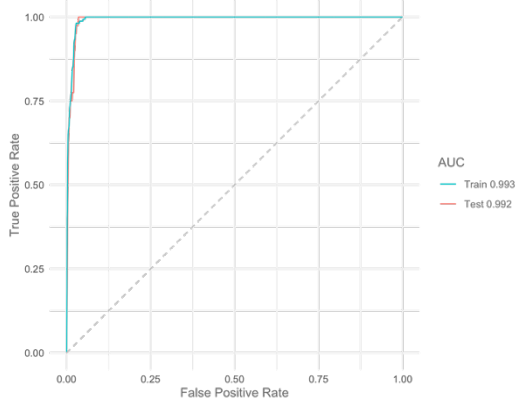
| Variable	Permutation_importance	sd
Biocl 10	70.6	0.022
DEM	17.1	0.006
treeTemperate	7.4	0.005
Biocl 14	1.3	0.002
Biocl 18	0.9	0.000
treeBoreal	0.9	0.001
Biocl 04	0.8	0.001
TRI	0.7	0.001
C3 gra	0.2	0.000
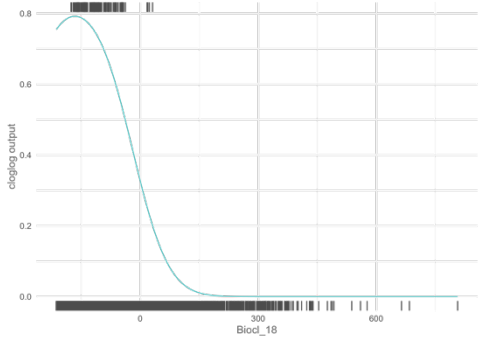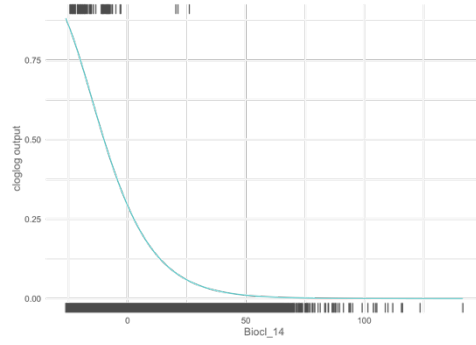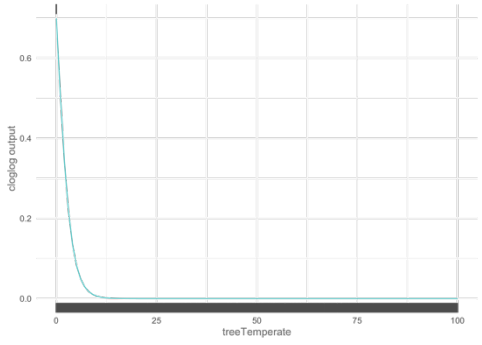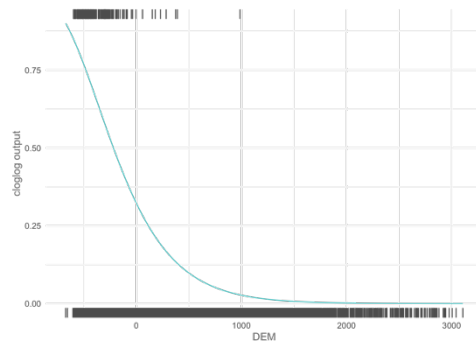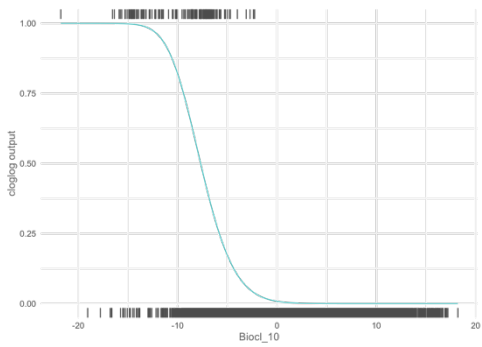
Biocl_10: Mean temperature of warmest quarter
DEM: Elevation
treeTemperate: Temperate tree fractional cover
Biocl_14: Precipitation of driest month
Biocl_18: Precipitation of warmest quarter

American bison
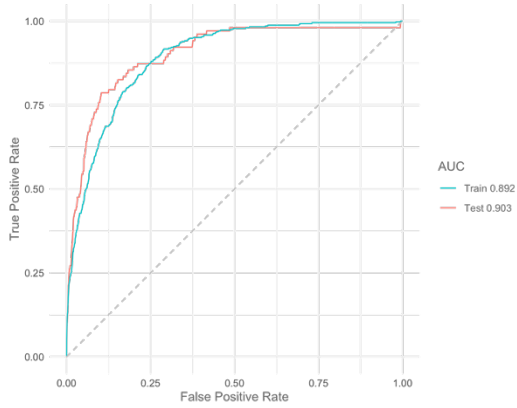
Variable	Permutation_importance	sd
Biocl 19	26.3	0.009
Biocl 18	23.3	0.006
Biocl 08	13.1	0.003
Biocl 02	10.9	0.005
AGR	9.6	0.004
treeBoreal	6.0	0.002
treeTemperate	3.0	0.003
TRI	2.7	0.002
BDS tem	2.1	0.002
C3 gra arc	1.5	0.002
C4 gra	1.0	0.001
DEM	0.5	0.001
Urban	0.0	0.001
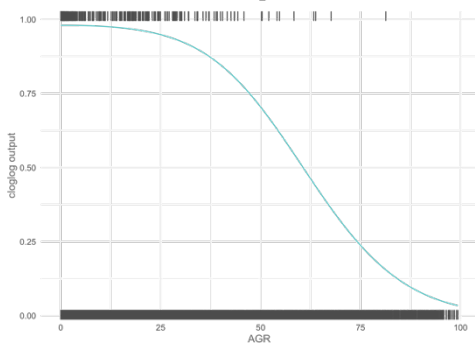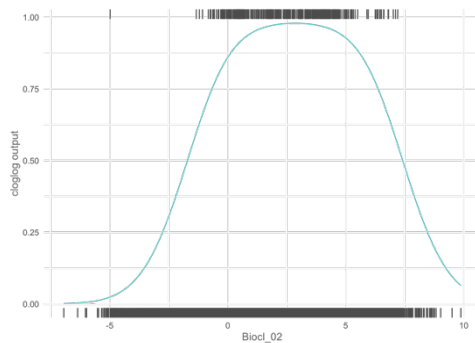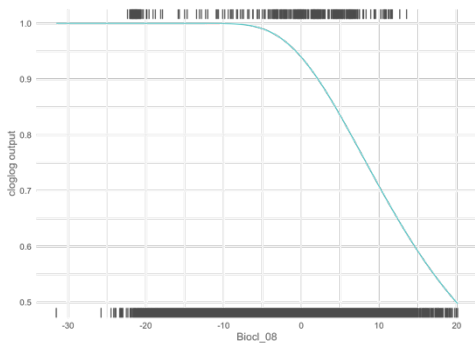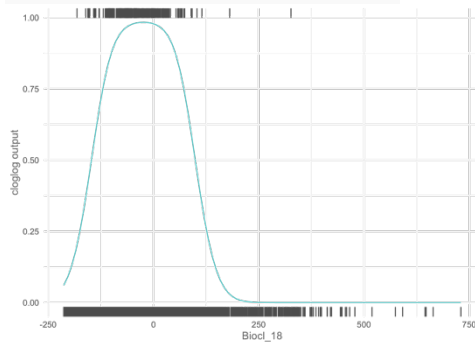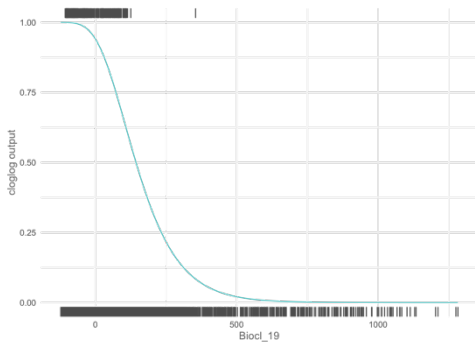
Biocl_19: Precipitation of coldest quarter
Biocl_18: Precipitation of warmest quarter
Biocl_08: Mean temperature of wettest quarter
Biocl_02: Mean diurnal range
AGR: Agriculture fractional cover